Role of megalin in albumin transport across the alveolar epithelium and its dysregulation by transforming growth factor β

Yasmin Buchäckert

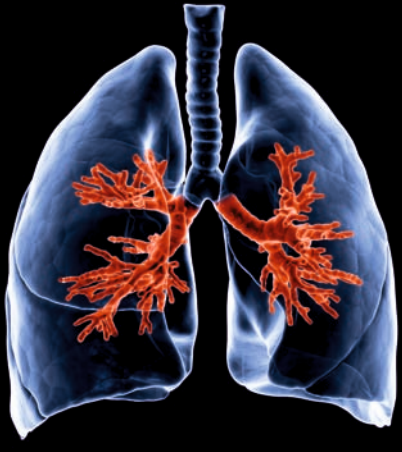

INAUGURALDISSERTATION
zur Erlangung des Grades eines **Doktors der Humanbiologie**
des Fachbereichs Medizin der Justus-Liebig-Universität Gießen

édition scientifique
VVB LAUFERSWEILER VERLAG

1. Auflage 2012

1st Edition 2012

Printed in Germany

édition scientifique
VVB LAUFERSWEILER VERLAG

STAUFENBERGRING 15, D-35396 GIESSEN
Tel: 0641-5599888 Fax: 0641-5599890
email: redaktion@doktorverlag.de

www.doktorverlag.de

Role of megalin
in albumin transport across the alveolar epithelium and its dysregulation by transforming growth factor β

INAUGURAL-DISSERTATION

zur Erlangung des Grades eines Doktors der Humanbiologie
des Fachbereichs Medizin
der Justus-Liebig-Universität Giessen

vorgelegt von

Yasmin Buchäckert

aus Ludwigshafen am Rhein

Giessen 2011

Aus dem Zentrum für Innere Medizin, Medizinische Klinik II,
Universitätsklinikum Gießen und Marburg GmbH
Standort Gießen
Direktor: Prof. Dr. W. Seeger

Gutachter: Prof. Dr. W. Seeger

Gutachter: Prof. Prof. h.c. Dr. Dr. Dr. h.c. R. Schnettler

Tag der Disputation: 09.10.2012

Viktor Braun gewidmet

Table of Contents

Abbreviations

^{125}I-albumin	^{125} Iodined bovine serum albumin
A	asymptote of the exponential curve
A549	human adeno-carcinoma cell line
AAC	area above the curve
Aβ	β-amyloid
AD	Alzheimer's disease
AEBSF	4-(2-aminoethyl)-benzenesulfonyl fluoride
ALI	acute lung injury
ANOVA	one-way analysis of variances
AP180	assembly protein 180
AP-2	adaptor protein-2
ARDS	acute respiratory distress syndrome
ATII cells	alveolar epithelial type II cells
ATI-like cells	alveolar epithelial type I-like cells
ATPase	adenosine triphosphatase
ATP	adenosine triphosphate
BAL	broncho-alveolar lavages
BSA	bovine serum albumin
CK	casein kinase
DMEM/F12	Dulbecco's modified Eagle´s medium/Ham´s F12 medium
DMSO	dimethyl sulfoxide
DPBS	Dulbecco's phosphate buffered saline
DPBS-G	Dulbecco's phosphate buffered saline supplemented with glucose
e	exponential function of the curve
EDTA	ethylenediaminetetraacetic acid
ELF	epithelial lining fluid
ENaC	epithelial sodium channel
FCS	fetal calf serum
FiO_2	fraction of inspired oxygen
FITC	fluorescein isothiocyanate
FXS	fragile X syndrome
gp60	albondin, albumin binding protein

GSK3	glycogen synthase kinase 3
HDL	high-density lipoprotein
IgA	immunoglobulin A
IgG	immunoglobulin G
LAP	left atrial pressure
LDL-R	low density lipoprotein-receptor
LVP	left ventricular pressure
MDCK	Madine Darby canine kidney cells
min	minutes
Na,K-ATPase	Na,K-adenosine triphosphate
NO	nitric oxide
PaO_2	partial arterial oxygen pressure
PAP	pulmonary artery pressure
PEEP	positive end-expiratory pressure
PK	protein kinase
PTH	parathyroid hormone
RAP	receptor associated protein
RLE-6TN	rat alveolar epithelial cells
rpm	revolutions per minute
SDS	sodium dodecyl sulfate
SD	standard deviation
SNARE	soluble *N*-ethylmaleimide-sensitive factor attachment protein receptor
TGF-β	transforming growth factor β
VP	ventilation pressure

1. Introduction

1.1 The acute respiratory distress syndrome

The acute respiratory distress syndrome (ARDS) has an incidence of approximately 200,000 patients annually in the United States with a mortality of around 40 % (Rubenfeld et al. 2005). The definition of acute lung injury (ALI) and ARDS that has been used over the past 15 years was stated by the American/European Consensus Conference in 1994 (Bernard and Artigas et al. 1994). By this definition patients with ALI present with bilateral pulmonary infiltrates with arterial hypoxemia using the concentration of arterial oxygen in the blood divided by the inspired fraction of oxygen (i.e., a PaO_2/FiO_2 ratio of less than 300 for ALI, PaO_2/FiO_2 ratio of less than 200 for ARDS). The arterial hypoxemia is caused by accumulation of edema fluid in the distal air spaces of the lung, resulting in impaired blood gas exchange (Matthay and Zemans 2011). To diagnose ALI or ARDS, the presence of left atrial hypertension should be excluded, although it was established in a clinical trial (Wiedemann et al. 2006) that the pulmonary arterial wedge pressure is greater than 18 mmHg in 29 % of patients with ALI/ARDS.

Numerous clinical disorders have been linked to the development of ALI/ARDS, although the presence of pulmonary or non pulmonary infection is most prevalent. The most common trigger is primary pneumonia caused by bacterial, viral or fungal infection (Bachofen and Weibel 1977; Ware and Matthay 2000). The syndrome can also be caused by severe sepsis, either associated with pneumonia or a non pulmonary infection, such as peritonitis. Other causes of ALI/ARDS include hemorrhage and shock following trauma, aspiration of gastric contents, severe acute pancreatitis, transfusion-associated lung injury and drug reactions (Ashbaugh et al. 1967; Ware and Matthay 2000; Eisner et al. 2001; Flori et al. 2005; Randolph 2009).

One of the initial causes of ALI/ARDS is lung endothelial injury. There is data demonstrating that permeability increases in the lung vasculature, which results in accumulation of protein-rich pulmonary edema even if the vascular pressure in the lung remains normal (Staub 1974, 1981). Several mechanisms can cause endothelial injury, neutrophil-mediated lung injury being the best documented (Flick and Perel, 1981; Matthay and Zimmerman, 2005). This has been shown in an in vivo mouse model of transfusion-

associated lung injury (Looney and Su, 2006) which was based on the passive transfusion of an MHC class I (MHC I). In both settings of lung injury, agglomeration and activation of neutrophils releases numerous toxic mediators, such as proteases, reactive oxygen species, proinflammatory cytokines and procoagulant molecules, which results in increased vascular permeability and impairs endothelial barrier function (Matthay and Zemans, 2011).

However, endothelial injury alone is not sufficient to cause ALI/ARDS without injury to the alveolar epithelium. It has been shown in large-animal studies that endothelial injury can occur without involvement of epithelial damage (Wiener-Kronish and Albertine, 1991). Endothelial injury was initiated by intravenous instillation of endotoxin. The development of alveolar edema could only be reported when epithelial barrier function was impaired by an additional instillation of live bacteria. These data established that epithelial injury is required for the development of ALI/ARDS.

The restoration of the alveolo-capillary barrier is crucial for a positive outcome in ALI/ARDS. The epithelial barrier is less permeable than the endothelial barrier. Thus, the integrity of epithelial barrier function is the critical step regarding the formation and resolution of edema.

1.2 Clinical relevance of protein clearance

The mechanisms of protein removal from the distal air spaces are poorly understood. It has been shown that the rate of albumin transport across the alveolo-capillary barrier is considerably slower than the transport of sodium. Because of the high transport rate of sodium, the protein concentration in the alveolar space increases over time, thereby generating oncotic pressure that impedes edema clearance and recovery (Hastings, Folkesson et al. 2004). This manifestation of alveolar edema causes severe impairment of gas exchange and therefore alveolar hypoxia and systemic hypoxemia which implicate further disruption of alveolar epithelial function and fluid balance (Vadasz and Sznajder 2006). Elevated levels of precipitated protein can be found in the alveolar space of ARDS patients. Non-survivors of ARDS exhibit threefold higher levels of precipitated protein in their edema fluid than survivors of the disease (Bachofen and Weibel 1977). In addition, excess protein in the alveolar compartment may contribute to hyaline membrane formation and induce fibrogenesis (Kobashi and Manabe 1993; Tomashefski 1990). Also, protein degradation products, such as

amino acids and peptides, may affect the epithelial barrier and enforce edema formation (Kim and Malik 2003). Thus, removal of excess protein from the alveolar space is fundamental for a positive outcome in ARDS.

1.3 Lung anatomy

The primary site of protein transport in the lung is the alveolo-capillary barrier, which consists of an epithelial and an endothelial monolayer, separated by a diminutive interstitial space. The alveolar epithelium contains flat type I (ATI) and cuboidal type II (ATII) pneumocytes. Although both of them are found in similar numbers in the lung (Yumoto et al. 2006), type I pneumocytes represent ~ 95 % of the alveolar surface area (Mutlu and Sznajder 2005). Since ATI cells contain transport proteins such as epithelial sodium channels and aquaporin water channels, they are actively regulating fluid balance of the lung (Johnson et al. 2002; Matthay et al. 2002). Additionally, because of the high abundance of microvesicles, ATI cells are considered to play a role in the transport of macromolecules (Gumbleton et al. 2003). ATII cells produce and secrete surfactant (Fehrenbach et al. 1998) and serve as progenitors of ATI cells (Adamson and Bowden 1975; Evans et al. 1975). Also, they have been reported to facilitate active transport of fluid and electrolytes (Mason et al. 1982).

Given that the endothelial monolayer possesses a much higher permeability, alveolar epithelial cells and their tight junctions form the primary barrier for solutes and electrolytes in the lung (Taylor and Gaar 1970).

1.4 Molecular mechanisms of protein clearance

Processes that have been associated with protein clearance from the distal air space involve mucociliary clearance, alveolar degradation and absorption of low molecular weight fragments by pneumocytes, endocytosis by alveolar macrophages and absorption by the alveolar and bronchial epithelium (Folkesson, Matthay et al. 1996).

Mucociliary clearance could move excess protein from the alveolar space up to the bronchial tree. This mechanism takes several days and does probably not play a major role in protein removal from the distal airspace, since it has been described that protein removal

takes place much faster (Berthiaume, Albertine et al. 1989). However, intratracheal instilled radio-labeled albumin has been detected in the upper airways, presenting evidence for protein movement via mucociliary clearance (Meyer, Ottaviano et al. 1977; Meyer, Ottaviano et al. 1978), even though it does barely contribute to alveolar protein clearance.

Alveolar macrophages degrade exogenous proteins and peptides (Steinman, Brodie et al. 1976), also they hold a higher endocytic capacity compared to type II pneumocytes (Hastings, Folkesson et al. 1995). Experiments have been conducted where autologous serum was instilled into sheep lungs which resulted in an increased macrophage number in the air spaces while protein clearance remained unaffected (Matthay, Berthiaume et al. 1985) in short-term experiments (1 – 2 days). In long-term studies (2 – 6 days) alveolar flood of macrophages increased massively and was linked to an increased accumulation of protein tracer in the macrophages (Berthiaume, Albertine et al. 1989). Nevertheless, the amount of ^{125}I-albumin found in the phagocytic cells was less than 1 % of the total instilled ^{125}I-albumin (Berthiaume, Albertine et al. 1989). It has been described though, that macrophages contribute to surfactant apoprotein clearance as well as to the clearance of surfactant protein A (Ueda, Ikegami et al. 1995). Still, their role in albumin clearance from the alveolar space is probably insignificant.

Another consideration regarding protein removal was protein degradation in the epithelial lining fluid (ELF) and subsequent absorption of low molecular weight fragments by pneumocytes. The most important proteases in the ELF are metallo and serine proteases (Gross 1995; Greenlee, Werb et al. 2007). Inhibition of metalloproteases by ethylenediaminetetraacetic acid (EDTA) (Chiancone, Thulin et al. 1986) and serine proteases by 4-(2-aminoethyl)-benzenesulfonyl fluoride (AEBSF) (Lunn and Sansone 1994) could be used to investigate the involvement of albumin degradation. But a number of studies have indicated that larger proteins, such as albumin, are most likely transported intact from the alveolar space to the vasculature. This was shown by determining intactness of alveolar instilled radio-labeled protein in the perfusion (Berthiaume, Albertine et al. 1989; Folkesson, Westrom et al. 1990; Folkesson, Westrom et al. 1992). Instillation of EDTA and AEBSF into the isolated, ventilated and perfused rabbit lung had no effect on ^{125}I-albumin clearance from the alveolar space, as previously reported by our group (Rummel 2007). Thus, albumin is most likely transported across the alveolar epithelium without undergoing degradation.

The alveolo-capillary barrier is impermeable to larger solutes, the epithelial monolayer features a reflection coefficient for proteins of ~ 0.95 whereas the much more permeable

capillary endothelium has a reflection coefficient of ~ 0.7 (Gorin and Stewart 1979). Alveolar epithelial type I and type II cells are linked by apical intercellular junctions, the apical junctional complex, consisting of tight junctions and adherens junctions (Gumbiner 1987). The semipermeable tight junctions control passive paracellular movement of fluid and small solutes, which in conjunction with transcellular vectorial transport creates distinct milieus in the alternate compartments. Therefore, tight junctions are important to maintain existing concentration gradients between the alveolar and the vascular compartment (Laukoetter, Bruewer et al. 2006). Adherens junctions basically consist of cadherins and catenins and are essential for intercellular adhesion (Mehta and Malik 2006). Consequently there is only minor paracellular movement of albumin across the alveolar epithelium in a healthy alveolus.

1.5 Protein uptake by alveolar epithelial cells

Active albumin transport has been described in epithelial cells of the proximal tubule of the kidney (Caruso-Neves, Kwon et al. 2005) and also in the mammary gland of lactating mice (Monks and Neville 2004). Albumin uptake by endocytosis has been well described in endothelial cells (Mehta and Malik 2006). In contrast, the mechanisms of albumin uptake by alveolar epithelial cells are incompletely comprehended, even though endocytosis is presumed to be the major process involved.

A non-specific fluid-phase uptake (macropinocytosis) can mediate endocytosis of macromolecules. The degree of uptake is proportional to the molecule concentration. Internalization of small extracellular fluid droplets by endocytic vesicles is extremely slow. Also, this process is neither saturable nor can it be affected by competitive inhibition in presence of other macromolecules (Conner and Schmid 2003). Horseradish peroxidase has been described to be taken up by alveolar epithelial cells through fluid-phase transport, but at a much lower rate as albumin (John, Vogel et al. 2001; Kim and Malik 2003). A much higher endocytosis efficiency can be obtained by receptor-mediated endocytosis involving specific high-affinity receptors (Conner and Schmid 2003). Two major receptor-mediated pathways have been established to this day, namely the caveolae-mediated and the clathrin-dependent pathway.

1.6 Caveolae-mediated endocytosis

In the endothelium, endocytosis is primarily mediated by caveolae. These 50-100 ηm small organelles form about 15 % of the total cell volume (Johansson 1979). Even though their structure is independent of the cell type, their arrangement and function may differ. They can either pass through current cycles of fission and fusion with the cell membrane or they can be statically stored in multi-caveolar structures (Pelkmans and Zerial 2005). The formation of caveolae requires caveolin-1, an integral membrane protein (Drab and Verkade et al. 2001). The involvement of another protein, caveolin-2, was implicated by Das and Lewis et al. (1999) but is controversial (Razani, Wang et al. 2002). Regulation of caveolin-1 oligomerisation, intracellular localization, as well as its sequestration to the plasma membrane is probably facilitated by several chemical reactions, such as phosphorylation, palmitoylation and contact with cellular cholesterol, which sustains structural integrity of caveolae vesicles (Sharma, Brown et al. 2004). Filipin, a cholesterol binding agent, removes cholesterol from the vesicles, thereby leading to their disassembly (Schnitzer, Oh et al. 1994). Previous studies in isolated rabbit lungs have demonstrated that filipin significantly impairs ^{125}I-albumin clearance from the distal airspace (Rummel 2007), implicating the involvement of caveolae-mediated endocytosis in protein transport across the alveolo-capillary barrier. In the context of caveolae-mediated endocytosis, gp60 has been identified as an albumin binding protein on the surface of endothelial cells (Tiruppathi, Finnegan et al. 1996; Tiruppathi, Song et al. 1997) and also in ATII cells (Hastings, Folkesson et al. 2004). In endothelial cells binding of albumin to gp60 activates specific kinases, conducting phosphorylation of caveolin-1 and inducing fission of the caveolae vesicle from the membrane. Subsequent transcytosis of albumin requires the soluble *N*-ethylmaleimide-sensitive factor attachment protein receptor (SNARE) machinery (Gerst 2003). SNARE enables fusion of the free vesicle with the target membrane and thus, facilitates exocytosis of albumin (Minshall, Tiruppathi et al. 2002).

1.7 Clathrin-dependent endocytosis

Clathrin-dependent endocytosis is induced by clathrin coat assembly on the plasma membrane followed by invagination and fission (Pearse 1976; Lin and Garbern et al. 1982) (**Figure 1**). Several adaptor proteins like adaptor protein 2 (AP-2), epsin and amphiphysin facilitate the

vesicles fission from the membrane (Wakeham, Ybe et al. 2000). Clathrin coats are the primary molecules of fluid-phase and receptor-mediated endocytosis from the membrane to early endosomes (Conner and Schmid 2003) and moreover, participate in transport mechanisms from the trans-Golgi network to late endosomes (Marsh and McMahon 1999). The formation of clathrin-coated vesicles can be averted by phenylarsine oxide, a membrane-permeable phosphotyrosine phosphatase inhibitor (Visser, Stevanovic et al. 2004). Chlorpromazine modulates AP-2 binding to the plasma membrane resulting in the loss of coated pits from the surface (Wang, Rothberg et al. 1993) and thus, just as phenylarsine oxide, impedes clathrin-dependent endocytosis.

Binding of albumin to the gp60 receptor changes the conformation of the receptor. This conformational change facilitates binding of AP-2 and clathrin to the receptor. Prior to binding to gp60, clathrin is recruited by the assembly protein AP180, epsin and amphiphysin (Marsh and McMahon 1999) as well as by epsin and amphiphysin.

Albumin transport across the endothelium is mainly induced by caveolae-mediated endocytosis (Mehta and Malik 2006). However, albumin uptake and transport across the alveolar epithelium is still under investigation. But precisely this transport mechanism is of high importance since any cumulating protein in the alveolar compartment has to transit the epithelium at first before it can trespass the endothelium. In isolated rat lungs clearance of albumin from the distal airspace was in part blocked by the caveolae-dissociating substance filipin (John, Vogel et al. 2001). On the contrary, mice lacking the caveolin-1 gene did not exhibit any dysfunctions in albumin transport (Drab and Verkade et al. 2001) even though there were no caveolae detectable. Clathrin has also been proposed to be involved in the uptake of albumin by cultured rat lung epithelial-T-antigen negative (RLE-6TN) cells (Yumoto, Nishikawa et al. 2006). This cell line is derived from rat alveolar type II cells transfected with SV40 (pRSV-T DNA) by lipofectin (Driscoll, Carter et al. 1995) and displays similar attributes as ATII cells.

Even though caveolae-mediated endocytosis seems to be involved in epithelial albumin uptake it does not appear to be the key mechanism. Therefore, the underlying mechanism for protein uptake by the alveolar epithelium requires further clarification.

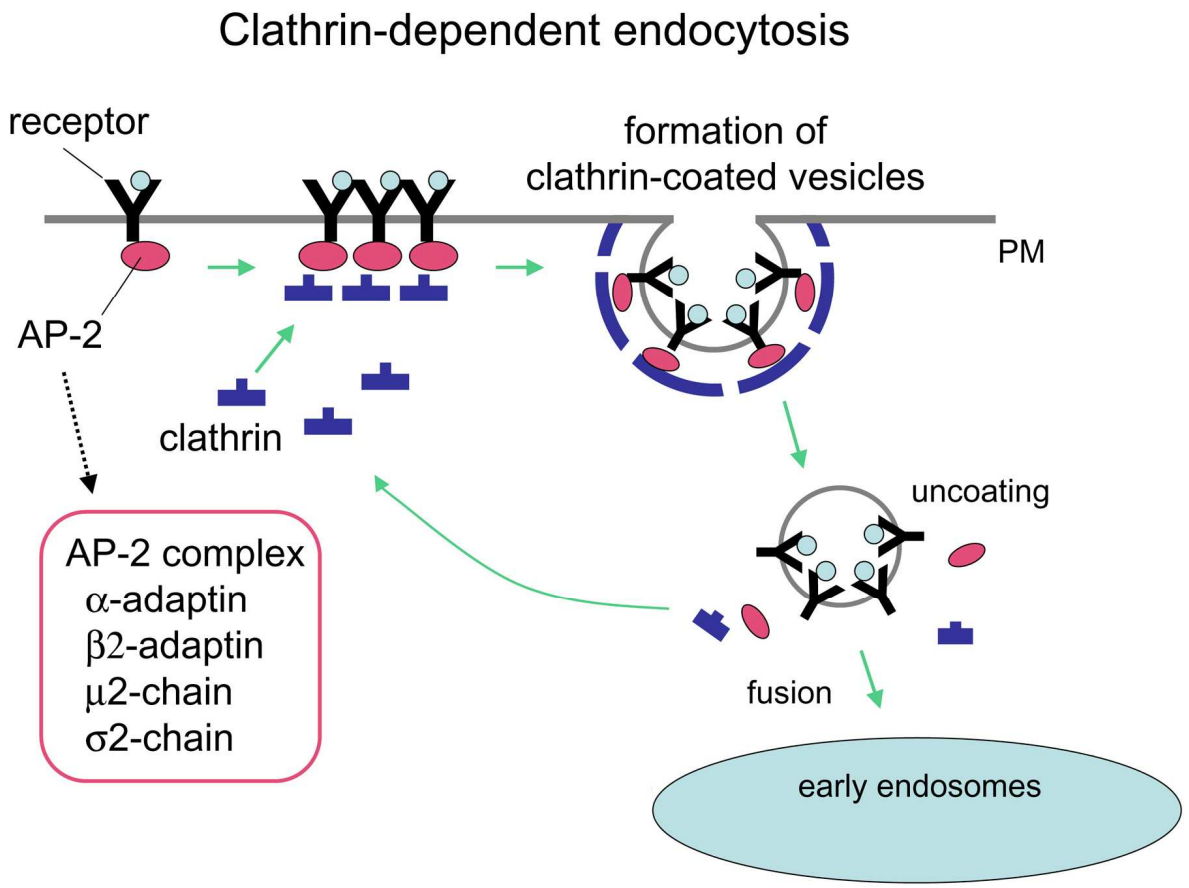

Figure 1: ***Clathrin-dependent endocytosis.***
Clathrin and target molecules are assembled into clathrin-coated pits on the plasma membrane. An adaptor complex called AP-2 links clathrin to transmembrane receptors, resulting in the formation of mature clathrin-coated vesicles which are then actively uncoated and transported to early endosomes. (Barth D. Grant and Miyuki Sato, 2006)

1.8 The tandem endocytic receptors megalin and cubilin

Megalin, a 600 kD glycoprotein, is a member of the low-density lipoprotein (LDL)-receptor family. It holds a single transmembrane domain and a large N-terminal extracellular domain. The extracellular domain is dominated by four clusters of low-density lipoprotein-receptor type A repeats that compose ligand binding regions (Saito, Pietromonaco, Loo et al. 1994). The sequences in the cytoplasmatic tail are presumed to mediate the receptors endocytosis by interaction with adaptor proteins such as ARH, Dab2 and GIPC (Saito and Sato, 2010). Additionally, the cytoplasmic tail may be involved in apical assembly of megalin and even provide signal transduction when disassociated from the membrane by γ-secretase (Willnow,

Nykjaer, Herz 1999). Megalin also interacts with intracellular adaptor proteins such as ARH, Dab2, and GIPC. Dab2 binds to motor proteins, myosin VI, and NMHC IIA, which may mediate endocytic trafficking of the molecular complexes through actin filaments. The cytoplasmic tail of megalin is released from the membrane by γ-secretase and is involved in intracellular signal transduction (Saito and Sato, 2010) (**Figure 2**).

Cubilin, is a 460 kD glycoprotein which is identical to the intestinal intrinsic factor receptor. It holds no transmembrane domain (Moestrup, Kozyraki, Kristiansen et al. 1998). Regarding its structure it has only minimal conformity to other known endocytic receptors. In addition, cubilin does not comprise any observable sites for interaction with mediators (e.g. adaptor proteins) of clathrin-dependent endocytosis. The extracellular domain is mostly determined by 27 complement subcomponents, the C1r/C1s, Uegf, and by bone morphogenic protein-1 (CUB) domains, which are assumed to contain ligand binding domains. The amino terminal region appears to facilitate attachment of cubilin to the membrane.

In the kidney, megalin and cubilin are almost exclusively expressed in the proximal tubules (Farquhar et al. 1995). But the two receptors co-localize in other tissues as well, in particular in absorptive epitheliums, as the epithelium of the small intestine (Birn et al. 2000), the visceral yolk sac as well as the placenta. Moreover, megalin is expressed in ependymal cells, epididymis, oviduct, the choroid plexus, labyrinthic cells (inner ear), alveolar type II cells, thyroid cells, the parathyroid hormone (PTH) secreting cells, the endometrium, the ciliary epithelium (eye), and embryonic tissues (Zheng et al. 1994). In comparison, the distribution of cubilin seems less extensive, even though it had been detected in the thymus (Hammad, Barth, Knaak et al. 2000) as well as in some other tissues.

1.9 Regulation of megalin

Megalins cytoplasmic tail contains numerous corresponding phosphorylation sites including four protein kinase (PK) C sites, eight casein kinase (CK) II sites and one PKA site (Saito 1994). All of these kinases are able to phosphorylate the megalin tail *in vitro*. Recent studies have shown that both CK II and PKA are not able to phosphorylate the megalin tail *in vivo* at all and that PKC, although it was able to phosphorylate megalin *in vivo*, does not play an important role in the regulation of the receptor's recycling and surface expression (Yuseff et al. 2007). Those studies identified a proline-rich region within the cytoplasmic domain,

featuring a conserved PPPSP motif. This PPPSP motif can also be found in the cytoplasmic tails of LRP5/6 and other members of the low density lipoprotein receptor (LDL-R) family (Tamai et al. 2004) and emerged to be the major determinant of the megalin receptors phosphorylation. It has been shown that this PPPSP motif represents a Glycogen synthase kinase 3 (GSK3) phosphorylation site and that activity of GSK3 is required for phosphorylation of megalin. Furthermore it has been well established that inactivation of GSK3 increases the cell surface levels of megalin by modifying its recycling efficiency and thereby, cell surface distribution (Yuseff et al. 2007).

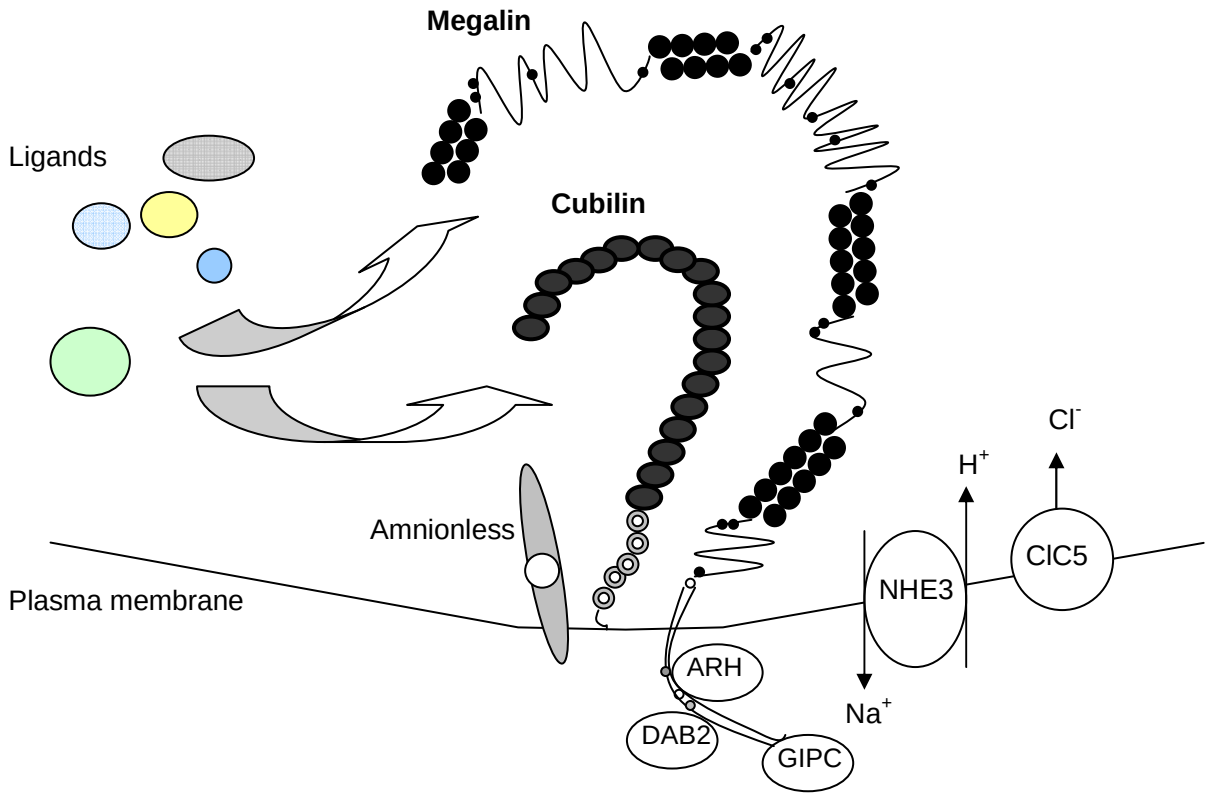

Figure 2: ***Megalin and its associated molecules in PTEC.***
Megalin interacts with the cubilin-amnionless complex (CUBAM), NHE3, and ClC5. Megalin and CUBAM directly bind numerous ligands, whereas NHE3 and ClC5 facilitate endosomal acidification in order to further process endocytosed proteins (Saito and Sato, 2010, modified) J Biomed Biotechnol. **2010**;**2010**:403272.

Glycogen synthase kinase 3 is a signaling molecule that participates in a variety of signaling pathways, including those activated by Wnts, hedgehog, growth factors, cytokines and G protein-coupled ligands (Wu and Pan 2010). GSK3 was first identified by Embi et al. in 1980. Mammals express two isoforms, GSK3 α (51 kDa) and GSK3 β (47 kDa) (Woodgett 1990).In the cell, GSK3 is constitutively phosphorylated and thereby inactivated. In order to get activated, the kinase must be dephosphorylated at Ser-21 (GSK3 α) or at Ser-9 (GSK3 β) (Cross et al. 1995). Several studies have pointed to an association of GSK3 dysregulation, particularly hyperactivation, with various pathological conditions, including diabetes mellitus, obesity, inflammation, neurological disorders and tumor development (Wada 2009; Rayasam 2009; Woodgett 2003). Thus, GSK3 inhibitors comprise an interesting group of potential therapeutics for human disease.

1.10 Albumin transcytosis throughout the alveolo-capillary barrier

After being taken up by the cell, proteins can either be transported across the cell without undergoing modifications (transcytosis) (Mehta and Malik 2006) or they can be degraded by lysosomes or proteasomes (Rivett 1990). Transcytosis is an actin-dependent process which allows the cell to move selected substances between two compartments without affecting their different compositions (Tuma and Hubbard 2003). An effective inhibitor of vesicle movement during endocytosis and transcytosis is phalloidin oleate, a membrane-permeable peptide which binds polymeric F-actin, stabilizes it and thus, impairs the function of actin-rich structures (Stenbeck and Horton 2004; Vadasz, Morty et al. 2005). In a polarized cell monolayer the molecule movement can occur from both sides (apical to basolateral or vice versa) depending on the molecule and the specific correlation of the transport process. A well established instance of transcytosis in epithelial cells is the clathrin-dependent movement of secretory immunoglobulin A (IgA) and its receptor IgA-R. IgA and IgA-R are conveyed from the basolateral to the apical cell surface (Mostov and Deitcher 1986). Comprehensive studies have been performed in Madine Darby canine kidney (MDCK) cells, describing particpation of a minimum of three cell compartments for this IgA-R transcytosis pathway. Those compartments imply basolateral early endosomes, a frequent endosome and an apical recycling endosome (Wang, Brown et al. 2000).

Another compelling inhibitor of transcytosis is monensin, an ionophore which interrupts the structure of the Golgi apparatus and thus, inhibits vesicle-mediated transport (Sakagami, Byron et al. 2002). Moreover, monensin adjusts the vesicle pH, disabling the vesicle recycling to the cell surface (Hastings, Wright et al. 1994). Albumin transcytosis has been well documented in endothelial cells. There, caveolae seem to be the determining vesicle carriers that are accountable for the transport of albumin across the cell (Mehta and Malik 2006). In contrast, it remains uncertain whether albumin transport across the epithelium is facilitated by transcytosis or if albumin is subjected to degradation.

The exact mechanisms of protein clearance from the alveolar space are incompletely understood, though removal of excess protein from the alveolar compartment is crucial for the resolution of ALI/ARDS. Determining the pathways of protein transport across alveolar epithelia cells and the alveolo-capillary barrier may eventually lead to novel therapeutic approaches and contribute to an improved outcome.

1.11 Transforming growth factor-β as mediator of ARDS

Transforming growth factor (TGF)-β is a cytokine, belonging to a family of growth and differentiation factors and holding multiple functions in a diversity of different organs (Bartram and Speer 2004). TGF-β is known for its capacity to modulate an array of cellular processes, among cell proliferation, differentiation and apoptosis (Grande 1997). Three isoforms of TGF-β are expressed, of which TGF-β1 is most abundant in general as well as most upregulated in response to tissue injury, and is most involved in the development of fibrosis (Singer and Clark 1999). Multiple cells produce TGF- β1, including epithelial cells. It is located at the cell surface as an inactive precursor. Activation can be triggered by a number of stimuli, such as plasmin, metalloproteinases (Mu 2002), reactive oxygen species, radiation and thrombospondin (Murphy-Ullrich 2000). These stimuli facilitate the binding of TGF- β1 to the integrin αvβ6, which is normally expressed at low levels but upregulated in response to injury and inflammation (Breuss 1995).

ARDS can be classified into three phases: (*i*) an early exudative phase of featuring edema and inflammation; (*ii*) a proliferative phase presenting with pneumocyte hyperplasia and proliferation of myofibroblasts; and (*iii*) a fibrotic phase implying collagen agglomeration, progressive lung fibrosis and obliteration of pulmonary microvasculature

(Tomashefski 2000). In cases of persistent inflammation fibroproliferation proceeds continuously (Pugin et al. 1999). It has recently been established that increased collagen turnover and fibroproliferation occur within 24 hours of acute lung injury (Marshall 2000). Since it is known for inducing procollagen gene expression (Kaminski 2000; Ghosh 2001) it has been proposed that TGF- β1 is a key molecule not only in the late fibroproliferative phase but also early acute injury (Fahy et al. 2003). The presence of active TGF- β1 in the bronchoalveolar lavage (BAL) fluid of patients with early ARDS (Fahy et al. 2003) implies that activation of latent TGF- β1 induces the early increase in collagen turnover. In a murine model of acute lung injury it has been demonstrated that activated TGF-β1 affected epithelial permeability and promoted pulmonary edema (Pittet et al. 2001), similar findings have been described in human ARDS patients (Fahy et al. 2003).

The role of TGF- β as a mediator of ARDS and fibrosis is well described. A correlation between pulmonary fibrosis and fatality in established cases of ARDS has already been determined (Martin et al. 1995). In fatal cases lung collagen content can increase 2- to 3-fold (Fukuda et al. 1987). The mechanism by which TGF- β affects protein clearance, thereby impairing edema resolution and recovery, remains unclear.

1.12 State of the art

Previous studies performed by our group have demonstrated that albumin clearance from the alveolar space is an active process (Rummel 2007). These studies were performed in the isolated, ventilated and perfused rabbit lung model, a well established model to investigate epithelial transport and alveolo-capillary barrier function, which has been used by several groups in the past two decades (Seeger, Walmrath et al. 1994). The isolated rabbit lung is a physiological model which enables to directly investigate alveolo-capillary barrier function in an intact *ex vivo* organ. Artificial ventilation and blood-free perfusion allow stable experimental conditions for several hours. This model allows to precisely analyze changes in alveolo-capillary barrier function in the absence of any input from the rest of the organism. Vadasz et al. (2005) employed this model to investigate the effect of thrombin on epithelial barrier function. Since involvement of the coagulation pathway was excluded due to blood-free perfusion, it has been demonstrated that thrombin directly leads to endocytosis of the Na^+,K^+-ATPase and thus, impairs edema resolution in ALI/ARDS.

To investigate protein transport across the alveolo-capillary barrier, ^{125}I-albumin was deposited to the alveolar space by ultrasonic aerosolization and tracer kinetics have been detected by real-time measurement *via* γ-detectors placed around the lungs and the perfusate reservoir. Under physiological conditions (37 °C), about 30 % of ^{125}I-albumin was cleared from the lungs by the end of the experiment. By conducting experiments at different temperatures, we established that movement of ^{125}I-albumin from the alveolar to the vascular space is a temperature-dependent process (**Figure 3**). At 4 °C the albumin transport rate has to be facilitated by passive movement, since active processes are shut down at this temperature (Rutschman, Olivera et al. 1993). Passive epithelial paracellular transport of small solutes was assessed by [^{3}H]mannitol clearance from the lung and was not affected by low temperature. These previous data established that the main proportion of ^{125}I-albumin transport was active (~88 %).

To further elucidate the characteristics of protein clearance, FITC-albumin was administered to the vasculature and the flux of FITC-albumin into the alveolar space was measured (Rummel 2007). Only 6 % of the applied FITC-albumin was detectable in the alveolar compartment of the lung. Furthermore, the same transport rate was detected when experiments were conducted at 4 °C, indicating that FITC-albumin movement was facilitated by passive paracellular transport. These data demonstrate a uni-directional transport of albumin from the alveolar space to the vasculature.

To prevent albumin from undergoing degradation, protease inhibitors were nebulized into the isolated rabbit lung. Inhibition of metallo- and serine-proteases by administration of EDTA (Chiancone, Thulin et al. 1986) and AEBSF (Lunn and Sansone 1994) had no effect on ^{125}I-albumin transport across the alveolo-capillary barrier (Rummel 2007), suggesting that albumin is taken up intact by the alveolar epithelium.

Figure 3: ***^{125}I-albumin clearance from isolated, ventilated and perfused rabbit lungs is inhibited by low temperature.***

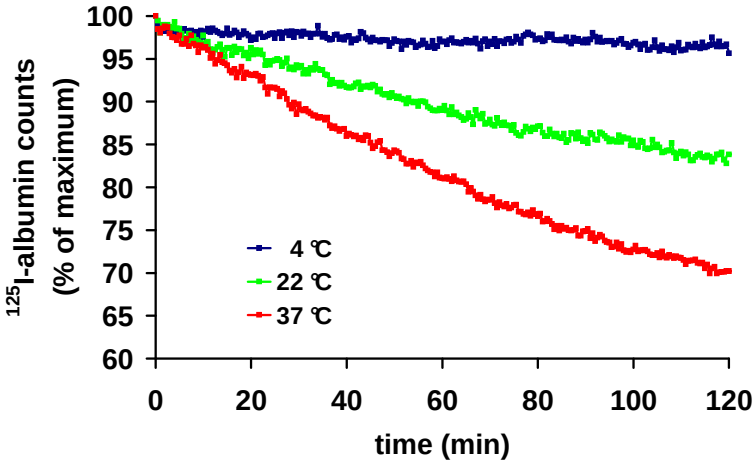

Lungs were maintained either at 37 °C (*red*), 22 °C (*green*) or 4 °C (*blue*) and ^{125}I-albumin was deposited into the alveolar space. Elimination of the tracer was monitored over 120 minutes. Counts were set at 100% immediately after nebulization of ^{125}I-albumin tracer.
(Rumel 2007).

To determine the mechanisms by which albumin was taken up by the alveolar epithelium, further experiments were performed in cultured monolayers of human epithelial cells A549 (ATCC-No.: CCL-185). This cell-line is of human adenocarcinoma origin and represents a well-characterized and excellent model system for primary alveolar epithelial type II cells. A549 monolayers were first treated with a 1000-fold molar excess of unlabeled albumin and subsequently incubated with ^{125}I-albumin to assess the effect of competition. Native albumin significantly inhibited the uptake of the radio-labeled tracer, indicating a competitive antagonistic effect (**Figure 4**). The γ-radiation that occurred in presence of native albumin was considered as binding of ^{125}I-albumin to the cell surface and therefore represents baseline condition.

Figure 4: ***Uptake of ^{125}I-albumin by human epithelial A549 cells was blocked by excess native albumin.***

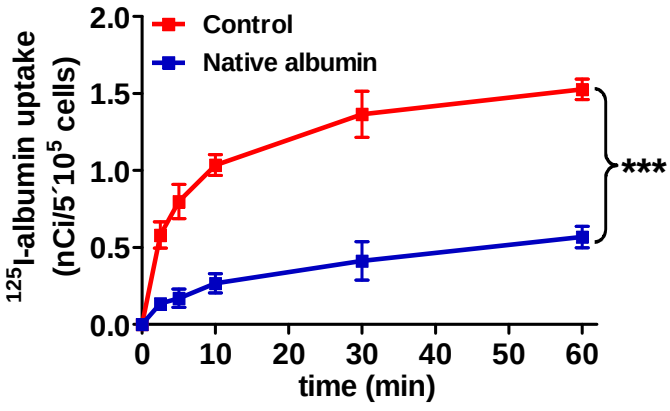

Subconfluent monolayers of A549 were pre-incubated for 30 min in absence or presence of excess native albumin. ^{125}I-albumin was applied to the cells and uptake of the radio-labeled protein was terminated after 2.5, 5, 10, 30 or 60 minutes from cellular lysates by gamma-emission counting. (n=4) ***$p < 0.001$, as compared to control.
(Rummel 2007)

These previous studies established that albumin is taken up intact by alveolar epithelial cells and transported across the alveolo-capillary barrier by an active process. However, the mechanisms by which albumin transport is undertaken have not been identified. Thus, we set out to investigate the role of clathrin-dependent endocytosis and the multi-ligand receptor megalin in the physiological significance of albumin transport. Moreover, we sought to determine the mechanisms of albumin transport in the pathophysiology of acute lung injury with regard to the role of TGF-β1.

1.13 Aims of the study

In the present study we set out to answer the following questions:

→ What are the mechanisms of albumin transport under physiological conditions?

- Is albumin transport across the alveolo-capillary barrier mediated by the multi-ligand receptor megalin *via* clathrin-dependent endocytosis?

→ What are the mechanisms of impaired albumin transport in the pathophysiology of ALI/ARDS?

- Does TGF-β1, a mediator of ALI/ARDS, affect albumin transport across the alveolo-capillary barrier?
- If albumin transport is dysregulated by TGF-β1, what are the underlying mechanisms?
- How can one interfere with the effect of TGF-β1 on albumin transport in the lung?

2. Material and Methods

2.1 Cellular experiments

To understand the mechanisms by which albumin is taken up by alveolar epithelial cells and transported across the alveolar epithelial monolayer, we conducted cellular transport studies. We isolated primary alveolar type II cells from rats and employed cultured rat lung epithelial cells (RLE-6TN; ATCC-No.: CRL-2300). The RLE-6TN (rat lung epithelial-T-antigen negative) cell line is derived from rat alveolar type II cells which were isolated from a 56 day old male F344 rat by using airway perfusion with a pronase solution. At passage 5, alveolar type II cells were transfected with SV40 (pRSV-T DNA) by lipofection. Expression of the SV40-T antigen was negative by nuclear immunostaining and by PCR, indicating these cells were derived by a spontaneous immortalization. The cell line exhibits characteristics of alveolar type II cells such as lipid-containing inclusion bodies (phosphine 3R staining and electron microscopy) and expression of cytokeratin 8 and 19. The cells do not express alkaline phosphatase activity. Also, expression of several chemotactic cytokines by RLE-6TN cells was reported to be similar to that of primary cultures of alveolar Type II cells (Driscoll et al. 1995).

2.1.1 Isolation of alveolar epithelial type II cells from rat lungs

The lungs from male Sprague Dawley (SD) rats (200–250 g) were perfused at 37 °C with

- Solution A: 0.9 % NaCl
  0.1 % glucose
  30 mM HEPES
  6 mM KCl
  0.1 mg/ml streptomycin sulfate, 0.07 mg/ml penicillin G
  0.07 mg/ml EGTA
  3 mM Na_2HPO_4
  3 mM NaH_2PO_4, pH 7.4

The lungs underwent lavage 8 to 10 times at 37 °C using

- Solution B: Solution A
  3 mM $MgSO_4$
  1.5 mM $CaCl_2$

The lungs were digested by instilling 7 – 8 ml elastase (3 U/ml in solution A) at 37 °C and incubating for 12 – 14 min. This process was repeated two times. After chopping with scissors for several times, the cell suspension was mixed with 100 mg/ml DNase I, incubated for 5 min at 37 °C with gentle rotation, and filtered through 160 and 37 mm nylon mesh once, and 15 mm nylon mesh twice. The cells were incubated in two rat IgG-coated polystyrene bacteriological 100 mm Petri dishes (1.5mg rat IgG/dish) sequentially at 37 °C, 30 min each. The unattached cells were centrifuged at 250 g for 8 min and resuspended with 10 ml

- Solution C: RPMI 1640 Medium containing
  25 mM HEPES
  1 % FBS
  100 mg/ml DNase I

at a concentration of 10 ~ 20 $\times 10^6$ cells/ml. To remove the remaining macrophages, the cells were incubated with rat IgG (40 mg/ml) at room temperature for 15 min with gentle rotation. After being washed twice with solution C, the cells were incubated with sheep anti-rat IgG magnetic beads (100 ml/rat) for 15 min at 41 °C. The beads were removed by a magnetic device. To remove leukocyte and AEC I contaminations, the cells were incubated with anti-LC (40 mg/ml) and rabbit anti-rat T1a (40 mg/ml) at 41 °C for 40 min, followed by incubation with goat anti-mouse IgG Dynabeads (100 ml/rat) and goat anti-rabbit IgG BioMags beads (500 ml/rat). After removing the beads, the resultant cells were used for the evaluation of cell yield. Subsequently, primary ATII cells were plated on permeable supports (**Figure 5**).

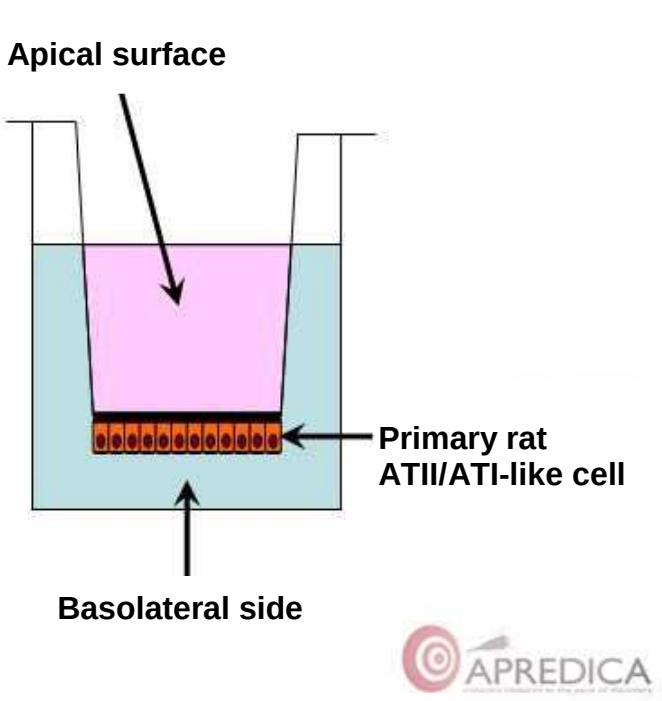

Figure 5: ***Rat primary ATII cells on permeable supports.***
After isolation, rat primary alveolar epithelial type II cells were plated on permeable supports and allowed to form tight monolayers.

2.1.2 Cell culture

Cells were incubated in a Haereus cell culture incubator (Haereus Instruments, Hanau, Germany) at a temperature of 37 °C, 80 – 90 % relative humidity and 5 % carbon dioxide in air atmosphere. Primary rat alveolar type II cells were cultured on permeable supports with a pore size of 0.4 µm (BD Falcon cell culture inserts; Fisher scientific GmbH) for six well tissue culture plates (Cellstar; Greiner Bio-One, Frickenhausen, Germany) in RPMI 1640 Medium containing 25 mM HEPES, 1 % FBS and 100 mg/ml DNase I, medium was changed every other day and cells were used for experiments on day four and day seven. RLE-6TN cells were cultured in

- Culture medium: Dulbecco´s modified Eagle´s medium/Ham's F12 medium ((DMEM/F12; GIBCO, Invitrogen, Karlsruhe, Germany)
  1 % [vol/vol] glutamine
  1 % [vol/vol] penicillin/streptomycin (both from PAN-Biotech, Aidenbach, Germany)

10 % [vol/vol] fetal calf serum (FCS; PAA Laboratories, Egelsbach, Germany)

in a 75 cm^2 tissue culture flasks (Cellstar; Greiner Bio-One, Frickenhausen, Germany). For subculturing, culture medium was removed and cells were rinsed in DPBS twice before adding 2ml of 0.25 % trypsin-EDTA (PAN-Biotech, Aidenbach, Germany) and incubating the cells for another 5 min to enhance cell detachment. To achieve full cell detachment, cells were resuspended in medium containing 1.5 ml fetal calf serum (FCS) and 5 ml DMEM/F12 and the suspended cells were transferred to a 15 ml tube (BD Bioscience, Heidelberg, Germany) and centrifuged in a Rotina 46 R centrifuge (Hettich, Kirchlengern, Germany) at 1200 revolution per minute at 15 °C for 10 min. The supernatant was discarded and the cell pellet was resuspended in culture medium and cells were seeded in a ratio 1:10 in 75 cm^2 tissue culture flasks for further subculturing. For experiments cells of passage 5 to 12 were employed and plated on permeable supports or cover slips, cells used for experiments at day two.

2.1.3 Protocol of cellular experiments

Primary rat alveolar epithelial cells were either used on day three as alveolar epithelial type II cells (ATII cells) or on day seven as alveolar epithelial type I-like cells (ATI-like cells). To assess the tightness of the cell monolayer on the permeable support transepithelial electrical resistance was measured and only monolayers presenting with a resistance of > 1500 Ω/ cm^2 were used for experiments.

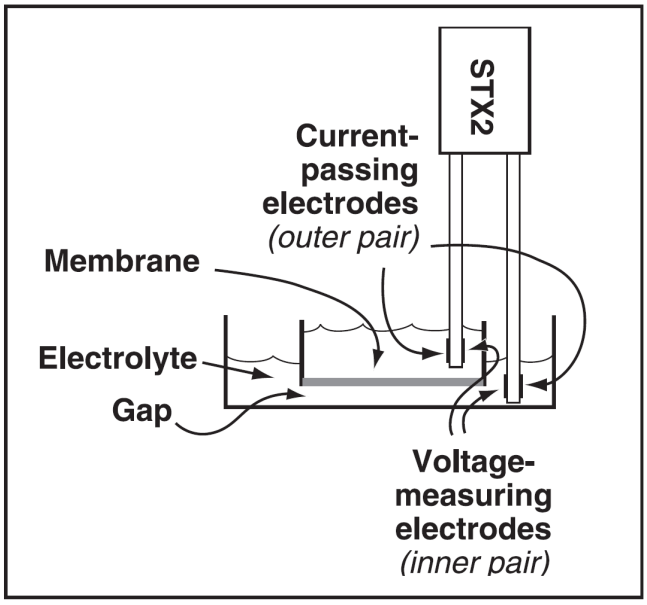

Figure 6: ***Transepithelial electrical resistance measurement.***
Tightness of the cell monolayers was assessed by transepithelial electrical resistance measurement. Only monolayers presenting with a resistance of > 1500 Ω/ cm^2 were used for experiments.

Media was removed from the cell culture plates and the permeable supports. Then cell layers were rinsed briefly with

- DPBS-G: Dulbecco's phosphate buffered saline (DPBS; PAN Biotech, Aidenbach, Germany)
  0.1 mM $CaCl_2$ dihydrate (Calbiochem, San Diego, USA)
  0.5 mM $MgCl_2$ $6H_2O$ (Sigma, St. Louis, USA)
  5mM glucose (Sigma, St. Louis, USA)

Cells were then pre-incubated for 10 min with 1.4 ml of DPBS-G followed by a pre-incubation with pharmacological agents or their vehicles. Applied agents and details of treatments are described in **Table I**. After treatment of the cells with these substances, 100 µl of DPBS-G containing ^{125}I-albumin was applied to the cells in presence or absence of the prior mentioned agents. To assess transepithelial transport of ^{125}I-albumin buffer samples were taken from the basolateral side of the permeable support after 30 min. Then experiments were terminated by aspiration of the medium and addition of ice-cold DPBS. The cell layers

were washed thoroughly with ice-cold DPBS to remove any residual tracer from the surface. Afterwards cells were incubated with a

- Solution X: DPBS-G
  0.5 mg/ml trypsin
  0.5 mg/ml proteinase K
  0.5 mM ethylenediaminetetraacetic acid (EDTA)

In order to lift them from the permeable supports (EDTA-trypsin) and to dissolve ^{125}I-albumin bound to the cell surface (proteinase K). This solution was spun down in a centrifuge to separate surface bound ^{125}I-albumin from ^{125}I-albumin which was taken up by the cells. Samples were collected to asses binding, uptake and transepithelial transport of ^{125}I-albumin and quantified by γ-emission counting in a Packard γ-counter (Packard, Dreieich, Germany).

Table I: ***Chemical agents applied in cellular experiments.***

Application	Agent	Vehicle	Concentration
Competitor	**BSA**	PBS	20 mg/ml
Competitor	**RAP**	H2O	1 μM
Transforming Growth Factor	**recombinant human TGF-β1**	4mM HCL 1mg/ml BSA	1 μg/ml
Inhibitor	**SB 216763**	DMSO	30 μM
serine protease	**Proteinase K**	PBS	0,5 mg/ml
serine protease	**Trypsin**		0,5 mg/ml
metallo proteinase inhibitor	**EDTA**		0,5 mM

2.1.4 Assessment of cell viability

Cell viability was assessed by the Trypan Blue exclusion dye method (Perry, Epstein et al. 1979). Cells were plated on permeable supports as described before and viability of control cells and those exposed to drugs or their vehicles was assessed by adding 50 µl of Trypan Blue solution (0.4 % [mass/vol] Trypan Blue in PBS) to the culture medium. After 1-2 min the number of dead cells, retaining in the dye, was compared to the total number to calculate mortality percentage.

2.1.5 Western blot analysis

Cells were cultured in six well tissue culture plates, and treated with the drug or reagent at the concentrations and time courses stated. At the end of treatment, cells were washed with phosphate-buffered saline (PBS) and treated with an

- Cell lysis buffer: 50 mM Tris-HCl, pH 7.4
  1 % Nonidet P-40
  0.25 % sodium deoxycholate
  150 mM NaCl
  1 mM EDTA
  1 mM phenylmethanesulfonyl fluoride
  1 mM sodium orthovanadate (Na_3VO_4)
  0.1 mM dithiothreitol
  0.4 g/ml leupeptin and pepstatin.

After incubating the cells in lysis buffer for 10 minutes they were scraped from the plates and the cell extract was stored at -20 °C until required. Protein samples were subjected to electrophoresis in 10 % SDS-polyacrylamide gel. Separated proteins were electroblotted to PVDF membranes and the blot was blocked for 1 h at room temperature with

- Blocking solution: 0.1 % TBST
  5 % fat-free dried milk powder.

The blot was then incubated with a primary antibody (1:2000 dilution) at 4 °C overnight. The blot was washed three times for 10 minutes with 0.1 % TBST and incubated with a horseradish peroxidase-conjugated (HPR-conjugated) secondary antibody (1:2000 dilution with 5% fat-free dried milk in 0.1 % TBST, blocking solution) for 1 h. The blot was washed again three times for 10 minutes and then incubated with ECL Western blotting detection reagent (GE Healthcare). If stripping was required the following procedure was carried out; the membrane was incubated in

- Stripping buffer: 100 mM 2-mercaptoethanol
  2 % SDS
  62.5 mM Tris-HCl, pH 6.8

at 50 °C for 30 min with occasional agitation, followed by washing the membrane in a large volume of 0.1 % TBST and blocking of the membrane for 1 h in blocking solution at room temperature. The antibodies used were as follows: rabbit polyclonal anti-rat p-GSK3-α/β, S21/9 (catalog number 9331; Cell Signaling Technologies**);** rabbit polyclonal anti-rat GSK-α/β (catalog number 5676; Cell Signaling Technologies**)**; rabbit polyclonal anti-rat megalin (H-245) (catalog number 25470; Santa Cruz biotechnology); goat anti rabbit IgG (catalog number 7074; Cell Signaling Technologies) (**Table II**). Bands were analized by density measurement in ImageJ.

2.1.6 Fluorescence microscopy

Cells were plated on cover slips and prepared for fluorescence microscopy at day three or day seven. Medium was aspirated and replaced with DPBS-G, after 10 min of pre-incubation, pharmacological agents were applied and subsequently 50 µg/ml albumin-fluorescein isothiocyanate conjugate (FITC-albumin) (catalog number 9771; Sigma Aldrich) was added to the cells. After 30 min, cover slips were washed thoroughly with ice-cold PBS for several times and cells were fixed by adding a 1:1 mixture of acetone/methanol for 10 min at -20 °C. After washing the cover slips three times they were blocked in Tris-buffered Saline containing 0.1 % of Tween 20 (TBST washing buffer) and 4 % bovine serum albumin (BSA) for 30 min at room temperature. Cover slips were then incubated overnight at 4 °C in rabbit polyclonal anti-rat megalin (H-245) (catalog number 25470; Santa Cruz biotechnology) in a 1:10 dilution

in blocking solution. The next day cover slips were washed with 0.1 % TBST and incubated in polyclonal donkey anti-rabbit cy3-conjugate secondary antibody (catalog number AP182C; Millipore) in a 1:100 dilution in blocking solution (**Table II**). Nuclei were stained with 4',6-diamidino-2-phenylindole (DAPI) (catalog number D21490; invitrogen), a nucleic acid stain, and cover slips were plated on glass slides with fluorescent mounting medium (catalog number 3023; Dako). Analysis was undertaken by using a fluorescence microscope (Leica DMLA Q550/W; Leica Microsystems), a digital camera (DC 300 FX; Leica Microsystems) and software (Q-Win; Leica Microsystems). Uptake of FITC-albumin was detected by density measurement *via* microscopic software (Q-Win; Leica Microsystems).

Table II: Antibodies used for western blot analysis and fluorescence microscopy

Antibodies	Source	Application	Dilution
megalin (H-245)	rabbit polyclonal IgG	WB, IF	1: 100
Phospho-GSK-3α/β (Ser21/9)	rabbit polyclonal IgG	WB	1 : 2000
GSK-3α/β (D75D3) XP™	rabbit monoclonal IgG	WB	1 : 2000
anti-rabbit IgG HRP-conjugated	goat polyclonal IgG	WB	1 : 1000
anti-rabbit IgG (cy3-conjugate)	donkey polyclonal IgG	IF	1 : 100

2.1.7 RNA interference of megalin

RLE-6TN cells were plated on permeable supports or cover slips and cultured until they were 40 – 60 % confluent. Medium was removed and cells were incubated in 2 ml of DMEM/F12 without any supplements. Rat megalin siRNA (catalog number 108041, Santa Cruz Biotechnology) consisted of three target-specific 19- to 25-nt siRNAs and the siRNA negative control contained a scrambled sequence (siRNA-A, catalog number 37007; Santa Cruz Biotechnology) and a cy3 labeled negative control was used as transfection control (Silencer

cy3 labeled negative control, catalog number AM 4621, Ambion). The siRNA-transfection reagent complexes, consisting of 6 µl Rat megalin siRNA (catalog number 108041, Santa Cruz Biotechnology) and 6 µl RNAi max lipofectamine (catalog number 56531; invitrogen) in DMEM/F12 were incubated for 30 min at room temperature and subsequently added to the washed cells. Cells were incubated in normal cell culture conditions for 6 h, and then fresh normal growth medium containing 10 % FCS but no antibiotics was added to maximize cell growth and prevent potential cytotoxicity. After 24 h of transfection cells were used to assess albumin uptake.

2.2 The isolated, ventilated and perfused rabbit lung model

For physiological trials the isolated, ventilated and perfused rabbit lung model was used. This model is well established for pulmonary research and has been expansively used by our group and others in the past twenty years (Seeger, Walmrath et al. 1994). This model permitted us to explore alveolar epithelial barrier function in an intact *ex vivo* organ. Due to artificial ventilation and blood-free perfusion experiments could be performed under stable conditions for several hours which enabled us to directly monitor changes in alveolo-capillary barrier function lacking any contribution from the rest of the organism. A graphic description of the isolated, ventilated and perfused rabbit lung model is illustrated in **Figure 7**.

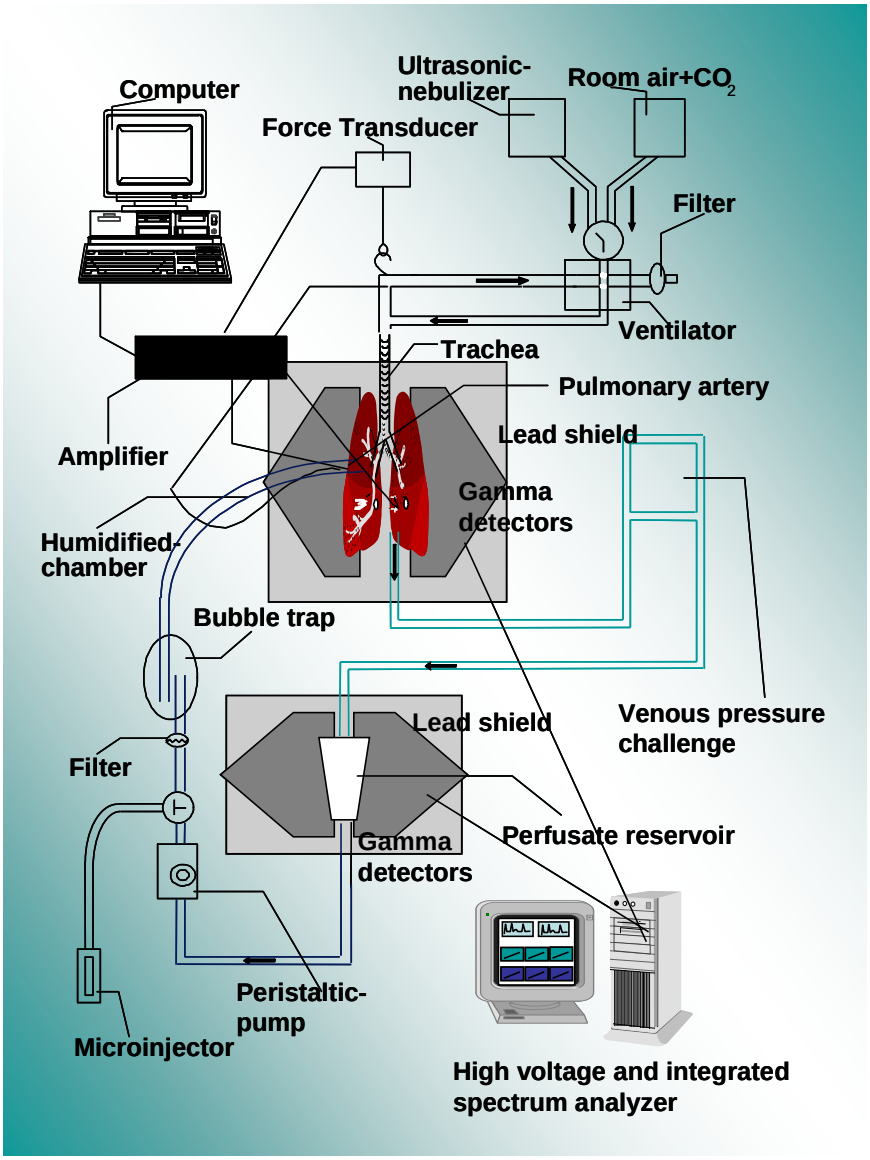

Figure 7: ***Schematic depicture of the isolated, ventilated and perfused rabbit lung model***
This scheme shows the isolated lung on a force transducer. Artificial respiration is illustrated by a schematic assembly of the ventilation circuit (including ventilator, nebulizer and air reservoir). The perfusion of the organ is driven by a peristaltic pump. Lungs and perfusate reservoir are surrounded by gamma detectors. Data are processed by a personal computer while the high voltage supply is delivered from a separate personal computer with an integrated power support.

2.2.1 Isolation of the rabbit lung and incorporation into perfusate and ventilation circuit

Lungs were isolated from adult male rabbits (New Zealand White, Charles River, Sulzfeld, Germany) weighing 3.0 ± 0.5 kg. An initial bolus of approximately 0.3 – 0.5 ml of a mixture of xylazine (Rompun 20 mg/ml; Bayer) and ketamine (Ketavet 100 mg/ml; Pfizer) in a ratio of 3:2 was administered intravenously. Also 1000 IU/kg heparin (Sodium heparin-25,000-ratiopharm, Ratiopharm) was applied for anticoagulation. Another 1 ml of anesthetics was administered progressively during a period of three minutes to ensure adequate anesthesia while still allowing spontaneous breathing. Animals were brought in a supine position. About 8 – 10 ml lidocaine (Xylocain 2 %, 20 mg/ml; AstraZeneca) were applied subcutaneously into the ventral area of the neck for local anesthesia of skin and tissue. After a median incision from chin to cranial thorax the trachea was uncovered by blunt dissection and partially transected, and a tracheal cannula with an inner diameter of 2 mm was inserted. Thereafter, animals were artificially ventilated with room air. Another median incision from the cranial thorax to the caudal end of the thorax including a small part of the upper abdomen and a mid-sternal thoracotomy were performed after the xyphoid process was fixed by a clamp and the diaphragm was dissected. To expose the heart and the ascendant aorta and the pulmonary trunk, parts of the parietal pleura, the thymus and a part of the pericardium were removed and the apex of the heart was clamped. A movable thread was placed around the aorta and the pulmonary artery; a bolus of 3 ml ketamine/xylazine was applied intravenously and an incision in the upper right ventricle was performed. A fluid-filled catheter of an inner diameter of 3 mm was inserted into the pulmonary artery through the opening in the upper right ventricle and fixed with a thread loop. The left atrium was opened by removing the apex of the heart and the descendent aorta was ligated. Through the pulmonary artery catheter, the lungs were perfused with a blood-free buffer which had a temperature of 4 °C at a perfusion rate of 15 ml/min. The lungs, trachea and heart were excised *en bloc* from the thorax. The mitral valves and the *chordae tendinae* were removed from the heart and another perfusion catheter with an inner diameter of 4 mm was placed into the left atrium via the left ventricle. The second catheter was fixed by using a tobacco pouch suture (Mersilene; Ethicon) in a way that allowed no leakage from the catheterization sites and no obstruction of the pulmonary circulation. At least 1 l of buffer was perfused through the lungs to remove blood from the system. After closure of the perfusion circuit for recirculation the perfusion rate was slowly

increased from 15 to 100 ml/h. At the same time, temperature was increased from 4 °C to 37 °C.

2.2.2 Artificial ventilation

After intratracheal intubation of the rabbit, spontaneous respiration was replaced with artificial ventilation with room air. A Harvard cat/rabbit ventilator (Hugo Sachs Elektronik) was used to facilitate steady gas exchange under deep anesthesia. After the lungs were isolated from the organism, room-air was supplemented with 4.5 % CO_2 to preserve the pH of the recirculating buffer among 7.37 – 7.37. The *ex vivo* lungs were ventilated with a ventilation rate of 30 breaths/minute, plateau pressure was set at 7.5 mmHg (0 mmHg was referenced at the hilum of the lungs) and a ratio of 1:1 referring to the ratio of inspiration to expiration was used to hold up regular ventilation. Furthermore, positive end-expiratory pressure (PEEP) was set at 2 mmHg to avoid atelectasis, altogether resulting in a tidal volume of about 6 ml/kg body weight which is considered lung protective (ARDSNet 2000).

2.2.3 Perfusion of the isolated lungs

A Krebs-Henseleit buffer (Elektrolytlösung IIN; Serag-Wiessner, Naila, Germany) containing 120 mM NaCl, 4.3 mKCl, 1.1 mM Ka_2PO_4, 2.4 mM $CaCl_2$, 1.3 mM magnesium phosphate, 0.24 % [mass/vol] glucose and 5 % [mass/vol] hydroxyethylamylopectin (for plasma expandation) was used to perfuse the lungs. About 25 ml $NaHCO_3$ (Nabic 8.4 %, Braun) was added to the buffer to preserve a pH of 7.35 – 7.37. The use of two independent reservoirs allowed a perfusate change from one reservoir to the other without interrupting the circulation. The flow of the perfusate was provided by a pump (Masterflex 7518-10; Cole Parmer) at a flow rate of 100 ml/min. After crossing the pulmonary artery and perfusing the lungs, the perfusate departed through a catheter placed in the left atrium to the “venous” part of the circulation. To attune the left atrial pressure (LAP) a catheter was positioned in the venous part of the system above the lung hilum. To keep the temperature of the perfusate at 37 °C, a thermostat-controlled water bath (Thermo-Frigomix Braun) and a tube coil dipped into an additional 37 °C water bath were installed. To monitor the pulmonary arterial pressure (PAP), a pressure sensor was situated into the pulmonary artery, and an additional pressure

sensor into the left atrium to measure LAP. As well, a filter of 0.2 μm mesh size (Pall Cardioplegia; Terumo) was positioned into the circulation system to elute residual cells or pyrogenic aggregates. After the desired flow rate of 100 ml/min was reached and the temperature was increased up to 37 °C, the filter system was detached and the buffer was recirculated to perfuse the lungs and heart. The recirculating buffer had a volume of 300 ml. After the preparation was completed and the lungs were freely balanced from a force transducer LAP was set at 2 mmHg. All through the experiment, a bubble trap was installed into the perfusion system to avoid air embolisms in the circulation.

2.2.4 Nebulization

To deliver Substances to the alveolar compartment of the lung an ultrasonic nebulizer (Optineb, NEBU-TEC) was incorporated into the inspiration loop of the ventilator. To avoid any contamination of the environment filters (Iso-Gard Filter S; Hudson) were installed in the outlet of the inspiration and expiration loop. Measurements of the mass median aerodynamic diameter assessed an average particle size of 3.2 μm for aerosolized substances. Throughout a 10 minute aerosolization period an amount of 1.6 – 1.8 ml of aerosol was produced, and a fraction (~ 60 %) of this aerosol (~ 1 ml) was deposited into the alveolar compartment of the lung.

2.2.5 Radio-labeled Tracers

^{125}I-bovine serum albumin (Perkin Elmer) was applied to detect protein transport in the lungs. The specific activity of the radio-labeled albumin was 3 μCi/μg protein and about 6μCi (~ 2μg) of albumin was deposited into the alveolar space during 10 min of ultrasonic nebulization. And about 12 μCi of [^{3}H]mannitol (Perkin Elmer) was nebulized to detect paracellular transport of small solutes.

2.2.6 Measurement of Tracer Exchange

Four Gamma-detectors (Target System Electronic), two of them placed around the lungs and two around the perfusate reservoir, were used to detect ^{125}I-albumin. They were linked to an automated high-voltage power supply which was incorporated into a personal computer system with data processing. This system allowed monitoring of ^{125}I-albumin movement in real-time. The [^{3}H]mannitol tracer kinetics were determined by sampling circulating perfusate at 0, 5, 10, 20, 40, 80, 120 min after nebulization and was subsequently quantified by scintillation counting in a Canberra β-counter (Packard).

2.2.7 Calculation of Tracer kinetics

Gamma emission of ^{125}I-albumin was recorded by gamma-detectors every 30 s over the entire time-course of the experiment. The starting point of a tracer clearance measurement was set at the end of tracer nebulization. At this time point the amount of radiation in the lungs was referenced to 100 % whereas the amount of radiation in the perfusate reservoir was referenced to 0 %. Measurement of the area above the curve (AAC) was used to calculate the clearance rate from the lungs and transit into the perfusate by the following equation:

$$AAC = [(100-A) \times T] - \{[- (100-A) / e] \times [1 – \exp (e \times T)]\}$$

2.2.8 Monitoring parameters

Catheters placed in the expiration loop of the ventilator, the left atrium and the pulmonary artery were used to detect ventilation pressure (VP), left atrial pressure (LAP) and pulmonary artery pressure (PAP). To digitalize this signals an electromechanical pressure converter (Combitrans, Braun) was installed. The weight of the *ex vivo* organ was measured and monitored by a force transducer. Analog signals were amplified and converted to digital signals and the PlotIT 3.1 software (Scientific Programming Enterprises, SPE, USA) allowed an on-line graphical demonstration of LAP, PAP, VP and weight on a personal computer.

2.2.9 Experimental protocol in the isolated lung

After the perfusion rate was set to its final flow rate of 100 ml/min and the temperature reached the physiological condition of 37 °C, we waited 30 minutes to establish a steady state condition. When all monitoring parameters remained constant, we nebulized either 0.5 ml of NaCl (vehicle) or 10 ηg of TGF-β1 (diluted in NaCl) into the lung which resulted in a transient weight gain. After 30 minutes, when baseline conditions were re-established, we aerosolized radiolabeled albumin to the alveolar compartment. About 1 ml of fluid containing ^{125}I-albumin was deposited to the alveolar space, resulting in a weight gain of ~ 1 g. The movement of the radio-labeled albumin from the alveolar to the vascular compartment was detected by γ-counters for 120 minutes.

2.3 Statistical analysis of data

Numerical are given as mean ± standard deviation (SD). Comparisons between two groups were made using an unpaired, two tailed Student's *t-test*. Intergroup differences of three or more experimental groups were assessed by using a one-way analysis of variance (ANOVA) with *post hoc* Newman-Keuls multiple comparison test or Dunnett-test, when values were only compared to controls. Statistical significance was defined as $p < 0.05$. GraphPad Prism 5 for Windows software (GraphPad Software; San Diego, USA) was used for data plotting and statistical analysis.

3. Results

3.1 Mechanisms of albumin transport in physiology

3.1.1 Transport of albumin across the alveolar epithelium is an active process

In our studies we were employing primary rat alveolar type II and type I-like cells. From our previous studies, which were conducted in the isolated rabbit lung and in A549 cells, we know that a 1000fold molar excess of native albumin (BSA) almost completely blocked labeled albumin uptake *via* competitive inhibition. To ensure same baseline conditions in primary epithelial cells, we used fluorescence microscopy to detect FITC-albumin uptake by density measurement. We employed both ATII and ATI-like cells to investigate their contribution to albumin uptake separately. After viability of the epithelial cells was assessed by phase-contrast microscopy (data not shown), we detected fluorescence in the cell. Pre-incubation of the primary cells with native albumin resulted in significant inhibition of FITC-albumin uptake in ATII cells (decreased by 72.47 ± 4.56 %) (**Figure 8**) and in ATI-like cells (decreased by 74.02 ± 3.50 %) (**Figure 9**). These data not only demonstrate an active uptake of albumin in alveolar epithelial cells, but an involvement of both major cell types in the alveolar epithelium.

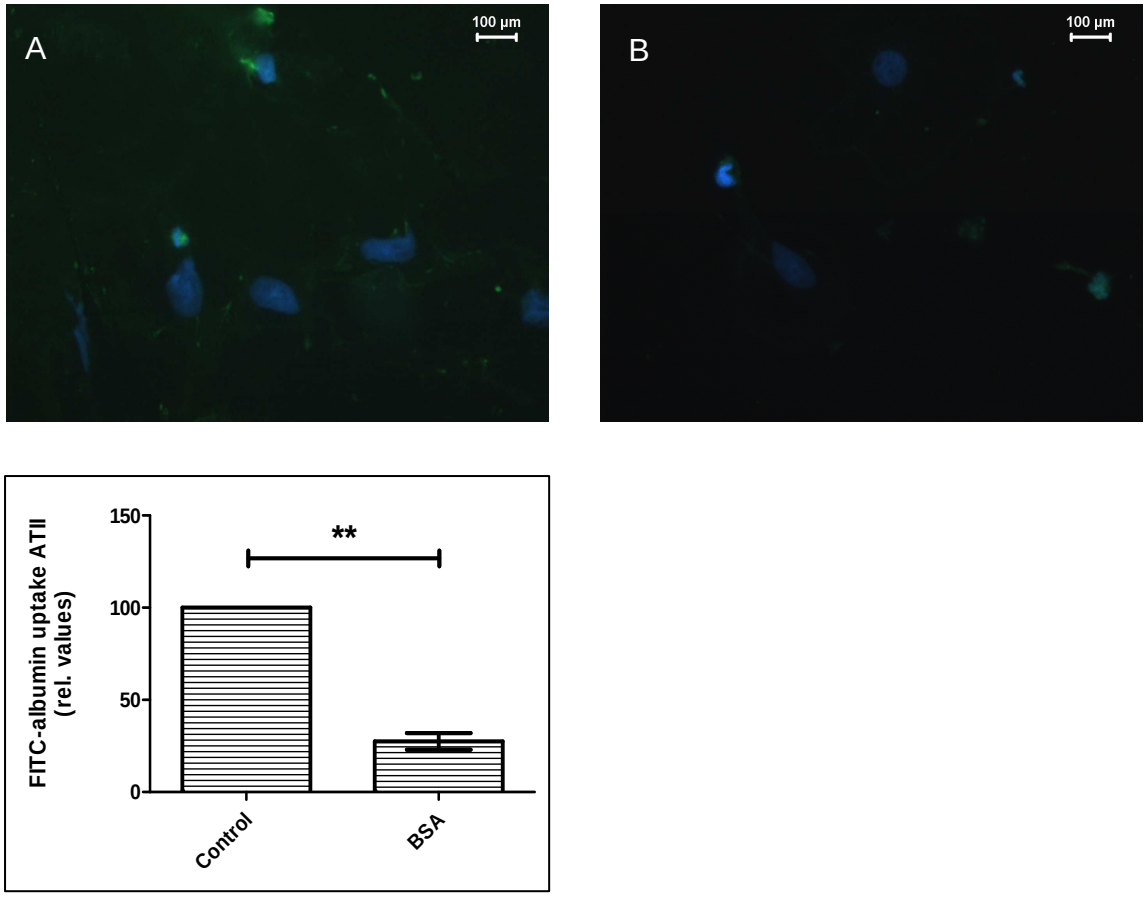

Figure 8: ***Uptake of FITC-albumin by primary rat alveolar epithelial type II (ATII) cells is blocked by excess native albumin.***
ATII cells were plated on cover slips and used for experiments on day 3. Cells were pre-incubated for 30 min in absence (A) or presence (B) of a 1000fold molar excess of native albumin prior to incubation with 50µg/ml of FITC-albumin. FITC-albumin uptake was assessed *via* density measurement. ***p<0.01; n=3.*

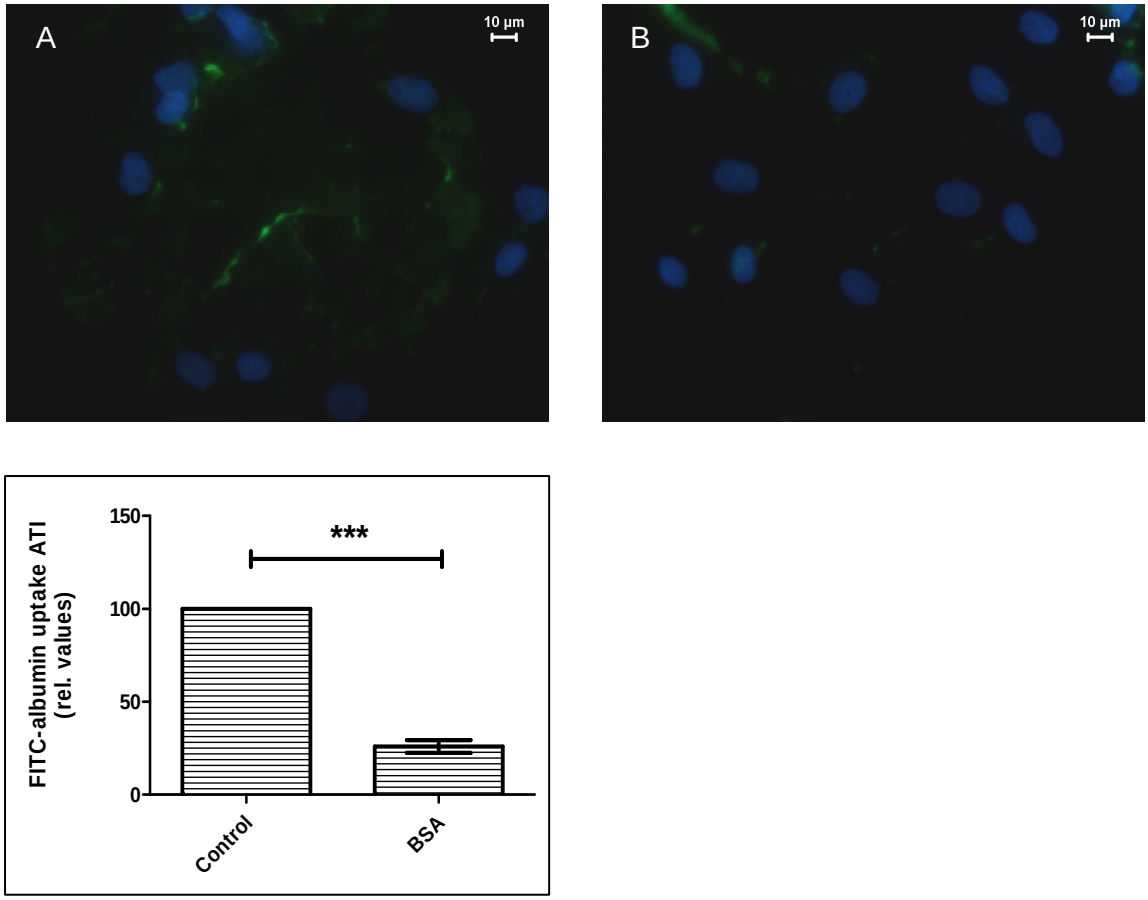

Figure 9: ***Uptake of FITC-albumin by primary rat alveolar epithelial type I-like (ATI) cells is blocked by excess native albumin.***
ATI cells were plated on cover slips and used for experiments on day 7. Cells were pre-incubated for 30 min in absence (A) or presence (B) of excess native albumin prior to incubation with 50 µg/ml of FITC-albumin for another 30 min. FITC-albumin uptake was assessed by density measurement. ****p<0.001; n=3.*

Former studies in the isolated rabbit lung (Rummel 2007), in which the membrane-permeable inhibitor of actin cytoskeletal rearrangement and thus transcytosis, phalloidin oleate (Stenbeck and Horton 2004) was pre-nebulized into the alveolar compartment, have shown significant inhibition of the active transport rate of ^{125}I-albumin. Another potent inhibitor of transcytosis, monensin (Sakagami, Byron et al. 2002) had the same effect on ^{125}I-albumin transport across the alveolo-capillary barrier, suggesting that transcellular trafficking is involved in albumin clearance from the distal air spaces (Rummel 2007). Since fluorescence microscopy is not completely objective, we additionally employed cellular transport studies, which is a more reliable quantifying method due to detection of γ-radiation. Thus, we set out to investigate the specific mechanisms of albumin clearance by conducting cellular transport studies. Cells were plated on permeable supports and allowed to form a tight

monolayer as described in “Material and Methods”. Again, cells were used for experiments either on day 3 (ATII) or day 7 (ATI) after isolation. After pre-treatment with a 1000-fold molar excess of unlabeled albumin for 30 minutes, ^{125}I-albumin was applied to the cells for antother 30 minutes. In detail, we sought to investigate the effect of excess native albumin on ^{125}I-albumin cell surface binding, ^{125}I-albumin uptake by epithelial cells and transepithelial transport across the epithelial monolayer. A mixture of proteinase K and trypsin/EDTA was used for detachment of the cells from the permeable supports and to dissolve labeled albumin which was bound to the cell surface of ATII and ATI-like cells. By centrifugation we separated surface bound albumin from albumin which was taken up by the cells. In presence of a 100fold molar excess native albumin the binding of ^{125}I-albumin to the epithelial cell surface was decreased by 71.4 ± 11.2 % in ATII cells and by similar amount in ATI-like cells (**Figure 10**).

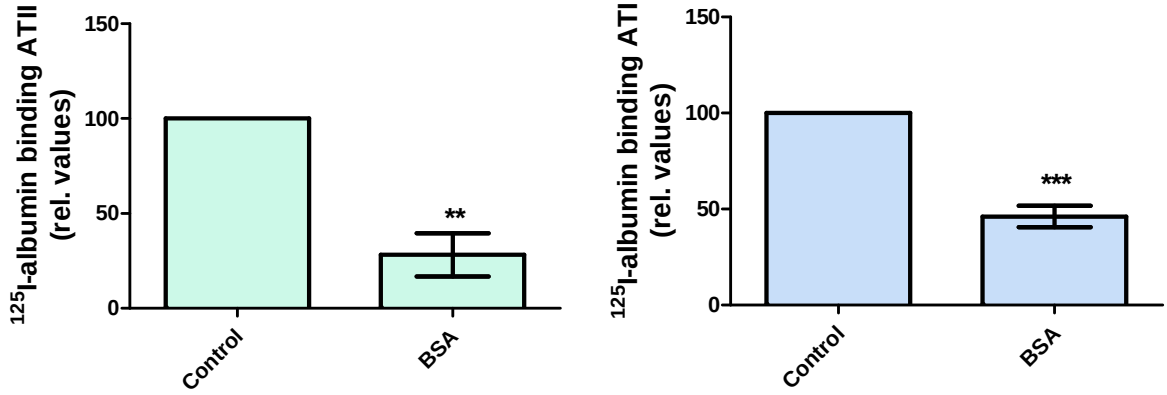

Figure 10: ***Binding of ^{125}I-albumin to primary rat alveolar epithelial type II (ATII) and type I-like (ATI) cells was strongly inhibited by excess native albumin.***
ATII cells were used for experiments on day 3 (ATII) or day 7 (ATI). Cells were pre-incubated in presence of excess native albumin and subsequently incubated with ^{125}I-albumin for another 30 min. The amount of surface bound ^{125}I-albumin was assessed by detection of γ-radiation. ****p<0.001; **p<0.01; n=4.*

After treatment of the epithelial cell monolayers with excess unlabeled albumin, uptake of ^{125}I-albumin by the cells was impaired by 92.8 ± 2.4 % in ATII cells and by 91.8 ± 2.0 % in ATI-like cells (**Figure 11**).

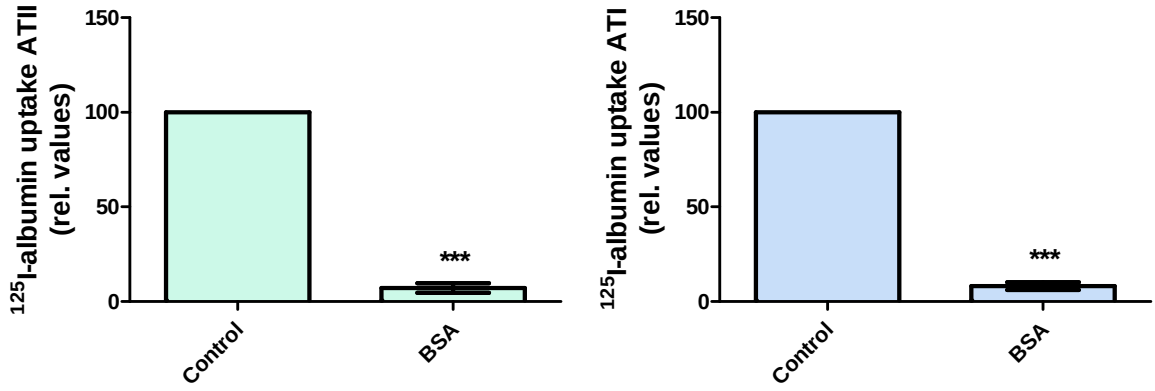

Figure 11: ***Uptake of ^{125}I-albumin by primary rat alveolar epithelial type II (ATII) and type I-like (ATI) cells is blocked by excess native albumin.***
Uptake of ^{125}I-albumin in absence or presence of excess unlabeled albumin was detected by γ-radiation. ****p<0.001; n=4.*

Transepithelial transport of ^{125}I-albumin, as assessed by taken samples from the basolateral side of the permeable supports, was significantly decreased after pre-incubation with an excess amount of cold albumin. Transepithelial movement was decelerated by 77.6 ± 4.8 % in ATII cells and by 67.5 ± 15.2 % in ATI-like cells (**Figure 12**). These data demonstrate that albumin uptake by alveolar epithelial cells as well as transepithelial transport across the alveolar epithelium is an active process which takes place in both alveolar epithelial cell types.

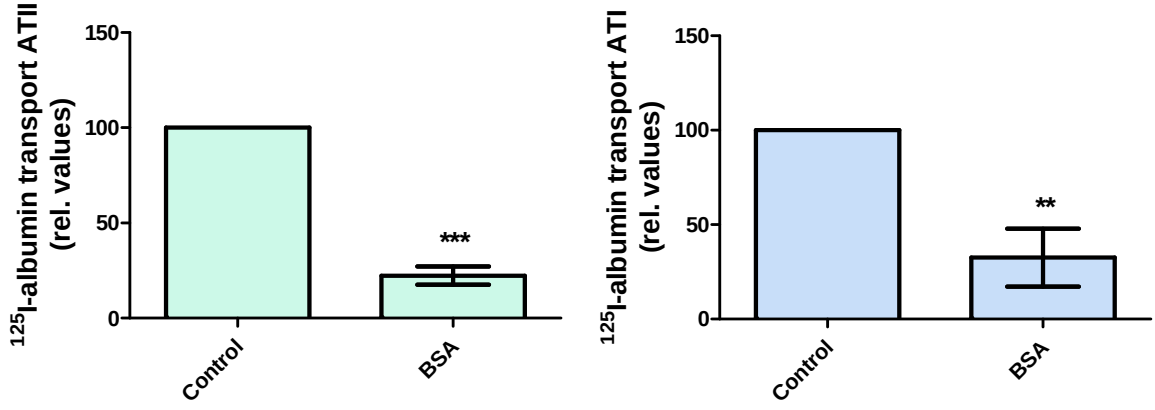

Figure 12: ***Transepithelial transport of ^{125}I-albumin across monolayers of primary rat alveolar epithelial type II (ATII) and type I-like (ATI) cells is blocked by excess native albumin.***
ATII cells were used on day 3 (ATII) or day 7 (ATI). The amount of ^{125}I-albumin which was transported across the epithelial monolayer (in absence or presence of an excess amount of BSA) was assessed by measurement of γ-radiation. ****p<0.001; **p<0.01; n=4.*

3.1.2 Albumin uptake in the alveolar epithelium is mediated by megalin via clathrin-dependent endocytosis

Endocytosis of albumin by alveolar epithelial cells has been proposed as a possible mechanism for protein clearance from the alveolar space (Kim and Malik 2003). In former studies of our group A549 cells were pre-treated with the two clathrin-dependent endocytosis inhibitors phenylarsine oxide (Visser, Stevanovic et al. 2004) and chlorpromazine (Wang, Rothberg et al.1993) which markedly inhibited ^{125}I-albumin uptake (Rummel 2007). These findings strongly suggest that clathrin-dependent endocytosis is required for albumin uptake in A549 cells. In isolated rabbit lungs inhibition of clathrin-dependent endocytosis by application of aerosolized phenylarsine oxide and chlorpromazine resulted in a significant decrease in active ^{125}I-albumin transit from the alveolar epithelium to the vascular compartment (Rummel 2007). These data accorded with former studies which had shown that FITC-albumin uptake requires clathrin-dependent endocytosis in RLE-6TN cells (Yumoto et al. 2006). Clathrin-dependent endocytosis is a receptor-mediated process. In the last years the two endocytic receptors megalin and cubilin emerged to be most important for the binding and uptake of albumin in the kidney´s epthelial cells of the proximal tubules (Birn and Christensen 2006). Megalin and cubilin are dependent on each other regarding their expression on the cell surface as well as their function. However, megalin seems to be the one responsible for albumin uptake, since only megalin has a transmembrane domain (Verrroust et al. 2002). It has already been proposed that the function of megalin and cubilin is required for FITC-albumin uptake in RLE-6TN cells (Yumoto et al. 2006).

We were using primary ATII and ATI-like cells to investigate the involvement of megalin in the binding, uptake and transepithelial transport of albumin. Thus, we were applying receptor associated protein (RAP) to the cells prior to incubation with either FITC-albumin or ^{125}I-albumin. RAP is one of megalins many ligands which binds megalin with high affinity and therefore, by competition, partially blocks albumin binding (Verroust et al. 2002). In our cellular transport studies RAP inhibited ^{125}I-albumin binding by 50.1 ± 4.5 % in ATII cells and by 39.2 ± 11.8 % in ATI-like cells (**Figure 13**).

Furthermore, RAP treatment inhibited the uptake of FITC-albumin by primary alveolar epithelial cells by 54.8 ± 9.8 % in ATII cells and by 64.2 ± 11.7 % in ATI-like cells, as assessed by fluorescence microscopy (**Figures 14 and 15**).

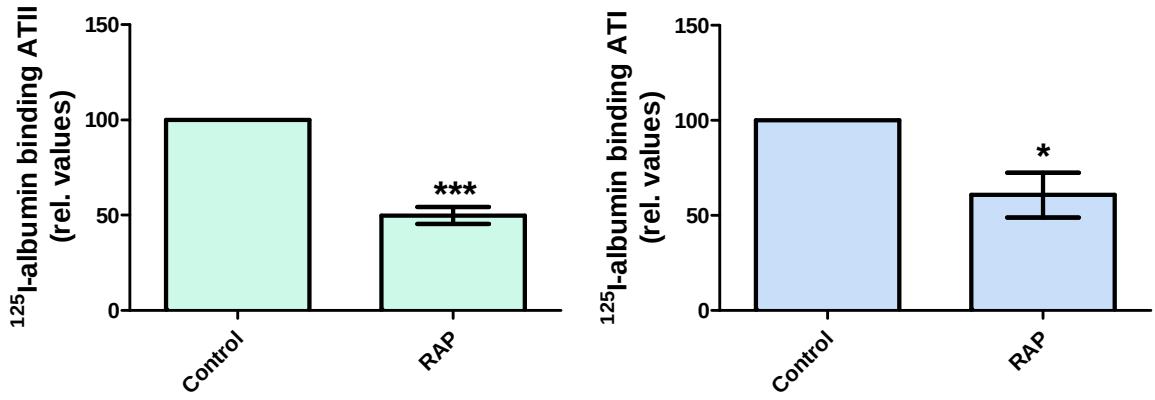

Figure 13: ***Binding of ^{125}I-albumin to primary rat alveolar epithelial type II (ATII) and type I-like (ATI) cells is inhibited by receptor associated protein (RAP).***
ATII cells were used for experiments on day 3 (ATII) or day 7 (ATI). Cells were pre-incubated with 1 µM RAP prior to incubation with ^{125}I-albumin. ****p<0.001; *p<0.05; n=3*

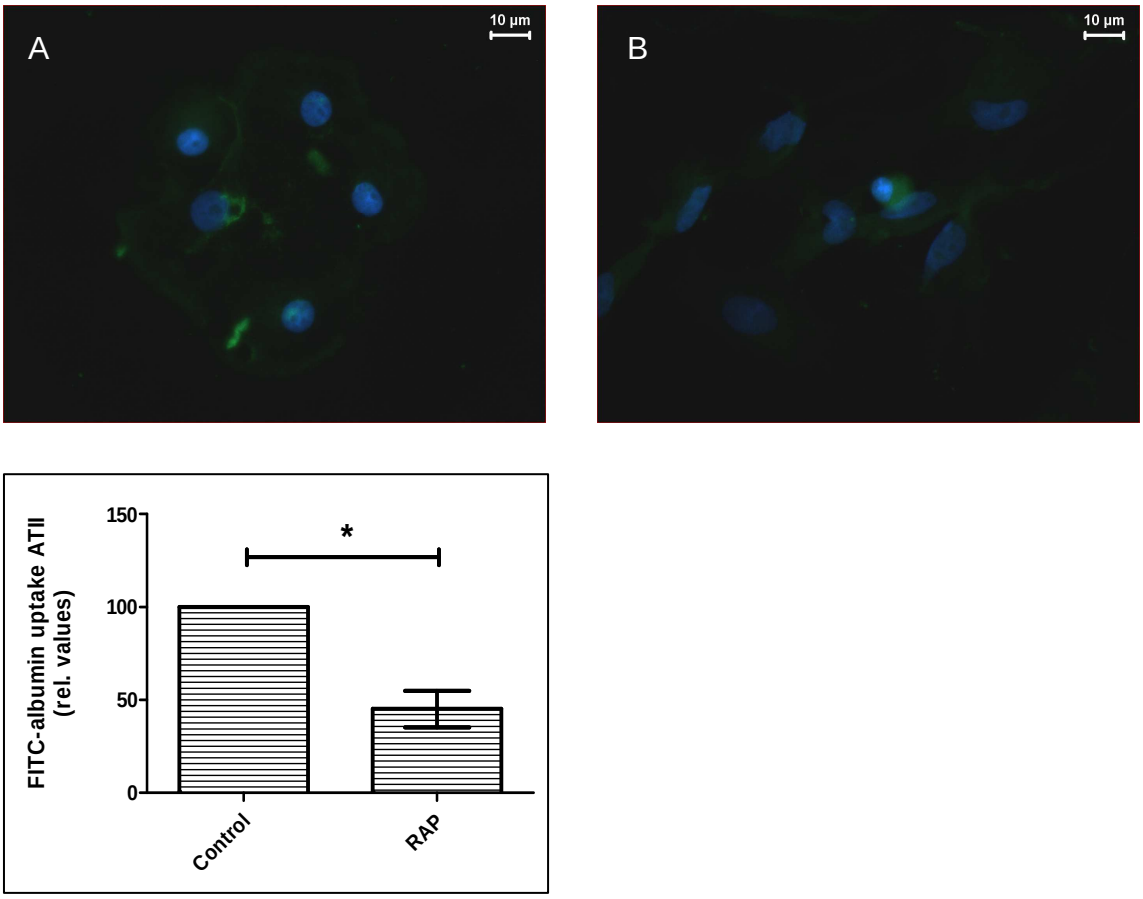

Figure 14: ***Uptake of FITC-albumin by primary rat alveolar epithelial type II (ATII) cells is impaired by Receptor associated protein (RAP).***
ATII cells were pre-incubated in absence (A) or presence (B) of 1µM RAP prior to incubation with 50µg/ml of FITC-albumin. FITC-albumin uptake was assessed by fluorescence microscopy. **p<0.05; n=3.*

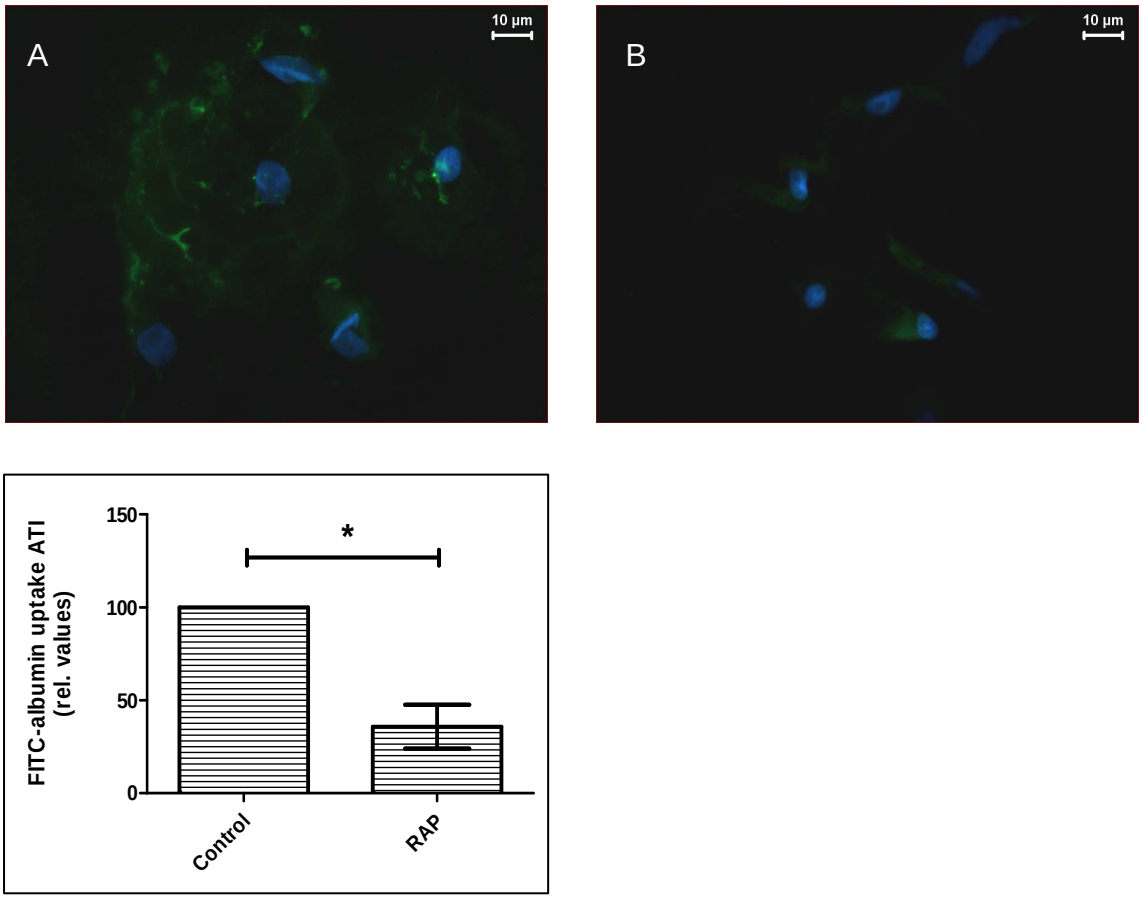

Figure 15: ***Uptake of FITC-albumin by primary rat alveolar epithelial type I-like (ATI) cells is inhibited by Receptor associated protein (RAP).***
ATI cells were pre-incubated for 30 min in absence (A) or presence (B) of 1µM RAP prior to incubation with 50µg/ml of FITC-albumin. FITC-albumin uptake was assessed by fluorescence microscopy. **p<0.05; n=3.*

The uptake of ^{125}I-albumin was also assessed by conducting cellular transport studies in primary ATII and ATI-like cells. After pre-treatment with RAP, the cell monolayers were incubated with ^{125}I-albumin for 30 minutes. Application of RAP inhibited the uptake of ^{125}I-albumin by 55.4 ± 7.7 % in ATII cells and by 36.8 ± 7.5 % in ATI-like cells (**Figure 16**).

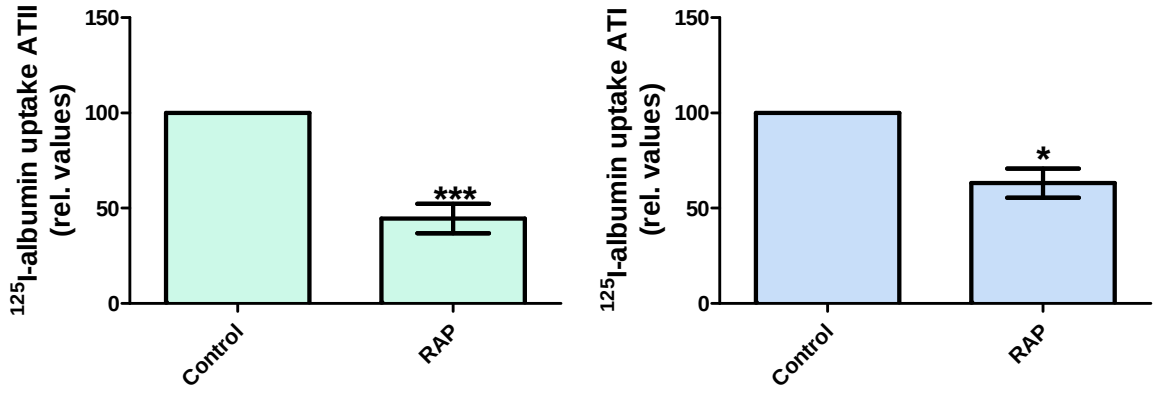

Figure 16: ***Uptake of ^{125}I-albumin by primary rat alveolar epithelial type II (ATII) and type I-like (ATI) cells was partially blocked by RAP.***
ATII cells were plated on permeable supports and used for experiments on day 3 (ATII) or day 7 (ATI). Cells were pre-incubated in absence or presence of 1µM RAP prior to incubation with ^{125}I-albumin. Uptake of ^{125}I-albumin was assessed by detection of γ-radiation. ****p<0.001;*p<0.05; n=4.*

Pre-incubation of the cells with 1µM RAP prior to the application of ^{125}I-albumin resulted in decelerated transepithelial transport rates. Transepithelial movement slowed down by 55.02 ± 4.987 % in ATII cells and by 37.18 ± 1.769 % in ATI-like cells (**Figure 17**). Altogether these data suggest that albumin uptake by alveolar epithelial cells as well as transepithelial transport across the alveolar epithelium is a receptor-mediated process which involves the multi-ligand endocytic receptors megalin and cublin.

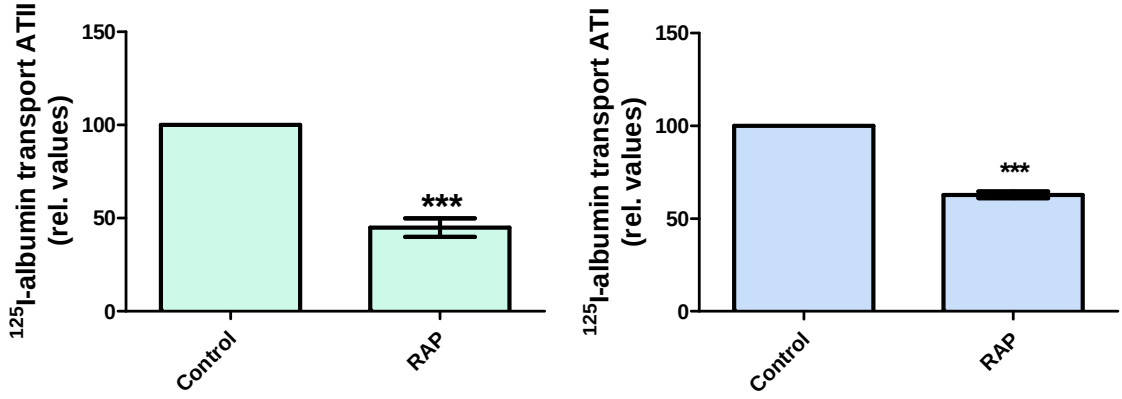

Figure 17: ***Transepithelial transport of ^{125}I-albumin across monolayers of primary rat alveolar epithelial type II (ATII) and type I-like (ATI) cells is partially blocked by RAP.***
ATII and ATI-like cells were pre-incubated with 1µM RAP and subsequently incubated with ^{125}I-albumin. The amount of ^{125}I-albumin which was transported across the epithelial monolayer was assessed by measurement of γ-radiation. ****p<0.001; n=4.*

To further elucidate the role of megalin as a potential receptor for albumin endocytosis in the alveolar epithelium, we evaluated the effect of silencing the megalin gene. We employed a cell line with high transfection efficiency, compared to that of primary alveolar epithelial type II cells, the RLE-6TN cell line. This cultured cell line was already evaluated as an *in vitro* model system for alveolar epithelial cells (Yumoto et al. 2006). RLE-6TN cells were shown to have some characteristic features of alveolar type II epithelial cells, such as alkaline phosphatase activity and the expression of cytokeratin 19 mRNA. To ensure we see the same base-line conditions in RLE-6TN cells as we saw in our primary alveolar epithelial cells, we evaluated the effect of an excess amount of native albumin on the uptake of labeled albumin. When cells were pre-incubated with a 1000-fold molar excess of cold albumin, the binding of ^{125}I-albumin to the cell surface was inhibited by 59.82 ± 3.53 % (**Figure 18**).

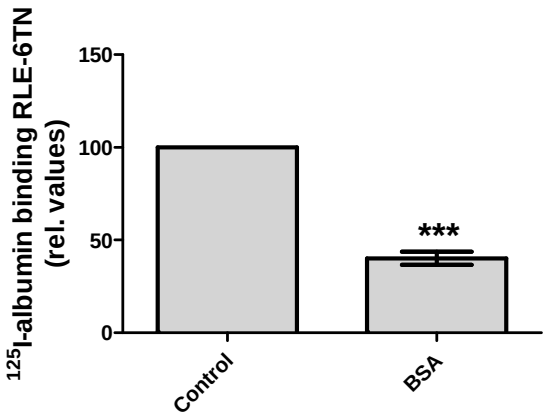

Figure 18: ***Binding of ^{125}I-albumin to RLE-6TN cells is blocked by excess native albumin.*** RLE-6TN cells were plated on permeable supports and used for experiments on day 7. Cells were pre-incubated in absence or presence of a 1000-fold molar excess of native albumin prior to incubation with ^{125}I-albumin. The amount of surface bound ^{125}I-albumin was assessed by detection of γ-radiation. ****p<0.001; n=4.*

The effect of excess native albumin on uptake of labeled albumin by RLE-6TN cells was also assessed by using fluorescence microscopy additional to cellular transport studies. The uptake of FITC-albumin by RLE-6TN cells was decreased by 69.62 ± 5.53 % when cells were pre-incubated with excess native albumin (**Figure 19**).

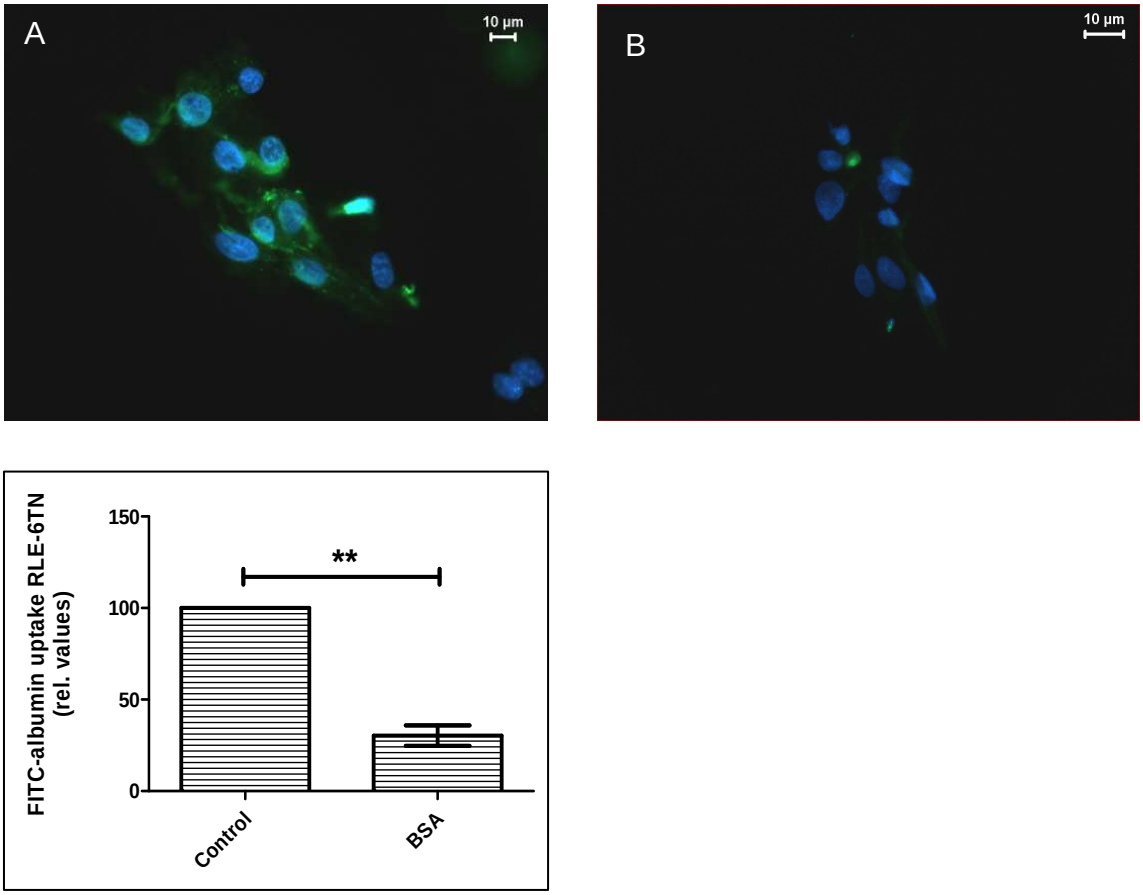

Figure 19: ***Uptake of FITC-albumin by RLE-6TN cells is blocked by excess native albumin.*** RLE-6TN cells were plated on cover slips and used for experiments on day 7. Cells were pre-incubated for 30 min in absence (A) or presence (B) of excess native albumin prior to incubation with 50 µg/ml of FITC-albumin. FITC-albumin uptake was assessed by density measurement. ***p<0.01;* n=*3.*

In cellular transport studies we assessed the effect of excess native albumin on the uptake of ^{125}I-albumin by RLE-6TN cells. As expected, a 1000-fold molar excess of cold albumin strongly inhibited the uptake of ^{125}I-albumin, namely by 92.0 ± 2.4 % (**Figure 20**). The effect of excess native albumin on transepithelial transport of ^{125}I-albumin across the cell monolayer was also similar to our findings in primary alveolar epithelial cells. In RLE-6TN cells the transport rate was slowed down by 43.8 ± 5.9 % after treatment with excess native albumin (**Figure 21**). These data suggest that the RLE-6TN cell line is an appropriate model for our studies. Since their behavior is similar to that of ATII cells, we can assume the same underlying mechanisms for albumin endocytosis and transcytosis.

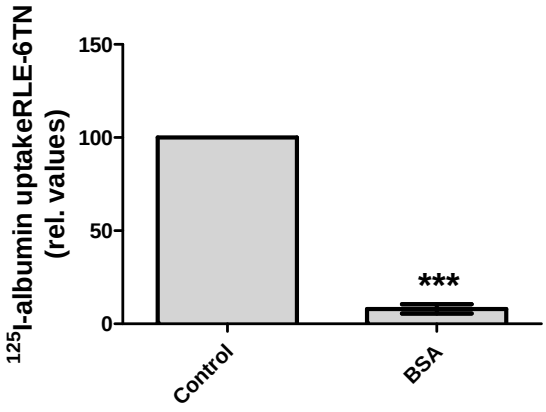

Figure 20: ***Uptake of ^{125}I-albumin by RLE-6TN cells.***
RLE-6TN cells were pre-incubated for 30 min in absence or presence of a 1000-fold molar excess of unlabeled albumin prior to incubation with ^{125}I-albumin. ^{125}I-albumin uptake was assessed by measurement of γ-radiation. ****p<0.001*; *n=4.*

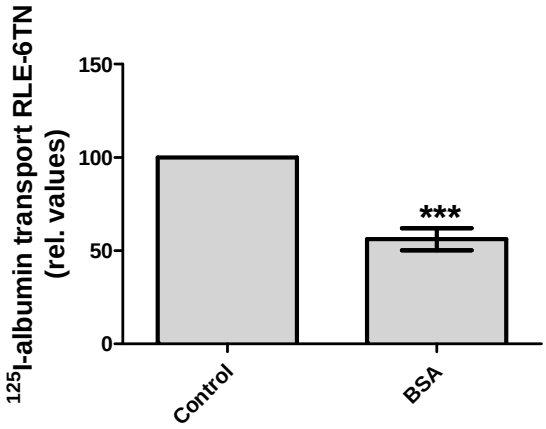

Figure 21: ***Transepithelial transport of ^{125}I-albumin across monolayers of RLE-6TN cells.***
RLE-6TN cells on permeable supports and used for experiments on day 7. Cells were incubated in absence or presence of a 1000-fold molar excess of cold albumin prior to incubation with ^{125}I-albumin. The amount of ^{125}I-albumin which was transported across the epithelial monolayer was assessed by measurement of γ-radiation. ****p<0.001; n=4.*

After we established that RLE-6TN cells present with same characteristics as primary alveolar epithelial cells we transfected them with rat megalin siRNA (Santa Cruz Biotechnology), which consisted of three target-specific 19- to 25-nt siRNAs to silence megalin gene expression. In addition we transfected a scrambled control siRNA (siRNA-A, Santa Cruz Biotechnology) or cy3 labeled negative control siRNA (Silencer cy3 labeled negative control siRNA, Ambion). We were plating RLE-6TN cells on cover slips and used them for transfection on day 6. Using fluorescence microscopy we established transfection efficiency,

eight out of ten cells were successfully transfected with cy3 labeled negative control siRNA after 24 h of transfection (**Figure 22**). In addition, we harvested the cells and performed gel electrophoresis and western blot analysis, using a rabbit polyclonal anti-rat megalin antibody (H-245, santa cruz biotechnology) and goat anti-rabbit IgG (catalog number 7074; Cell Signaling Technologies) to detect protein expression (**Figur 22**).

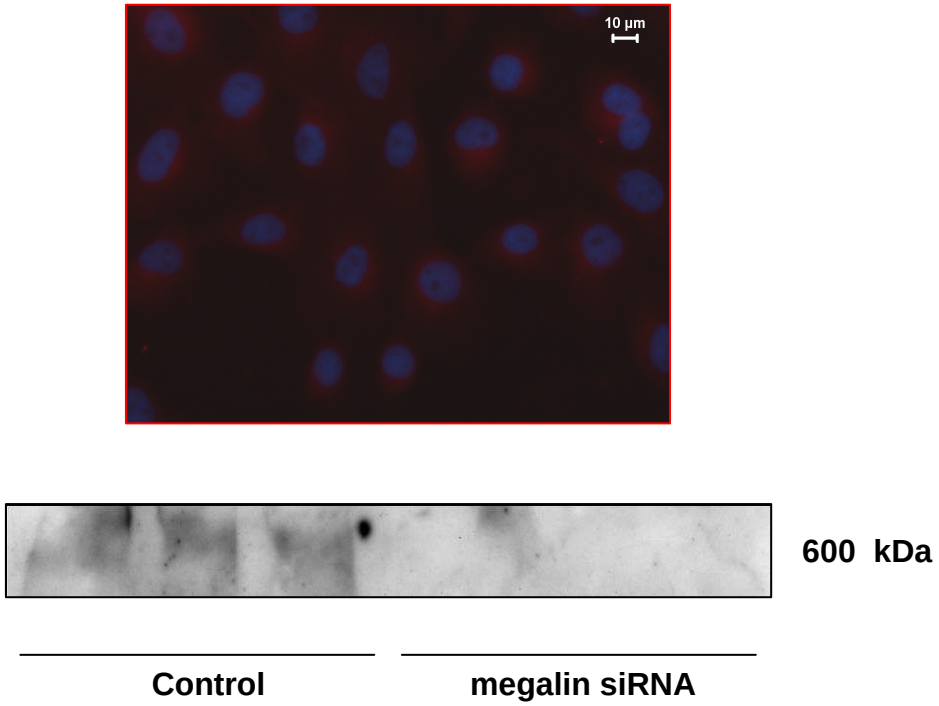

Figure 22: ***RNA interference of megalin in RLE-6TN cells.***
The upper panel illustrates efficiency of transfection with cy3 labeled negative control siRNA. Transfection with 50 ρM rat megalin siRNA (lower panel) resulted in decreased expression of megalin (600 kDa) after 24 hours as assessed by western blot analysis. *n = 3.*

After 24 hours of transfection we applied FITC-albumin to the megalin knockdown cells. After fixation the cells were incubated with rabbit polyclonal anti-rat megalin antibody (H-245, santa cruz biotechnology) and used a donkey polyclonal anti-rabbit antibody which was cy3-conjugated (AP182C; Millipore) for detection by immunofluorescence. Megalin expression was reduced by 76.5 ± 4.8 % after gene silencing by RNA interference (**Figure 23**). The uptake rate of FITC-albumin was reduced by 71.2 ± 5.2 % after gene silencing of megalin (**Figure 24**). Cells transfected with scrambled siRNA did not show any significant difference to controls, neither in megalin expression nor in FITC-albumin uptake.

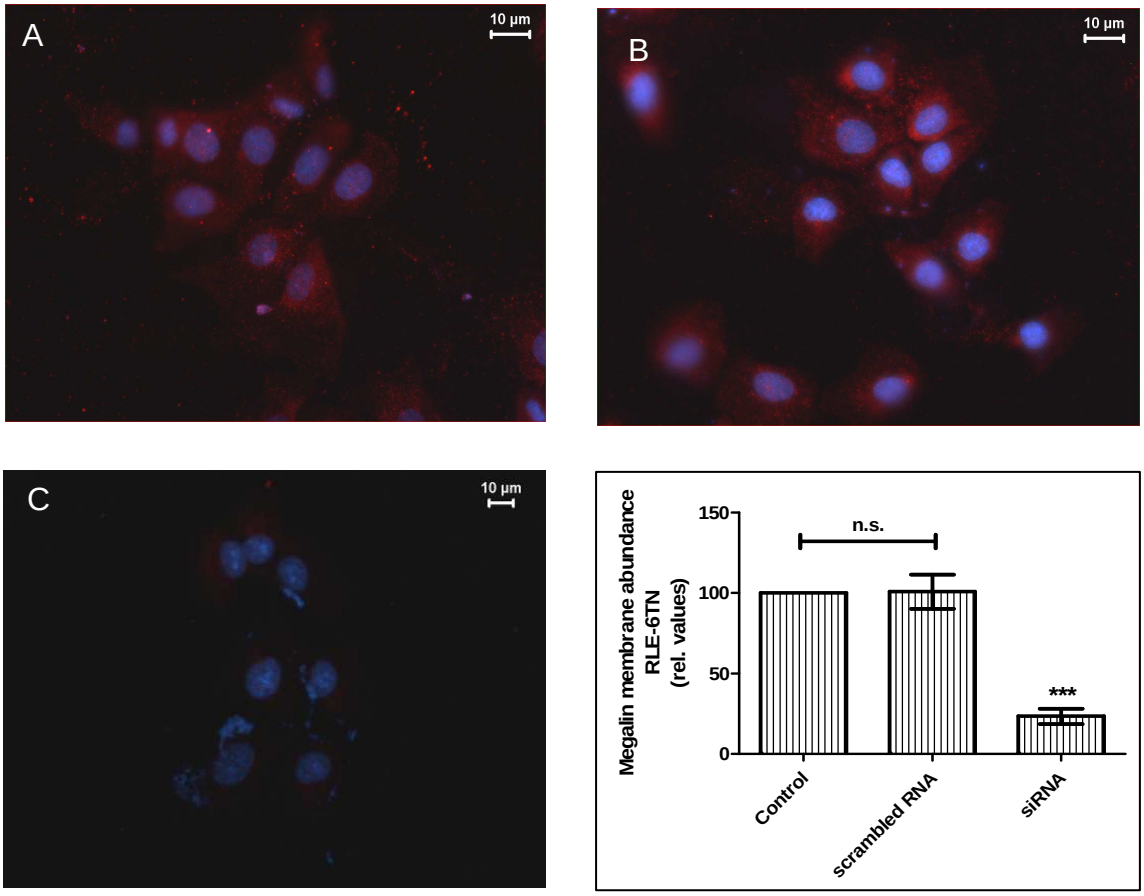

Figure 23: ***Megalin expression in RLE-6TN cells 24 hours after gene silencing with megalin siRNA.***
Megalin expression was detected by immunofluorescence. (A) Untransfected control, (B) transfected with 50 ρM scrambled siRNA, (C) transfected with 50 ρM rat megalin siRNA, (D) 50 ρM cy3-control siRNA. ****p<0.001; n=3.*

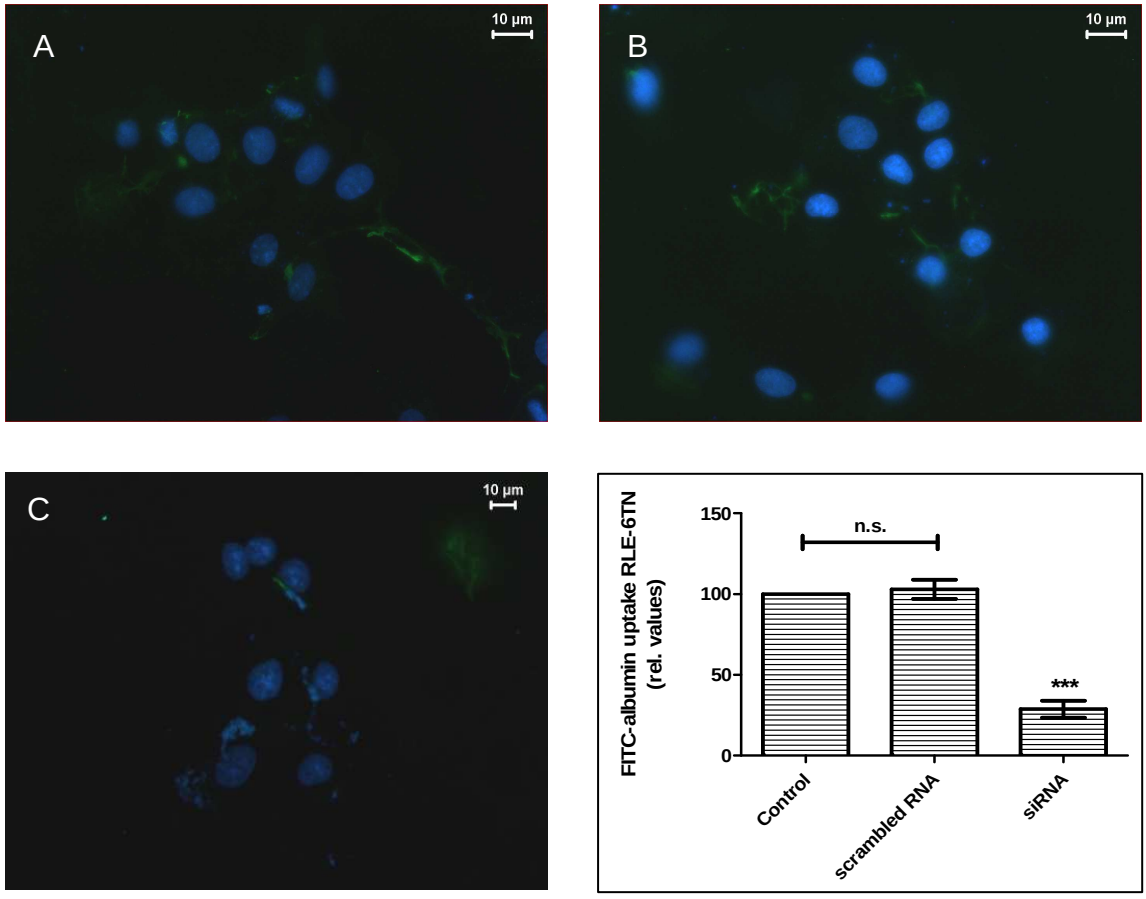

Figure 24: ***FITC-albumin uptake by RLE-6TN cells 24 hours after gene silencing with megalin siRNA.***
After transfection with rat megalin siRNA, cells were incubated with FITC-albumin. Uptake of FITC-albumin was detected by fluorescence microscopy. (A) Untransfected control, (B) transfected with 50 ρM scrambled siRNA, (C) transfected with 50 ρM rat megalin siRNA. ****p<0.001; n=3.*

We also knocked down megalin in RLE-6TN cells which were plated on permeable supports to conduct cellular transport studies and assess binding, uptake and transepithelial transport of ^{125}I-albumin. Cells were transfected with rat megalin siRNA on day 6 and experiments were conducted on day 7. Albumin binding was blocked by 85.7 ± 2.8 % after gene silencing of megalin (**Figure 25**).

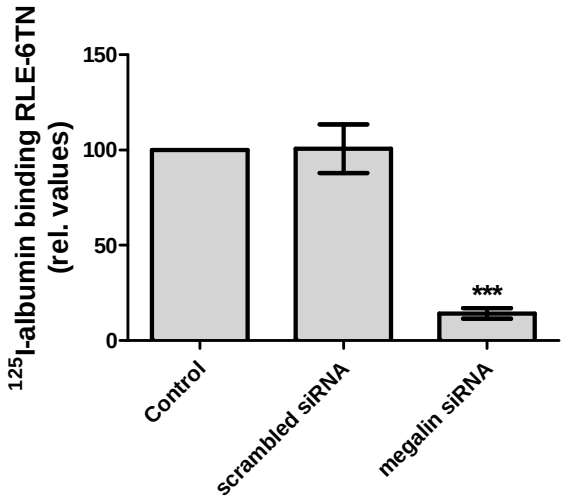

Figure 25: ***Binding of ^{125}I-albumin to RLE-6TN cells was blocked by gene silencing of megalin.***
RLE-6TN cells were plated on permeable supports, transfected with megalin siRNA on day 6 and used for experiments on day 7. Binding of ^{125}I-albumin to the cell surface was assessed by measuring γ-radiation, 30 minutes after administration. ****p<0.001; n=3.*

^{125}I-albumin uptake by RLE-6TN cells was impaired by 88.9 ± 3.2 % after RNA interference of megalin (**Figure 26**).

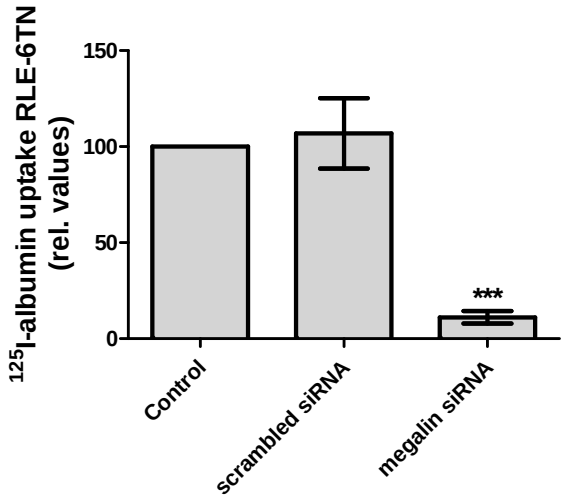

Figure 26: ***Uptake of ^{125}I-albumin by RLE-6TN cells was significantly impaired by gene silencing of megalin.***
Uptake of ^{125}I-albumin was assessed by measuring the γ-radiation of the cell lysate, 30 minutes after administration of labeled albumin. ****p<0.001; n=3.*

Transepithelial transport across the RLE-6TN monolayer was decreased by 85.4 ± 2.7 % when megalin gene expression was silenced by RNA interference (**Figure 27**).

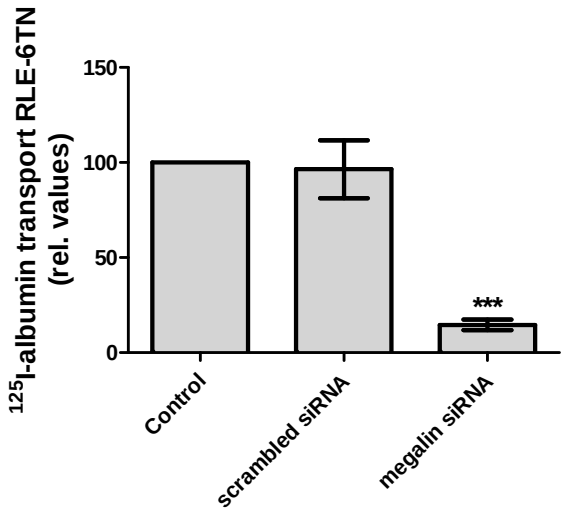

Figure 27: ***Transepithelial transport of ^{125}I-albumin across monolayers of RLE-6TN cells after gene silencing of megalin.***
RLE-6TN cells were plated on permeable supports and used for experiments on day 7. 30 minutes after administration of ^{125}I-albumin samples were taken from the basolateral side of the monolayer and the amount of ^{125}I-albumin which was transported across the epithelial monolayer was assessed by measurement of γ-radiation. ****p<0.001; n=3.*

Silencing megalin gene expression by short interference RNA resulted in significantly reduced FITC-albumin uptake in RLE-6TN cells. Our cellular transport studies confirmed that binding, uptake and transepithelial transport of ^{125}I-albumin was strongly decelerated in megalin knockdown cells. Transfecting the cells with a siRNA negative control, that contained a scrambled sequence had no significant effect on albumin transport. Altogether these data suggest that the multi-ligand endocytic receptor megalin facilitates albumin transport across the alveolar epithelium.

3.2 Mechanisms of impaired albumin transport in the pathophysiology of acute lung injury and the acute respiratory distress syndrome

3.2.1 TGF-β1 impairs uptake and transepithelial transport of albumin across the alveolar epithelium

TGF-β was identified a key mediator for ARDS and the promotion of end-stage fibrosis (Fahy et al. 2003). The initial step of fibrogenesis is protein-precipitation, which is unavoidable linked to acute lung injury, since there the concentration of albumin increases up to 75-95 % of the plasma level when it comes to pulmonary edema (Tagawa et al. 2008). A correlation between pulmonary fibrosis and fatality in established cases of ARDS has already been described (Martin et al. 1995). However, whether TGF- β impairs protein clearance from the alveolar space remains unclear.

We aerosolized a pathologically relevant concentration of human recombinant TGF-β1 (R&D systems) into the isolated, ventilated and perfused rabbit lung. Subsequently we deposited ^{125}I-albumin to the alveolar space by ultrasonic nebulization. We detected ^{125}I-albumin clearance from the alveolar compartment by real-time measurement of γ-radiation. When physiological saline was instilled into the lung prior to ^{125}I-albumin deposition, 29.8 ± 2.1 % of radio-labeled albumin was cleared from the lung by the end of the experiment (120 min). Instillation of TGF- β1 resulted in significantly decreased ^{125}I-albumin clearance (15.3 ± 0.7 %) (**Figure 28**). As previously established by our group approximately 88 % of albumin clearance is facilitated by active transport processes. In conclusion, TGF- β1 blocks 48.1 ± 0.4 % of total active transport capacity, as assessed by measuring the difference between the areas above the curve.

In cellular experiments we employed three different kind of alveolar epithelial cell monolayers and incubated them with a pathologically relevant concentration of TGF- β1 for 30 minutes. Afterwards we incubated them with ^{125}I-albumin for another 30 minutes and subsequently assessed binding, uptake and transepithelial transport of the radio-labeled albumin by measuring γ-radiation. In the rat alveolar epithelial cell line RLE-6TN, TGF-β reduced ^{125}I-albumin binding to the cell surface by 73.9 ± 0.6 % , by 50.5 ± 4.0 % in rat alveolar type II cells and by 61.3 ± 8.6 % in rat alveolar type I-like cells compared to control conditions (**Figure 29**).

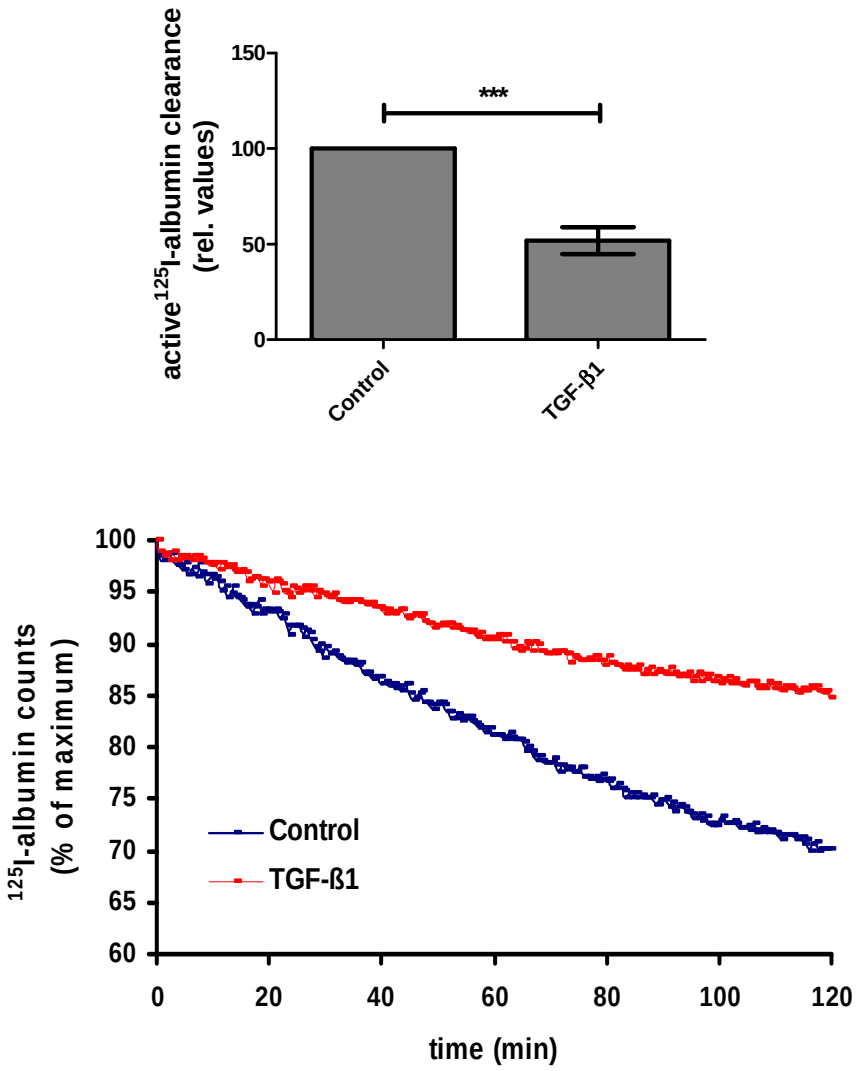

Figure 28: ***^{125}I-albumin clearance from isolated, ventilated and perfused rabbit lungs is impaired by TGF- ß1.***

After establishing steady-state equilibrium (30 min), TGF- β1 was applied to the lungs. After another 30 min, ^{125}I-albumin was deposited into the alveolar space by aerosolization. Clearance of radio-labeled albumin was monitored for 120 min *via* γ-detectors. The upper panel illustrates relative values of active ^{125}I-albumin transport, controls are set at 100 %. The lower panel represents the original graph as obtained from real-time measurement of tracer kinetics. ****p<0,001; n=6.*

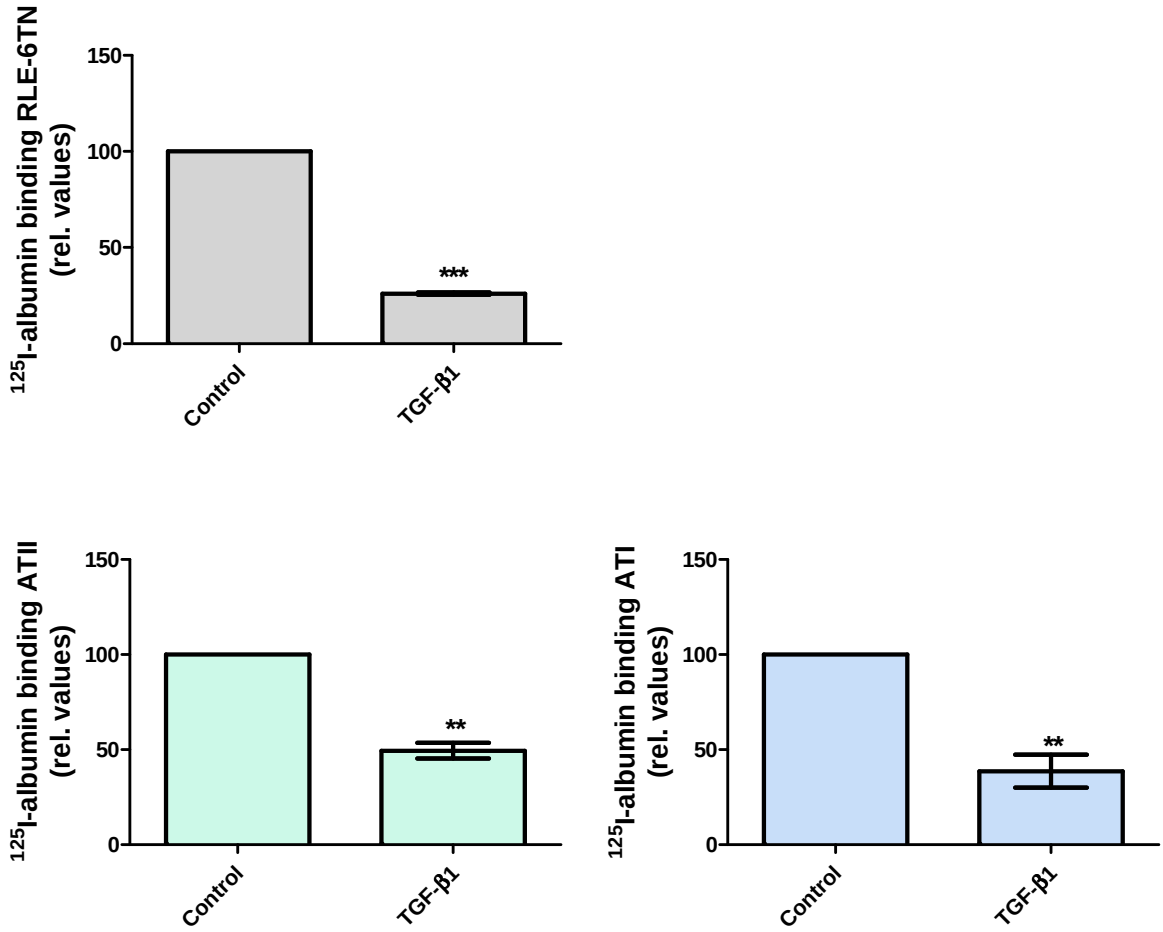

Figure 29: ***Binding of ^{125}I-albumin to the cell surface of RLE-6TN, ATII and ATI-like cells was impaired by TGF-β1.***
Cells were plated on permeable supports, used for experiments on day 3 (ATII) or day 7 (ATI and RLE-6TN) and pre-treated with 2 ηg of TGF-β1 for 30 minutes prior to incubation with ^{125}I-albumin. Binding was assessed by γ-radiation. ****p<0,001;**p<0,01; n=3.*

The effect of TGF-β1 on albumin uptake by alveolar epithelial cells was assessed by measuring the uptake of ^{125}I-albumin by γ-radiation. In RLE-6TN cells albumin uptake was decreased by 47.4 ± 1.7 % after TGF-β1 treatment, in ATII cells uptake was inhibited by 54.6 ± 4.5 % and in ATI-like cells uptake was impaired by 50.4 ± 2.6 % compared to control conditions (**Figure 30**).

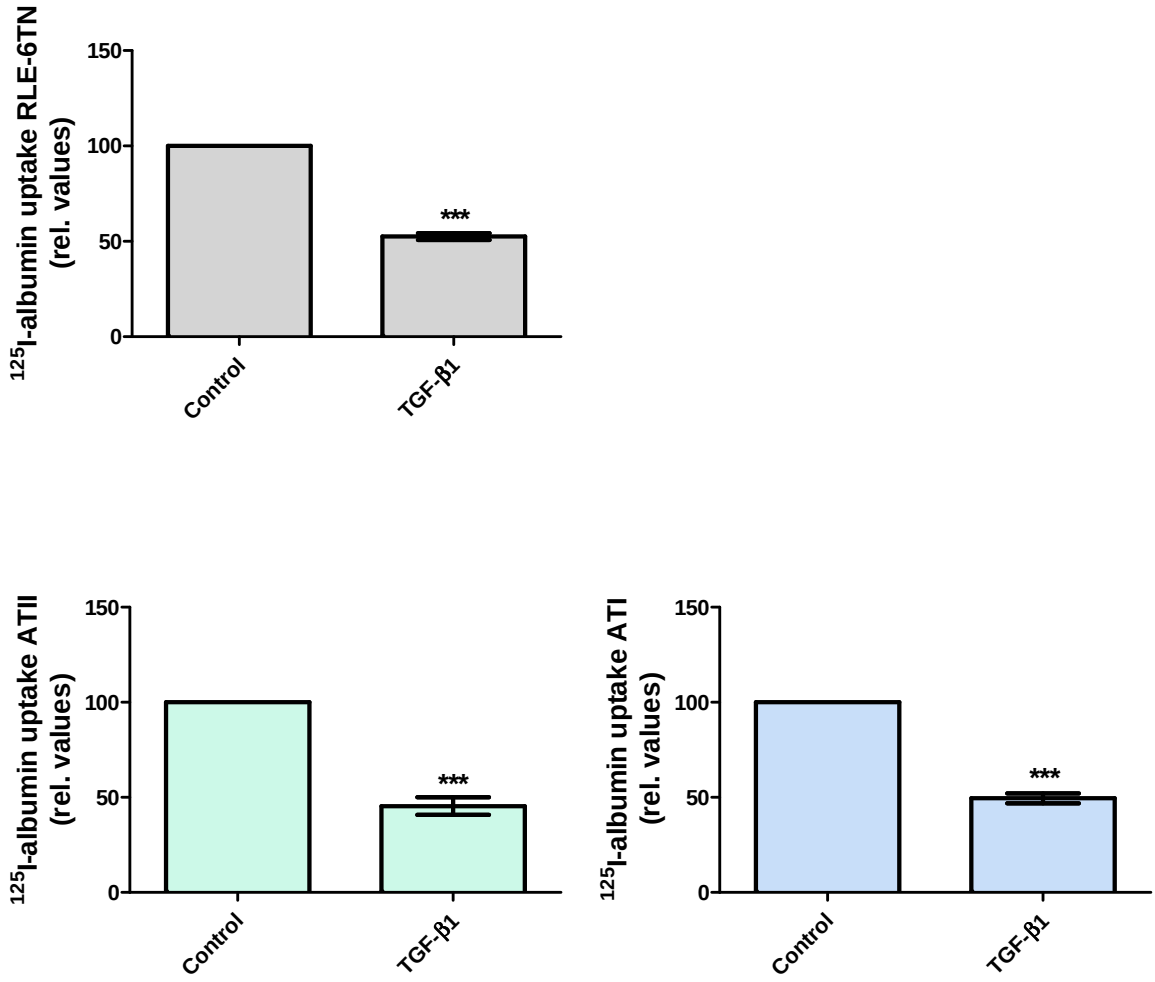

Figure 30: ***Uptake of ^{125}I-albumin by RLE-6TN, ATII and ATI-like cells was impaired by TGF-β1.***
Cells were plated on permeable supports and used for experiments on day 3 (ATII) or day 7 (ATI and RLE-6TN). Cells were pre-treated with TGF-β1 prior to incubation with ^{125}I-albumin. Uptake was assessed by γ-radiation. ****p<0,001; n=3.*

To assess the effect of TGF-β1 on transepithelial albumin transport, buffer samples were taken from the basolateral side of the cell monolayers and the amount of ^{125}I-albumin was detected. TGF-β1 reduced ^{125}I-albumin transport rates in RLE-6TN cells by 66.6 ± 6.8 % , by 68.7 ± 3.0 % in rat alveolar type II cells and by 65.5 ± 5.6 % in rat alveolar type I-like cells (**Figure 31**) These data strongly suggest that the presence of TGF-β1 significantly inhibits binding, uptake and transepithelial transport of albumin in the alveolar epithelium.

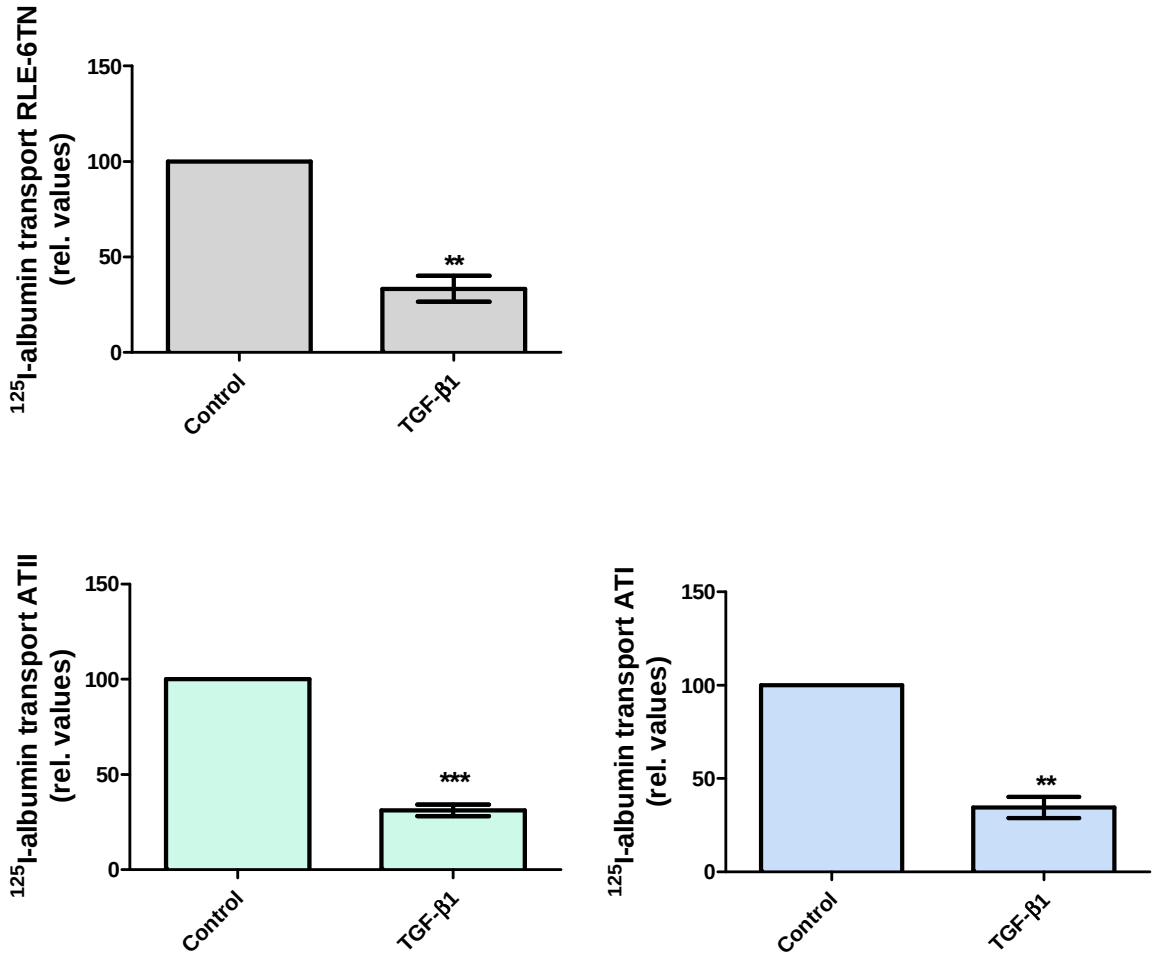

Figure 31: ***Transepithelial transport of ^{125}I-albumin across monolayers of RLE-6TN, ATII and ATI-like cells was significantly decreased by TGF-β1.***
Cells on permeable supports were used for experiments on day 3 (ATII) or day 7 (ATI and RLE-6TN). Cells were pre-treated with TGF-β1 for 30 minutes prior to incubation with ^{125}I-albumin. Transepithelial transport was assessed by γ-radiation. ****p<0,001;**p<0,01; n=3.*

Our cellular transport studies demonstrated the inhibitive effect of TGF-β1 on binding, uptake and transepithelial transport of ^{125}I-albumin in alveolar epithelial cells. This effect was not only visible in type II cells but also in type I cells which display 50 % of the alveolar epithelium. These data suggest a direct involvement of TGF-β1 in the decelerated albumin clearance in ARDS patients.

3.2.2 TGF-β1 decreases megalin surface distribution

After treatment with a pathological relevant concentration of TGF-β1 for 30 minutes, we detected megalin membrane distribution by immunofluorescence. In presence of TGF-β1 membrane abundance of megalin was significantly reduced compared to control conditions. In RLE-6TN cells we saw a reduction by 43.1 ± 6.9 % when cells were challenged with TGF-β1 (**Figure 32**). In primary ATII cells megalin abundance was reduced by 72.3 ± 6.3 % after TGF-β1 treatment (**Figure 33**) and in ATI-like cells we saw a decrease by 82.2 ± 4.9 % compared to control conditions (**Figure 34**).

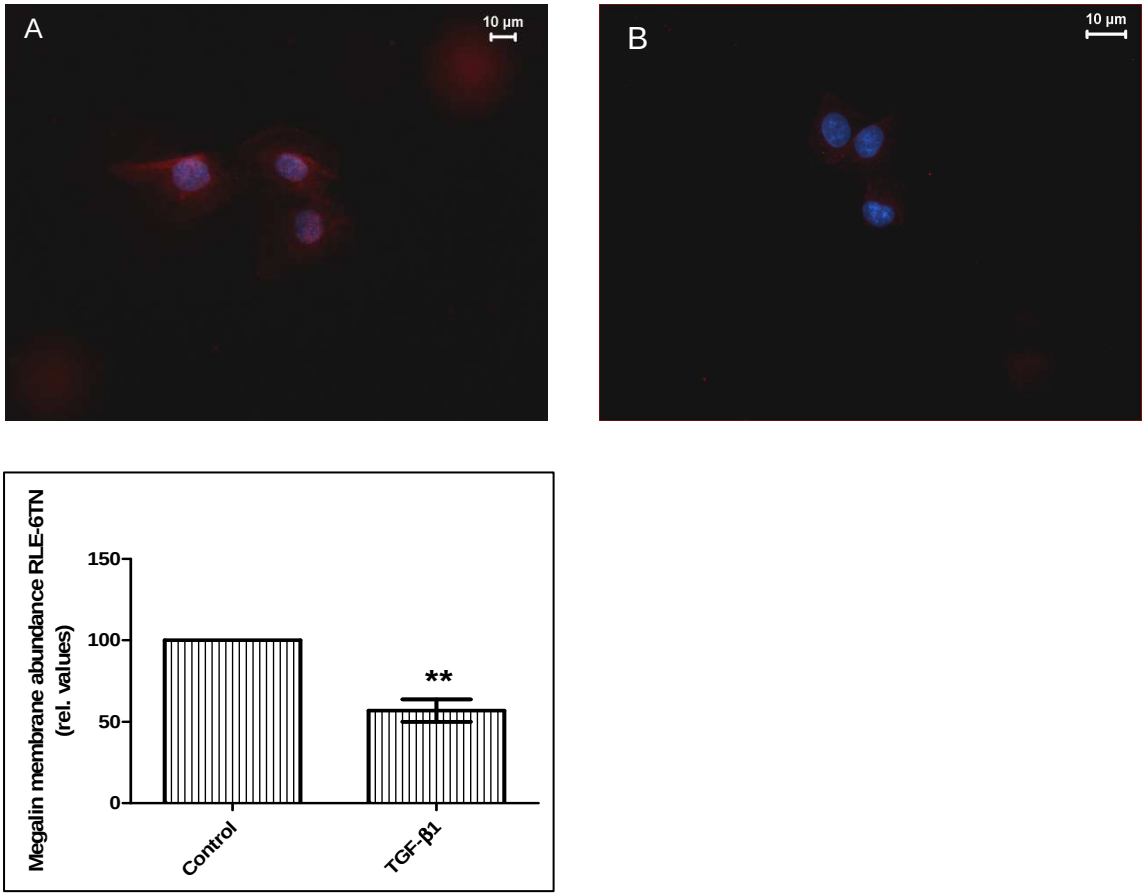

Figure 32: ***Reduced megalin membrane abundance after TGF-β1 treatment in RLE-6TN cells.***
After treatment with 2ηg TGF-β1, megalin membrane abundance was detected by immunofluorescence. (A) Control; (B) TGF-β1; ***p<0,01*; *n=3*.

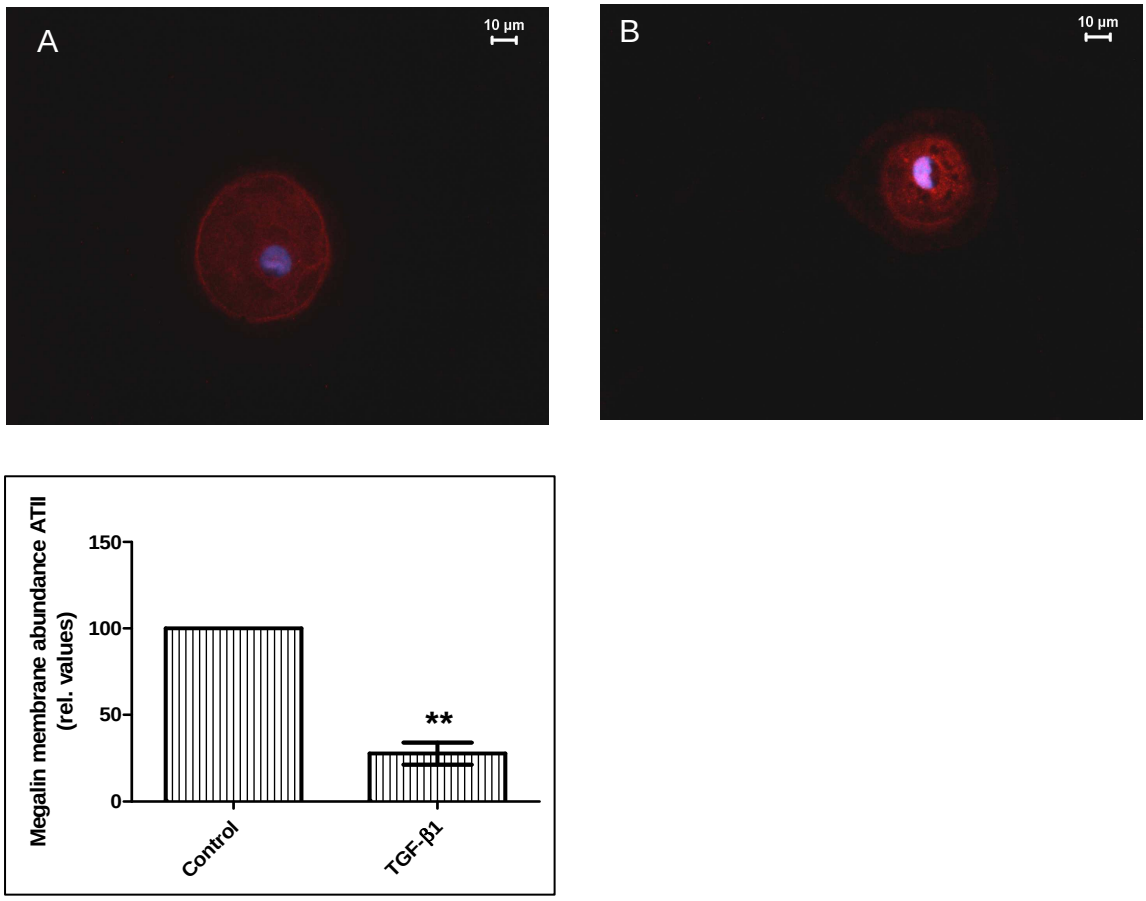

Figure 33: ***Megalin membrane abundance after TGF-β1 stimulation in primary ATII cells.*** After treatment with TGF-β1 primary ATII cells were incubated with rabbit anti-rat megalin and cy3-conjugated donkey anti-rabbit IgG. Megalin membrane abundance was detected by immunofluorescence. (A) Control; (B) TGF-β1; ***p<0,01*; *n=3*

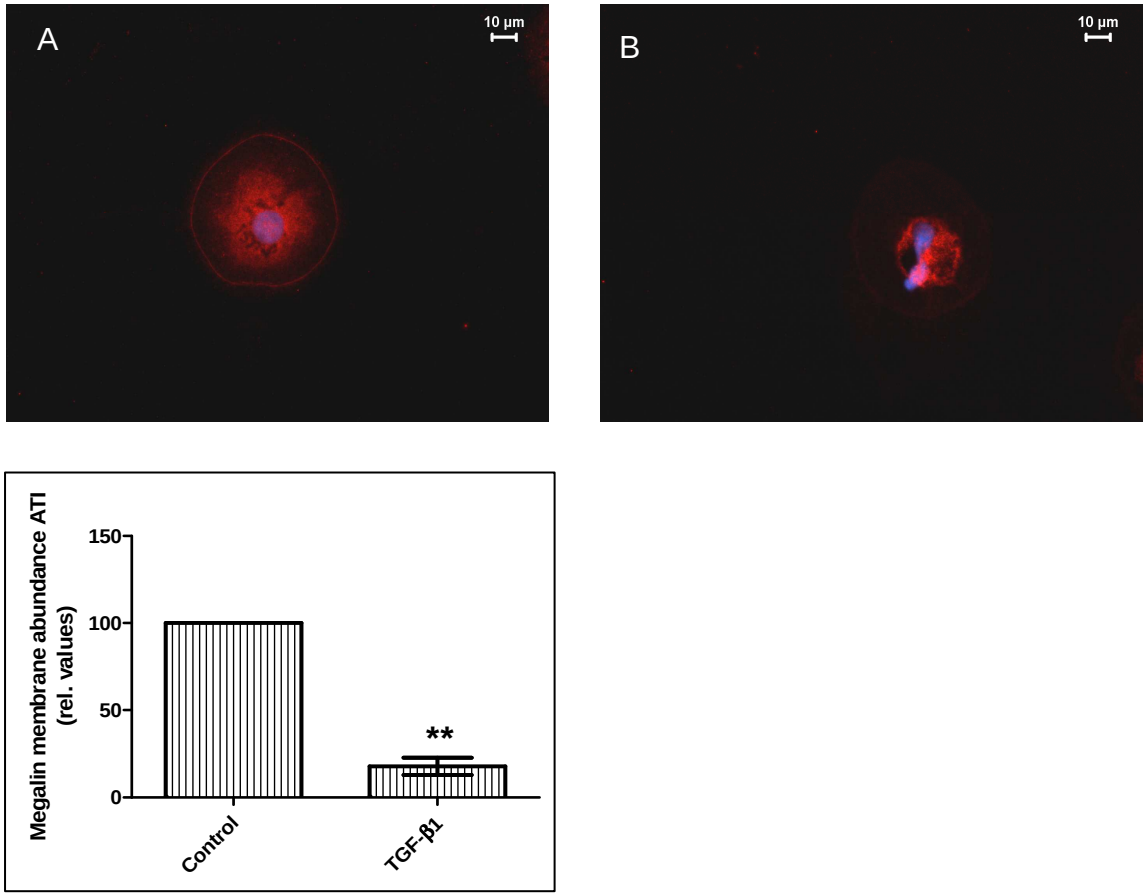

Figure 34: ***Decreased megalin membrane abundance after TGF-β1 challenge in primary ATI-like cells.***
After treatment of ATI-like cells with 2ηg TGF-β1, megalin membrane abundance was detected by fluorescence microscopy. (A) Control; (B) TGF-β1; ***p<0,01; n=3*

3.2.3 TGF-β1 activates glycogen synthase kinase 3 (GSK3) in a time-dependent manner

It has been well documented that glycogen synthase kinase 3 (GSK3) is the major regulator of megalins' surface expression in the cell (Tamai et al. 2004). Active GSK3 phosphorylates the cytoplasmic region of megalin at a PPPSP motif, thereby modifies megalin's recycling efficiency and thus, decreases surface expression of the receptor. GSK3 is constitutively phosphorylated in the cell, representing the inactive form of the kinase. In order to get activated, GSK3 needs to get dephosphorylated on either Ser 21 (α-subunit) or Ser 9 (β-subunit). The more dephosphorylated the kinase gets, the more activated it will be. To assess the effect of ARDS mediator TGF-β1 on GSK3 activity and thus, megalin cell surface distribution, we challenged primary rat ATII cells with TGF-β1 and detected GSK3 phosphorylation over a time-course of 45 minutes. Cell lysates were prepared for western blot analysis at different time points (0, 1, 5, 10, 20, 45 minutes after application of TGF-β1). Blots were probed against rabbit polyclonal anti-rat phospho-GSK3-α/β (catalog number 9331; Cell Signaling Technologies**)** and rabbit polyclonal anti-rat GSK3-α/β (catalog number 5676; Cell Signaling Technologies**)**. Our blots clearly demonstrated a time-dependent dephosphorylation of both GSK3 subunits under TGF- β1 stimulation leading to activation of the kinase (**Figure 35**).

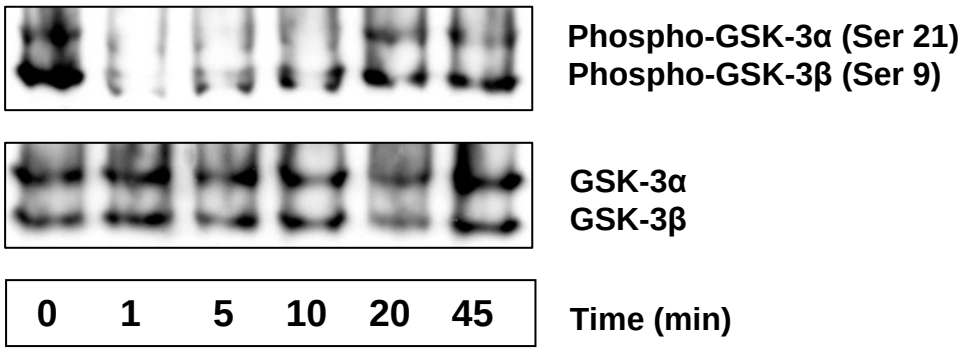

Figure 35: ***TGF-β1 dephosphorylates GSK3- α/β in a time-dependent manner.***
Primary rat alveolar epithelial type II cells were treated withTGF-β1 over a time-course of 45 minutes. Cells were lysed at different time points and GSK3 phosphorylation was detected by gel electrophoresis and western blot analysis. *n=3*

3.2.4 Reduced megalin membrane abundance by TGF-β1-mediated GSK3 activation results in partially blocked albumin uptake

To further elucidate the correlation between megalin membrane abundance and albumin uptake we applied FITC-albumin to the cells before they were fixed and incubated with rabbit anti-megalin and a cy3-conjugated donkey anti-rabbit IgG. By fluorescence microscopy we detected FITC-albumin uptake and megalin membrane abundance in presence or absence of TGF-β1. In RLE-6TN cells, after TGF-β1 treatment, the membrane abundance of megalin was reduced by 43.1 ± 6.9 %, at the same time FITC-albumin uptake was inhibited by 60 ± 6.2 % compared to control conditions (**Figure 36**). In primary ATII cells the presence of TGF-β1 reduced megalin surface expression by 72.3 ± 6.3 %, and therefore blocked FITC-albumin uptake by 72.2 ± 2.1 % (**Figure 37**). Similar results were obtained from primary ATI-like cells, were we saw a reduction of megalin membrane abundance by 82.2 ± 4.9 % and an inhibition of FITC-albumin uptake by 62.1 ± 3.6 % (**Figure 38**).

These data suggest a direct correlation between TGF-β1-mediated GSK3 activation and megalin membrane distribution. Activated GSK3 phosphorylates megalin, leading to endocytosis of the receptor and to an impaired uptake of albumin.

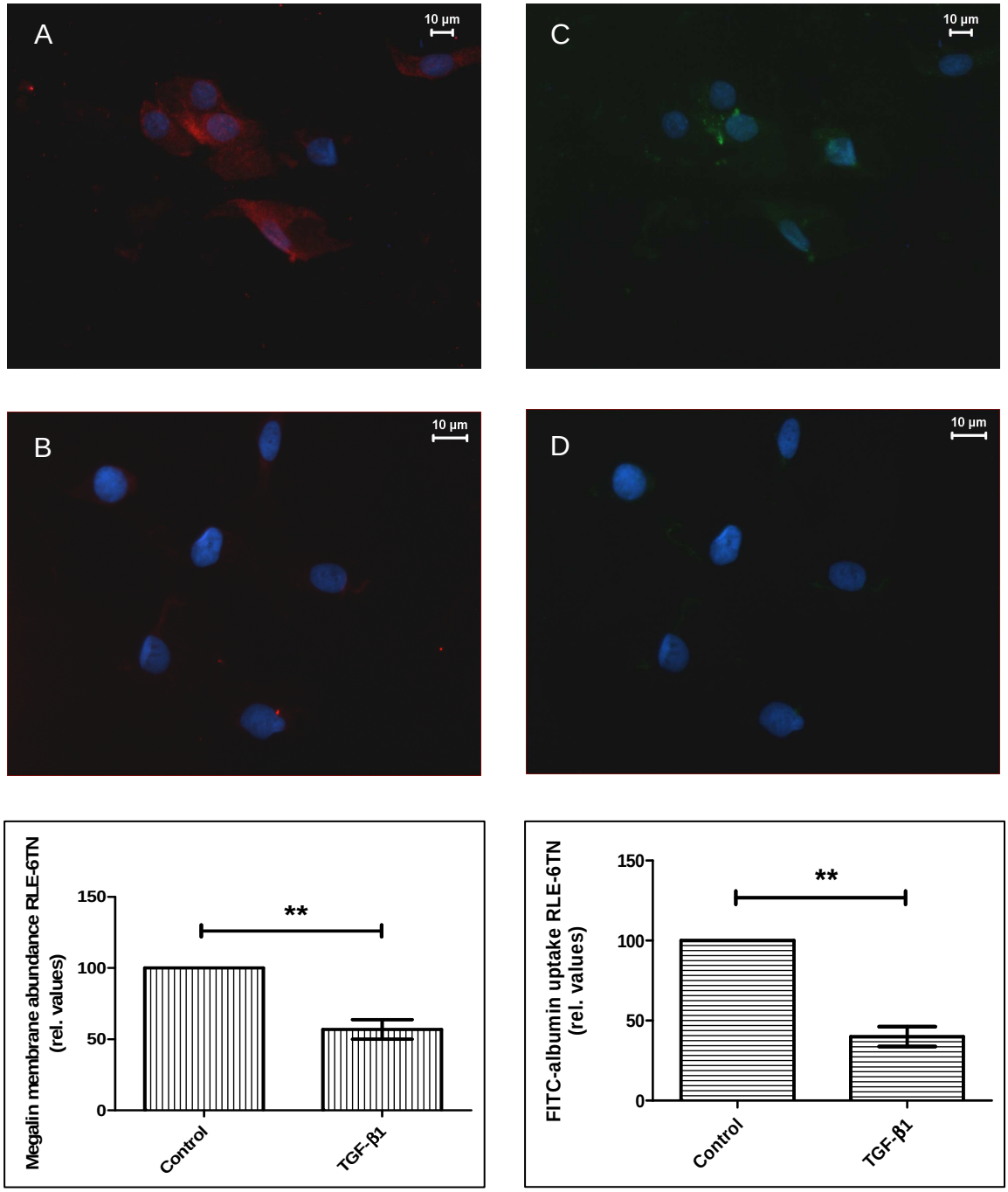

Figure 36: ***TGF-β1 mediated downregulation of megalin membrane abundance and impaired FITC-albumin uptake in RLE-6TN cells.***
Megalin membrane distribution in absence (A) or presence (B) of TGF-β1 and FITC-albumin uptake in absence (C) or presence (D) of TGF-β1. ***p<0,01; n=3*

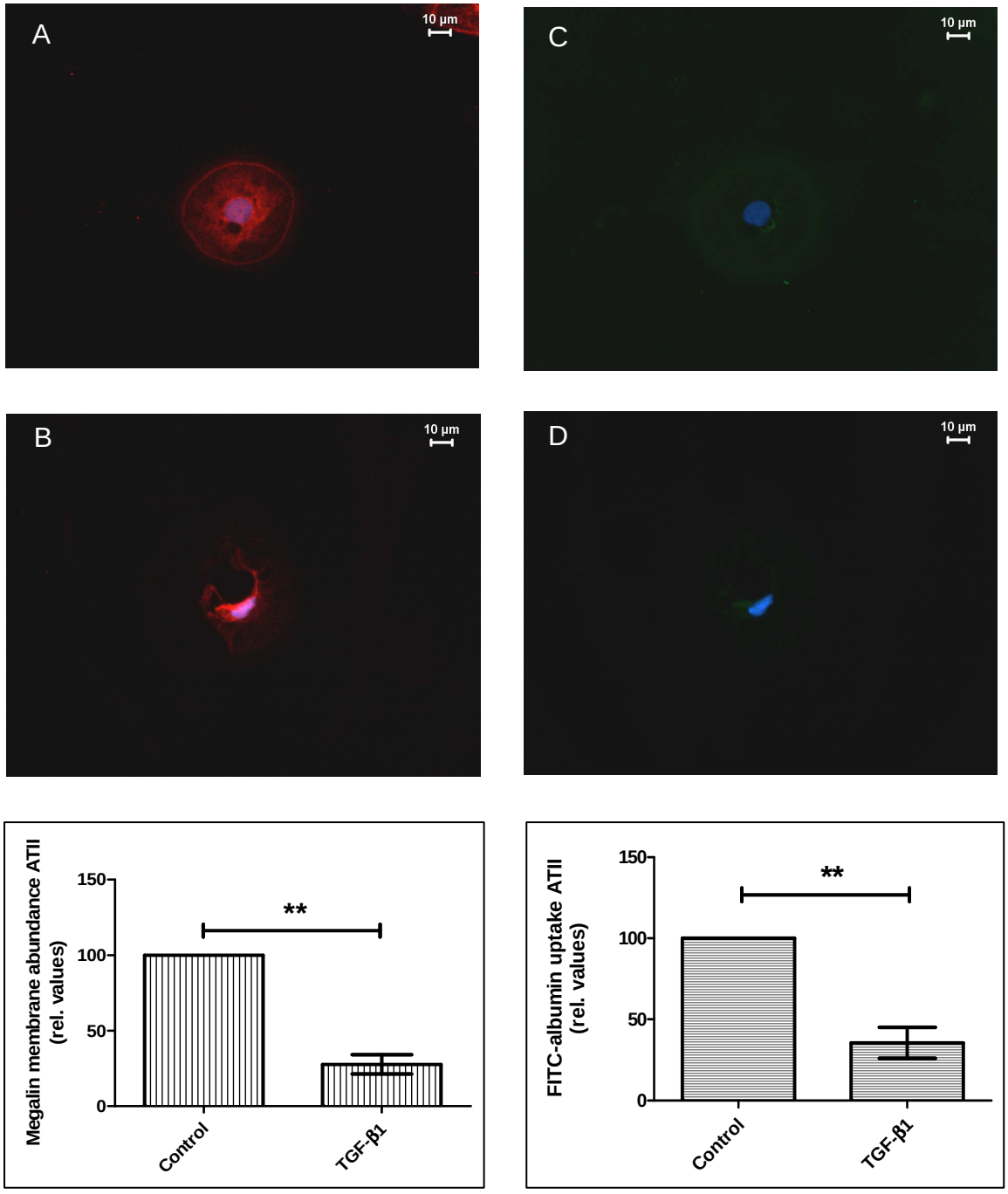

Figure 37: ***TGF-β1 mediated downregulation of megalin cell surface expression and reduced FITC-albumin uptake in primary ATII cells.***
Megalin membrane distribution in absence (A) or presence (B) of TGF-β1 and FITC-albumin uptake in absence (C) or presence (D) of TGF-β1. ****p<0,001; n=3*

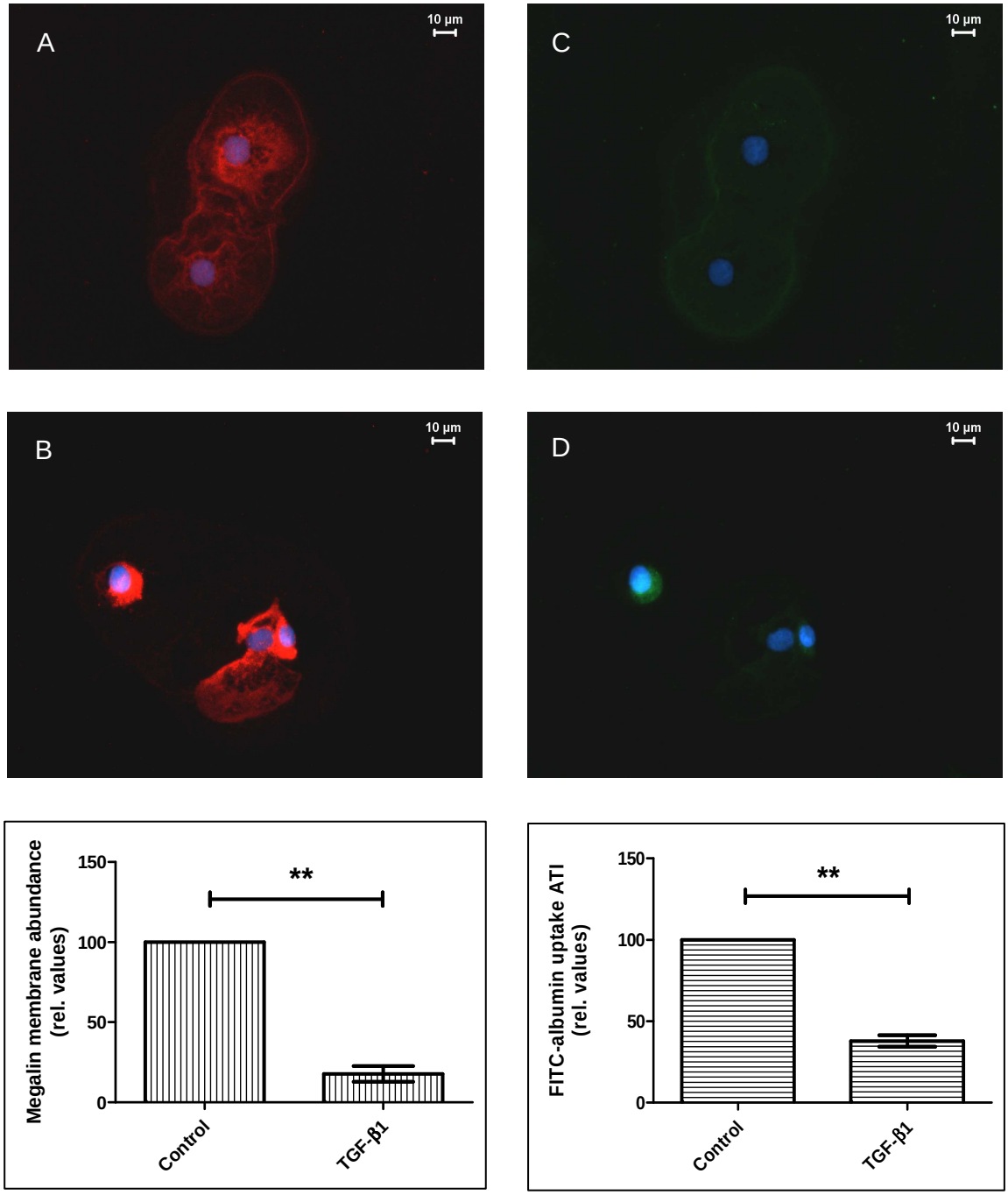

Figure 38: ***TGF-β1 induced downregulation of megalin membrane abundance and decreased FITC-albumin uptake in primary ATI-like cells.***
Megalin membrane distribution in absence (A) or presence (B) of TGF-β1 and FITC-albumin uptake in absence (C) or presence (D) of TGF-β1. ***p<0,01; n=3*

3.2.5 Inhibition of GSK3 activity prevents the effect of TGF-β1 on albumin uptake and transport

SB 216763 (Sigma Aldrich) is a maleimide which inhibits GSK-3α and GSK-3β *in vitro.* Inhibition is facilitated by ATP competition (Cross et al. 2001; Smith et al. 2001) and selectivity of the inhibitor was established by testing it against 26 different kinases, none of which were affected at concentrations where GSK3 was already significantly inhibited.

We plated alveolar epithelial cells on cover slips, treated them with SB 216763 for 30 minutes and subsequently challenged them with TGF-β1 for another 30 minutes. By using a rabbit anti-rat megalin antibody and a cy3-conjugated donkey anti-rabbit secondary antibody we assessed megalin cell surface abundance by immunofluorescence. FITC-albumin was administered to the cells for 30 minutes after treatment with the inhibitor and TGF-β1, uptake of FITC-albumin by the cells was assessed *via* density measurement. In RLE-6TN cells a megalin surface abundance of 96.3 ± 3.2 % and FITC-albumin uptake of 97 ± 1.6 % (**Figure 39 and 40**) was detectable when SB 216763 was applied prior to TGF-β1. In rat primary ATII cells, pretreatment with SB 216763 restored a megalin surface abundance of 98.5 ± 8 % and a FITC-albumin uptake of 97.9 ± 9.7 % (**Figure 41 and 42**) after TGF-β1 challenge. In primary ATI-like cells, the inhibitor prevented the effect of TGF-β1 and elevated megalin surface expression to 95.8 ± 24.6 % while .FITC-albumin uptake was increased by 2.3 ± 12.6 % (**Figure 43 and 44**). The inhibitor alone had no significant effect, neither on megalin membrane abundance nor on FITC-albumin uptake.

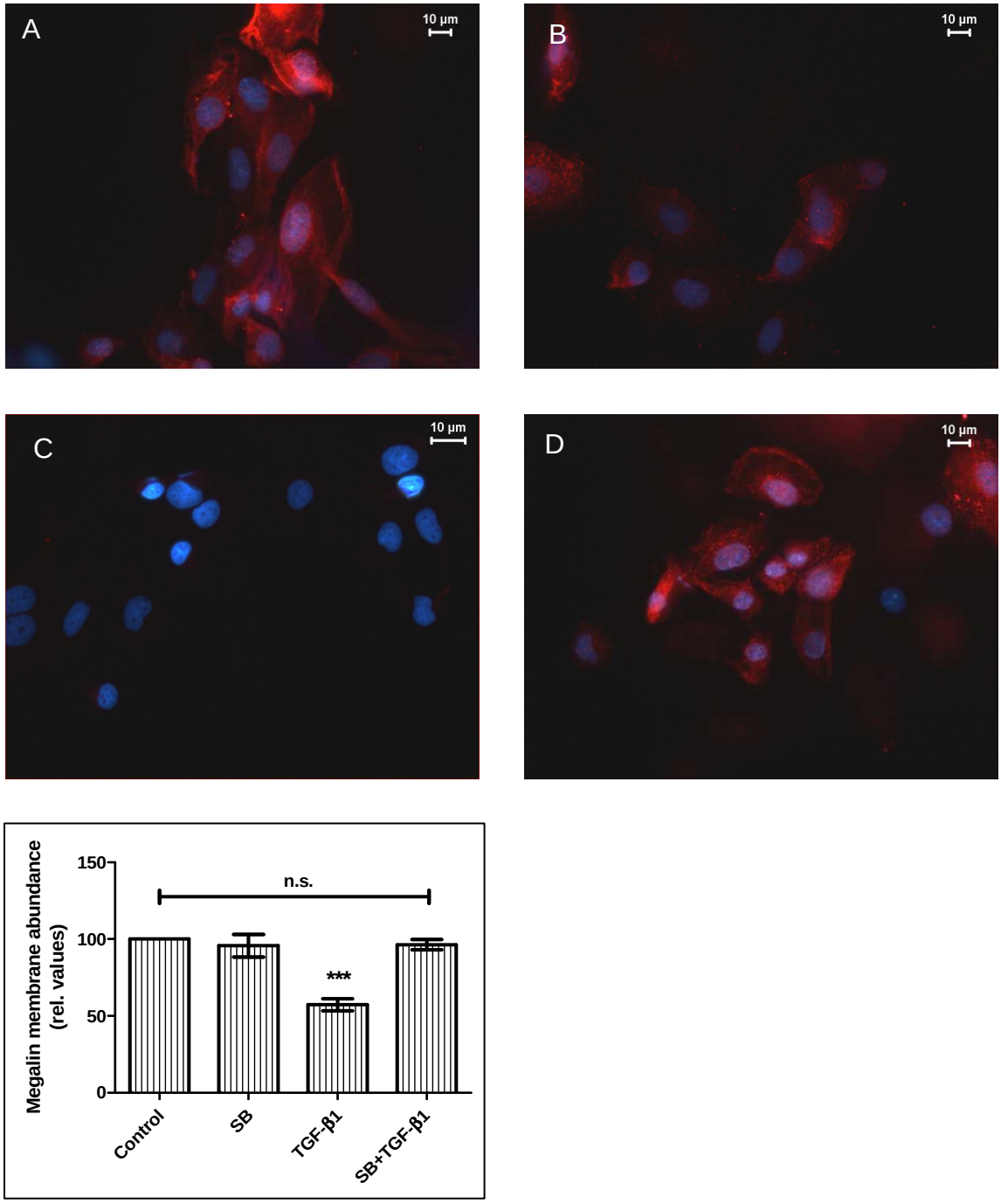

Figure 39: ***Inhibition of GSK3 prevents the effect of TGF-β1 on megalin surface expression in RLE-6TN cells.***
Megalin surface distribution in absence (A) or presence (C) of TGF-β1, 30µM SB 216763 (B) and pretreatment with 30µM SB 216763 before TGF-β1 challenge (D). ****p<0,001*; n=3

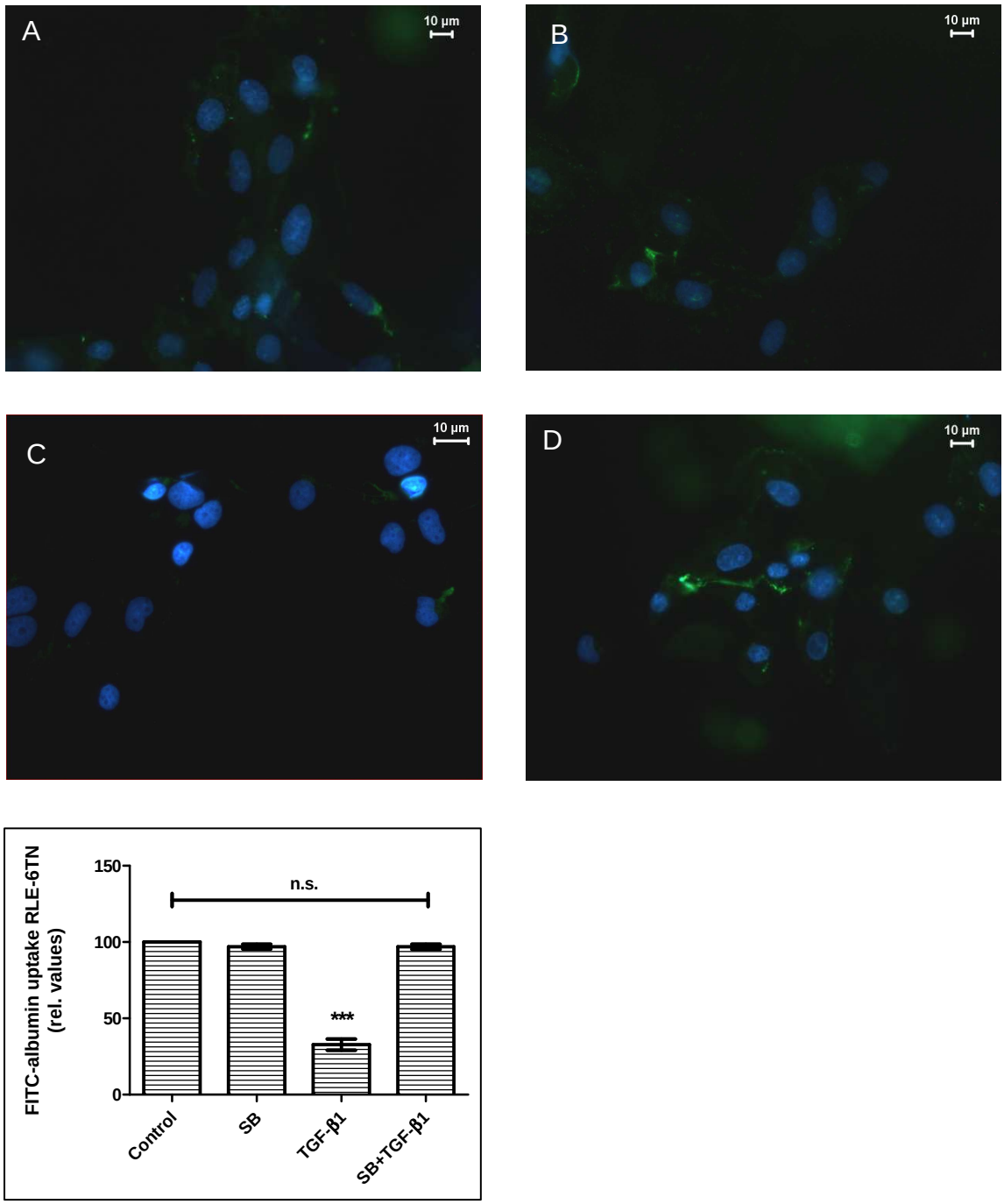

Figure 40: ***Inhibition of GSK3 prevents the effect of TGF-β1 on FITC-albumin uptake in RLE-6TN cells.***
FITC-albumin uptake in absence (A) or presence (C) of TGF-β1, SB 216763 alone (B) and in combination with TGF-β1 (D). ****p<0,001*; n=3

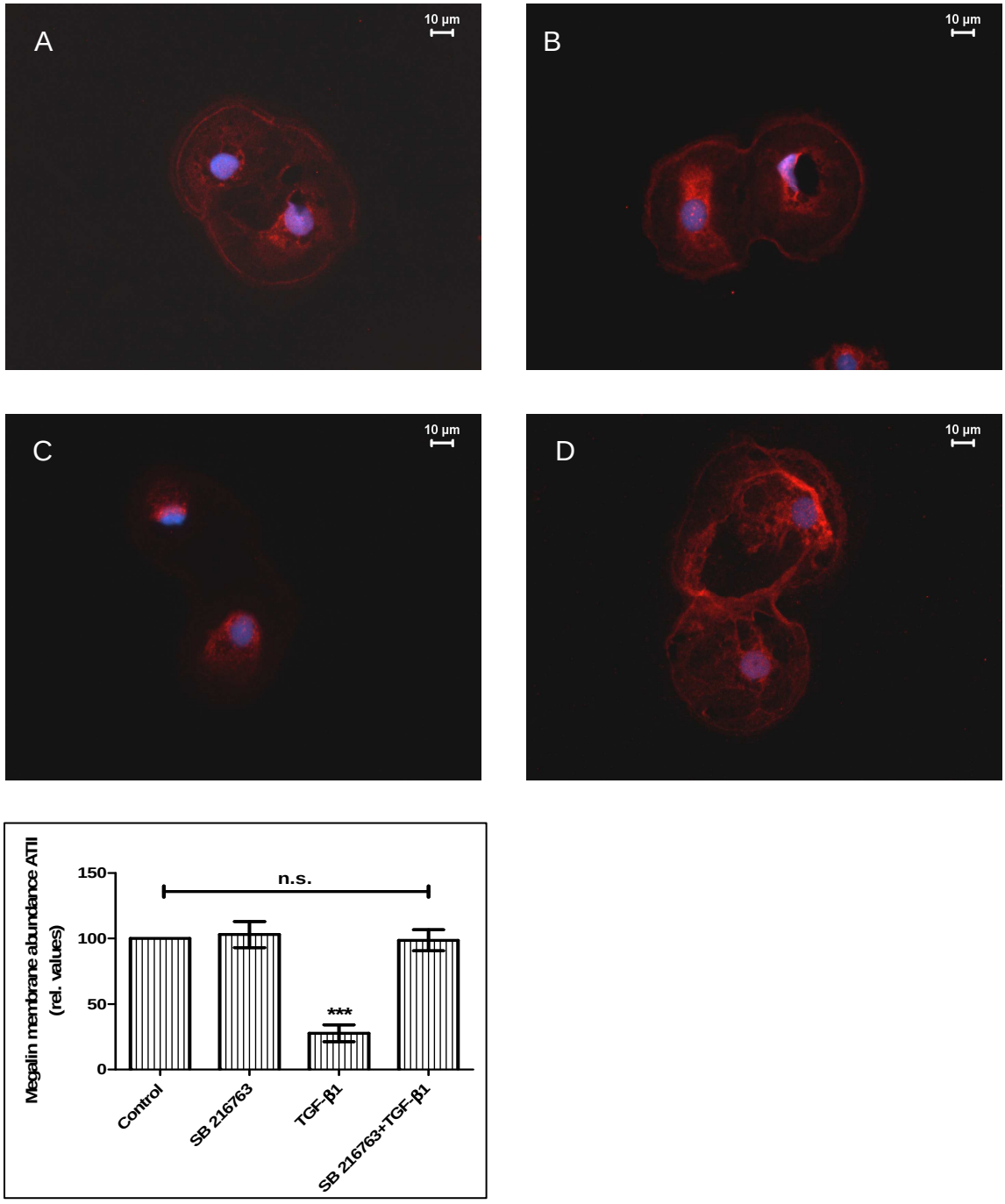

Figure 41: ***Inhibition of GSK3 prevents the effect of TGF-β1 on megalin surface distribution in primary rat ATII cells.***
Megalin surface distribution in absence (A) or presence (C) of TGF-β1, SB 216763 (B) and SB 216763 in combination with TGF-β1 (D). ****p<0,001*; n=3

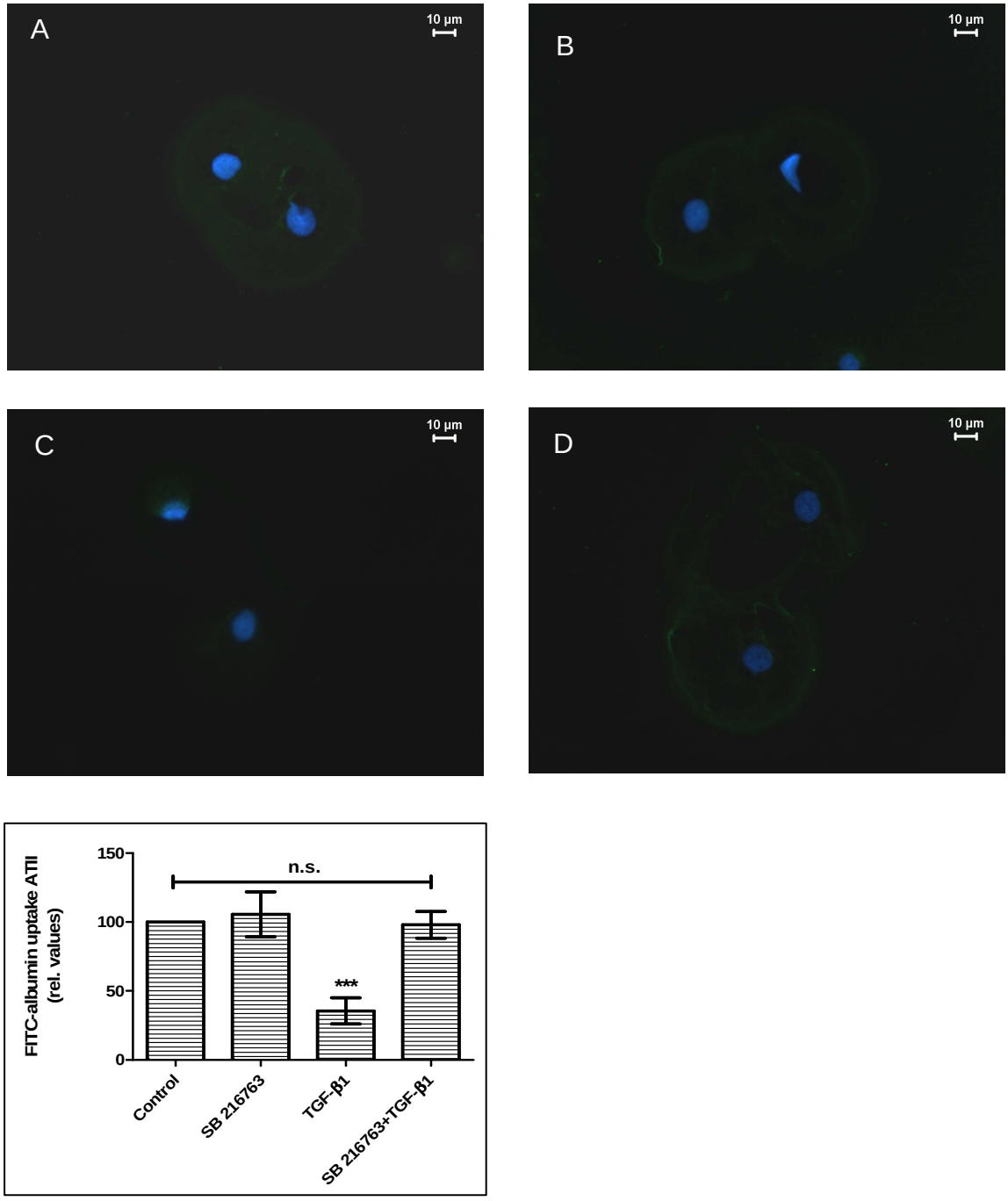

Figure 42: ***Inhibition of GSK3 prevents the effect of TGF-β1 on FITC-albumin uptake in primary rat ATII cells.***
FITC-albumin uptake in absence (A) or presence (C) of TGF-β1, SB 216763 alone (B) and combined with TGF-β1 (D). ****p<0,001*; n=3

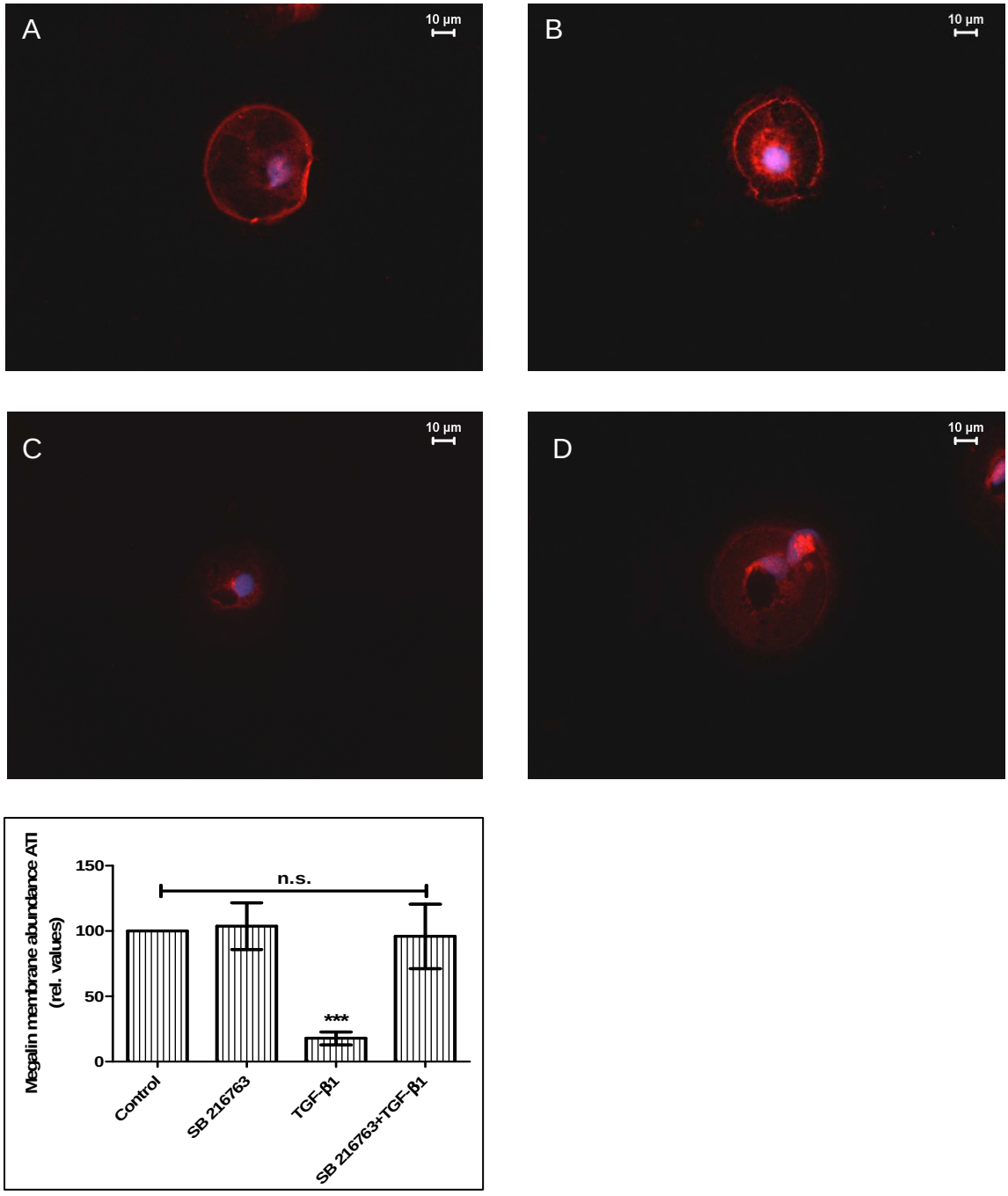

Figure 43: ***Inhibition of GSK3 prevents the effect of TGF-β1 on megalin surface abundance in primary rat ATI-like cells.***
Megalin surface distribution in absence (A) or presence (C) of TGF-β1, SB 216763 (B) and SB 216763 with TGF-β1 (D). ****p<0,001*; n=3

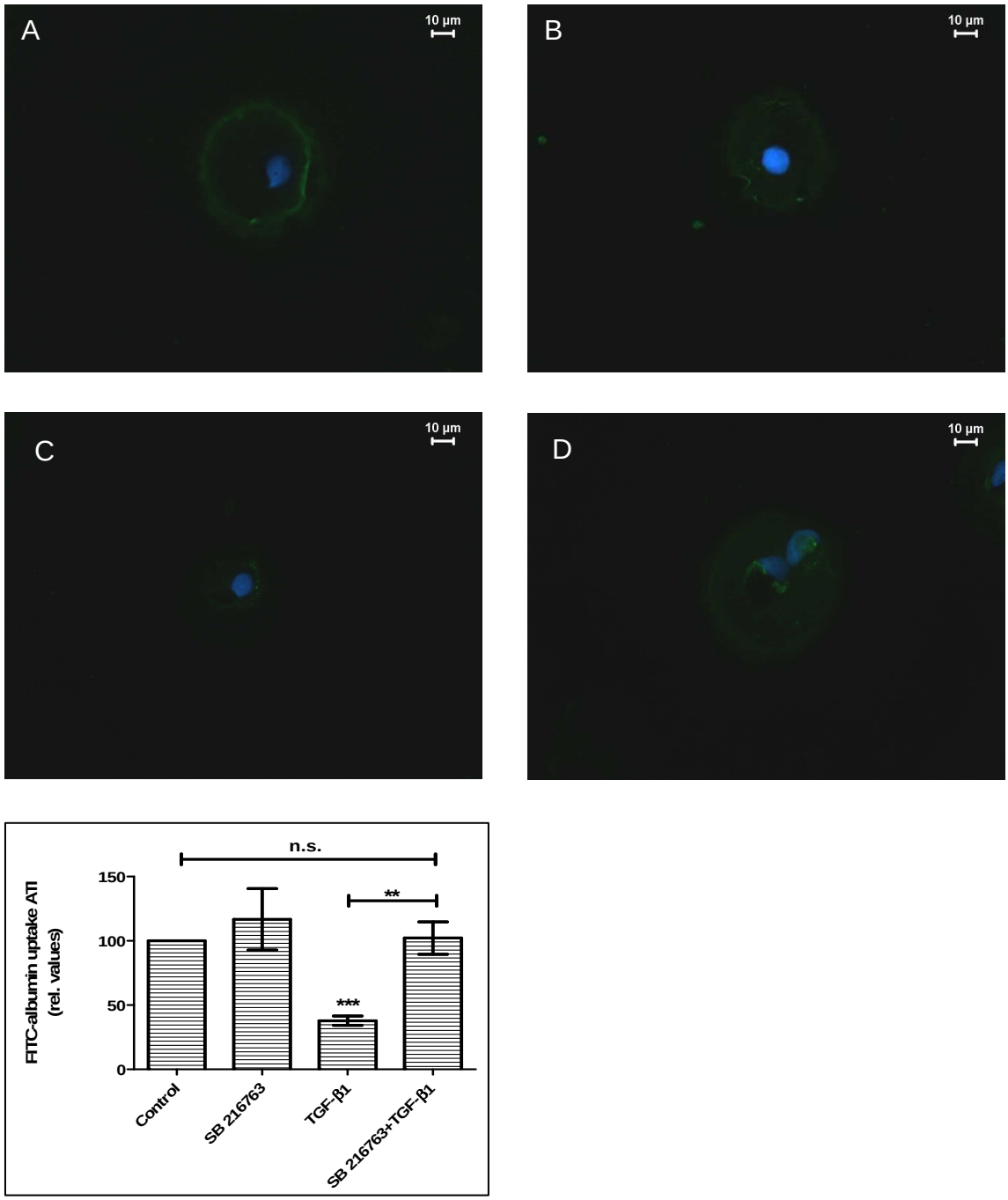

Figure 44: ***Inhibition of GSK3 prevents the effect of TGF-β1 on FITC-albumin uptake in primary rat ATI-like cells.***
FITC-albumin uptake in absence (A) or presence (C) of TGF-β1, SB 216763 (B) and combined with TGF-β1 (D). ****p<0,001*; n=3

To confirm these findings we performed cellular transport studies on permeable supports. We pre-incubated our cells with the GSK3 inhibitor SB 216763 before we challenged them with TGF- β1, each for 30 minutes, and measured its effect on binding, uptake and transepithelial transport of ^{125}I-albumin. For these experiments, once again, RLE-6TN cells, primary ATII cells and primary ATI-like cells were employed.

In presence of TGF- β1 only 27.9 ± 3.8 % of ^{125}I-albumin was bound to the cell surface in RLE-6TN cells; 47.4 ± 5,3 % in primary ATII cells and 38.3 ± 7.0 % in primary ATI-like cells, when compared to vehicle controls. When GSK3 was blocked before TGF- β1 application, 93.5 ± 5.1 % of ^{125}I-albumin was bound to RLE-6TN cells; 90.1 ± 5.5 % in ATII cells and 94.9 ± 5.7 % in ATI-like cells (**Figure 45**).

Uptake of ^{125}I-albumin by the cells was decreased to 51.7 ± 1.8 % in RLE-6TN cells; to 48.8 ± 8.0 % in ATII cells and to 50.2 ± 2.4 % in ATI-like cells when TGF- β1 was applied. Inhibition of GSK3 prevented the effect of TGF- β1, uptake was elevated to 98.1 ± 9.8 % in RLE-6TN cells; to 92.8 ± 5.3 % in ATII cells and to 97.0 ± 5.8 % in ATI-like cells. (**Figure 46**).

Transepithelial transport of ^{125}I-albumin after TGF- β1 challenge was decelerated to 35 ± 5.4 % in RLE-6TN cells; to 28.5 ± 2.5 % in ATII cells and to 36.3 ± 5.9 % in ATI-like cells. Inhibition of GSK3 abolished this effect, transport rates were at 96.7 ± 8.6 % in RLE-6TN cells; at 94.8 ±6.3 % in ATII cells and at 97.0 ± 5.8 % in ATI-like cells. (**Figure 47**).

The inhibitor, when applied alone, did not have any noteworthy effect on albumin binding, uptake or transepithelial transport in all three cell lines.

These data are in line with our results from immunofluorescence and FITC-albumin uptake, showing that the effect of TGF- β1 on albumin uptake by alveolar epithelial cells and albumin transport across the alveolar epithelium requires activity of GSK3.

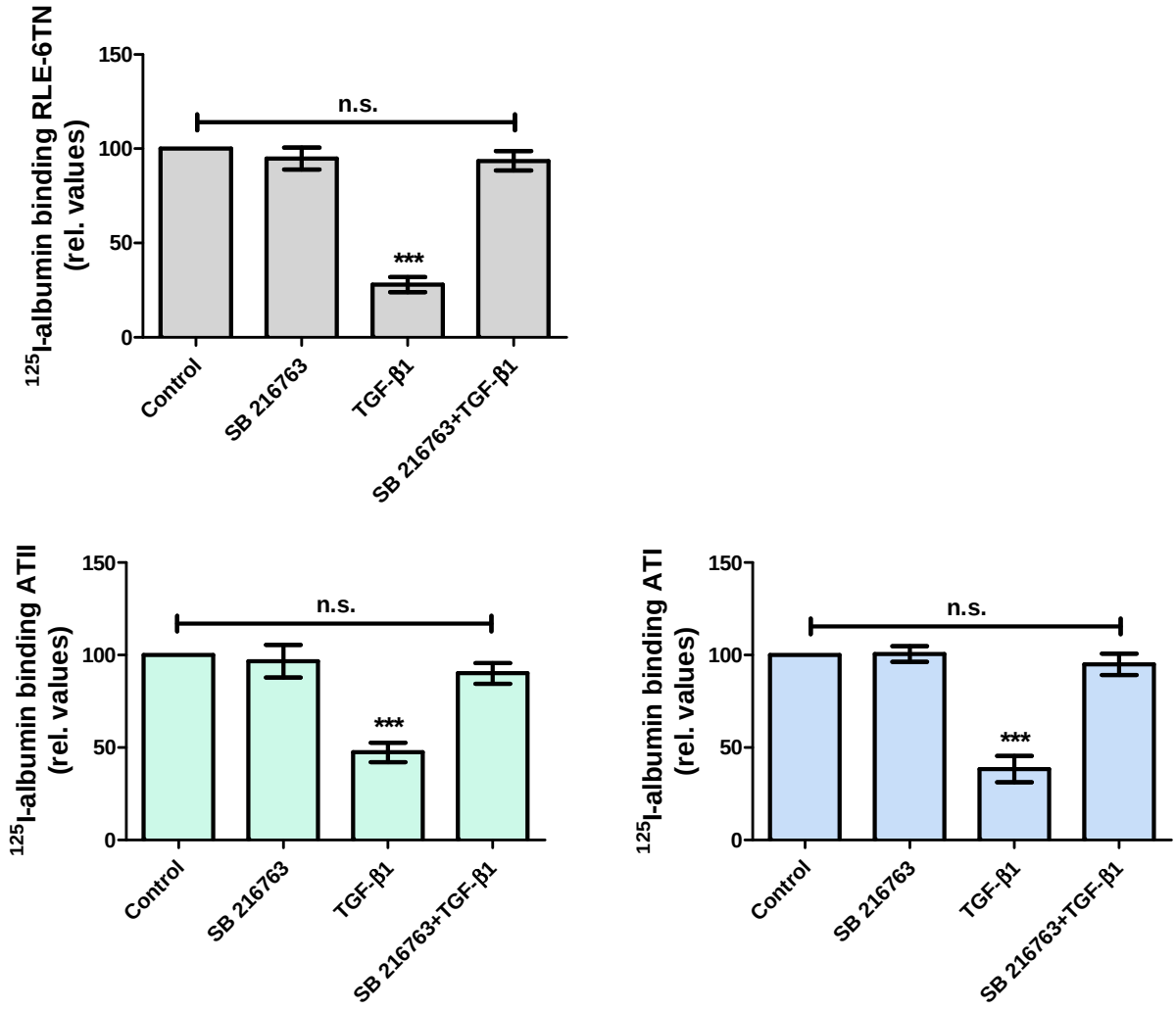

Figure 45: ***Binding of ^{125}I-albumin to RLE-6TN cells, primary rat alveolar epithelial type II (ATII) and type I-like (ATI) cells.***
Cells were pre-incubated in absence or presence of 30 μM SB 216763 prior to TGF-β1 challenge. The amount of surface bound ^{125}I-albumin was assessed by γ-radiation. ****p<0.001;* n=4

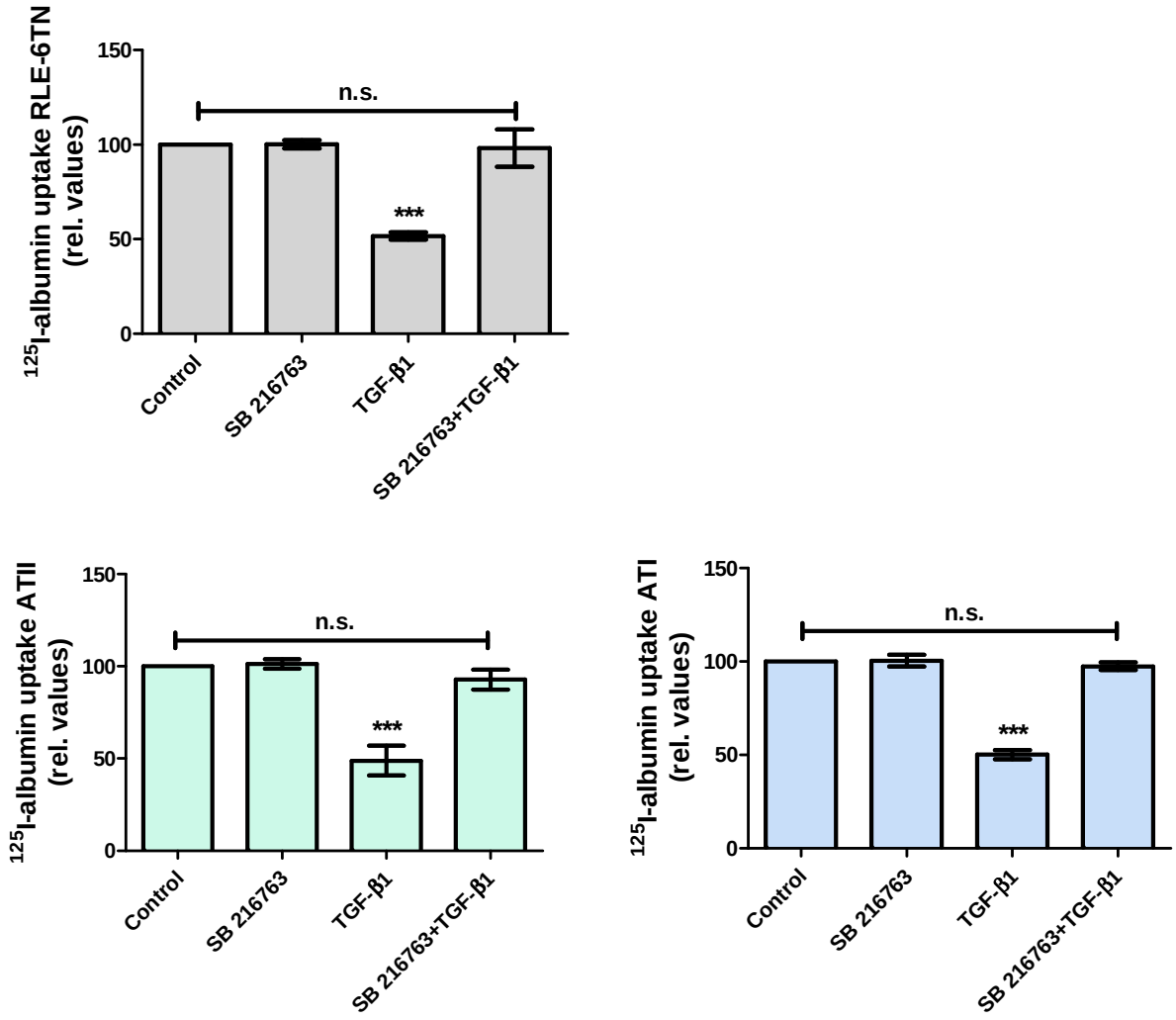

Figure 46: ***Uptake of ^{125}I-albumin by RLE-6TN cells, primary rat alveolar epithelial type II (ATII) and type I-like (ATI) cells.***

Cells were pre-incubated for 30 min in absence or presence of SB 216763 and subsequently challenged with TGF-β1. ^{125}I-albumin uptake was assessed by γ-radiation. ****p<0.001;* n=4

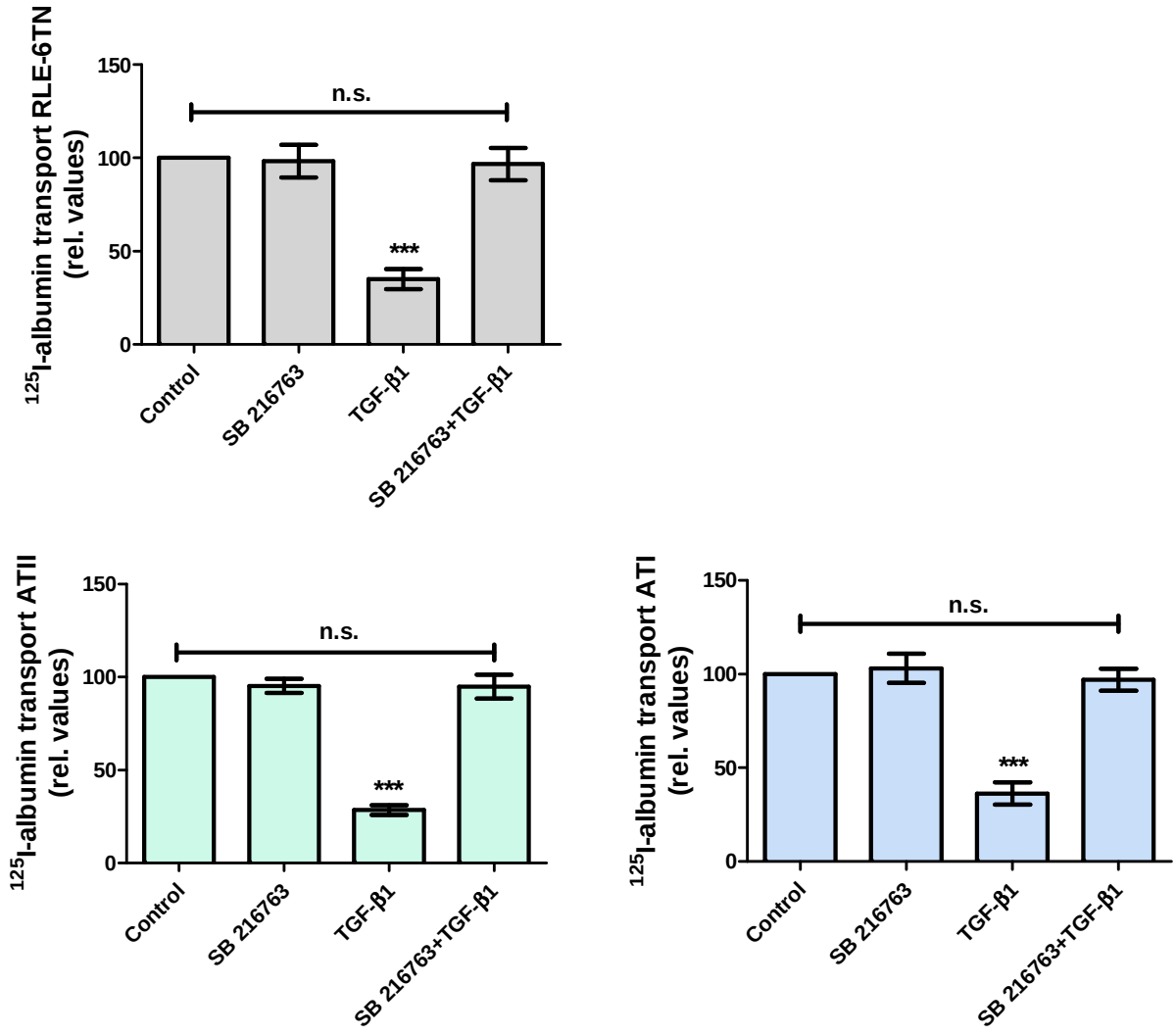

Figure 47: ***Transepithelial transport of ^{125}I-albumin across monolayers of RLE-6TN cells, primary rat alveolar epithelial type II (ATII) and type I-like (ATI) cells***
The amount of ^{125}I-albumin which was transported across the epithelial monolayer, with or without pre-treatment with SB 216763, was assessed by γ-radiation. ****p<0.001;* n=4

3.2.6 Inhibition of GSK3 as a therapeutic approach

There are several pathways using GSK3 as a regulator, some of them have been linked to human disease. As a component of the Wnt and the hedgehog pathway, it is involved in cell fate determination and morphology and thus, plays a role in several forms of cancer (Doble and Woodgett 2003). Lithium, an unspecific inhibitor of GSK3 (Stambolic et al. 1996), has been used as a therapy for bipolar disorders for decades. GSK3 has also been shown to play a role in non-insulin-dependent diabetes mellitus and its inhibition has ben discussed as a therapeutic tool (Kaidanovic and Eldar-Finkelman 2002).

We have already established that GSK3 is involved in the mechanism by which TGF-β1 impairs alveolar protein clearance in ARDS. When GSK3 was inhibited by application of the specific GSK3 inhibitor, SB 216763, the presence of TGF-β1 had almost no impact on albumin uptake and transport. To explore the use of SB 216763 as a therapeutic instrument in ARDS, we applied the GSK3 inhibitor to epithelial cells after TGF-β1 challenge and detected its effect on megalin surface distribution and FITC-albumin uptake by immunofluorescence.

Treatment of RLE-6TN cells with SB 216763 after TGF- β1 stimulation resulted in an elevated megalin surface expression of 99.0 ± 2.1 % and FITC-albumin uptake of 90.9 ± 12.4 % (**Figures 48 and 49**).

We found similar results in primary ATII cells. When SB 216763 was applied after TGF-β1 challenge, megalin abundance went up to 88.9 ± 7.2 % and FITC-albumin uptake elevated to 92.0 ± 3.6 % (**Figures 50 and 51**).

In ATI-like cells, megalin surface expression was restored to 93.4 ± 5.4 % and FITC-albumin uptake increased to 94.6 ± 1.3 % after treatment with SB 216763 (**Figures 52 and 53**).

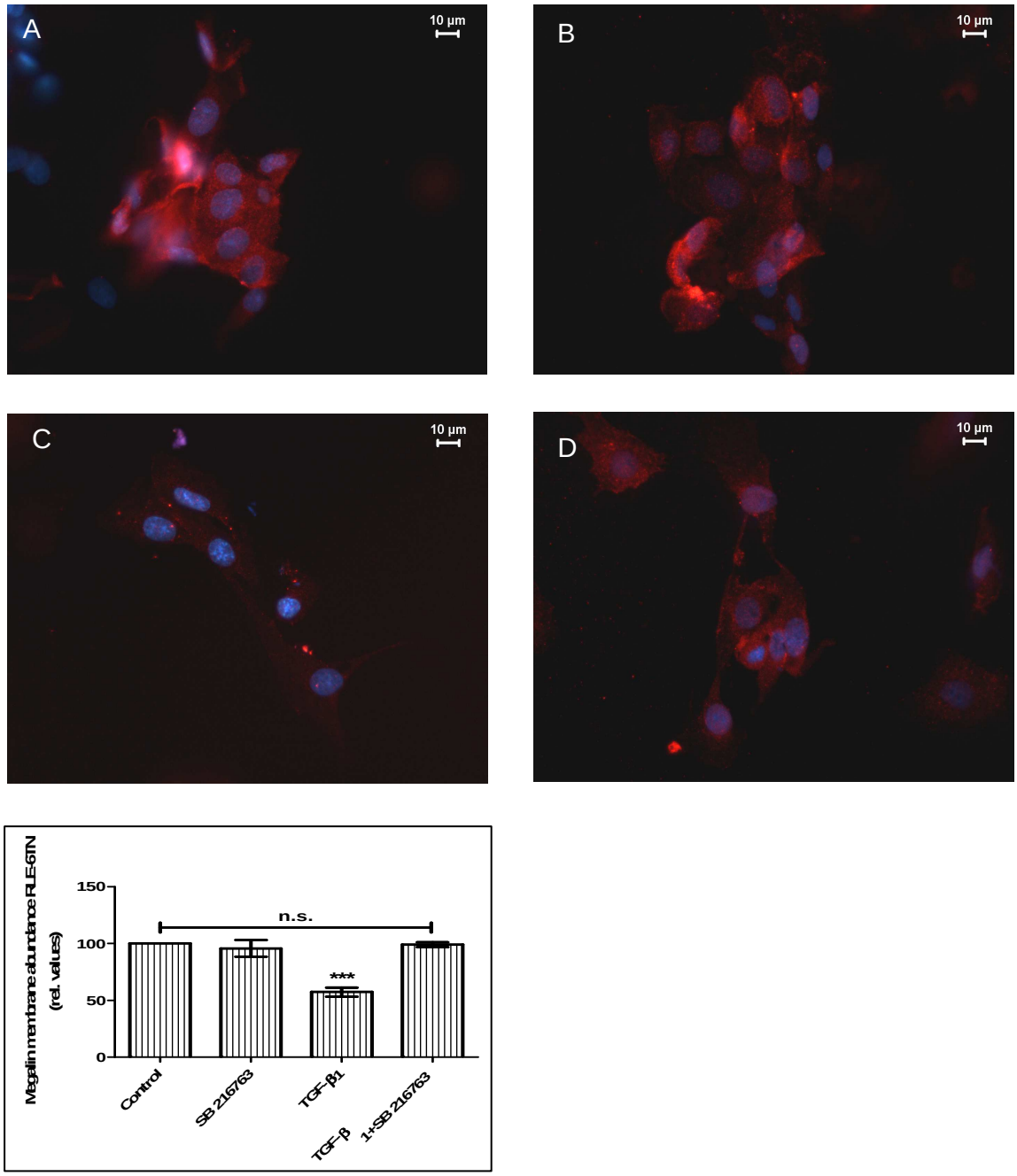

Figure 48: ***Treatment with SB 216763 restores megalin surface distribution in RLE-6TN cells.***
RLE-6TN cells were treated with SB 216763 after challenge with TGF-β1. Megalin membrane abundance was assessed by immunofluorescence.****p<0,001; n=3.*

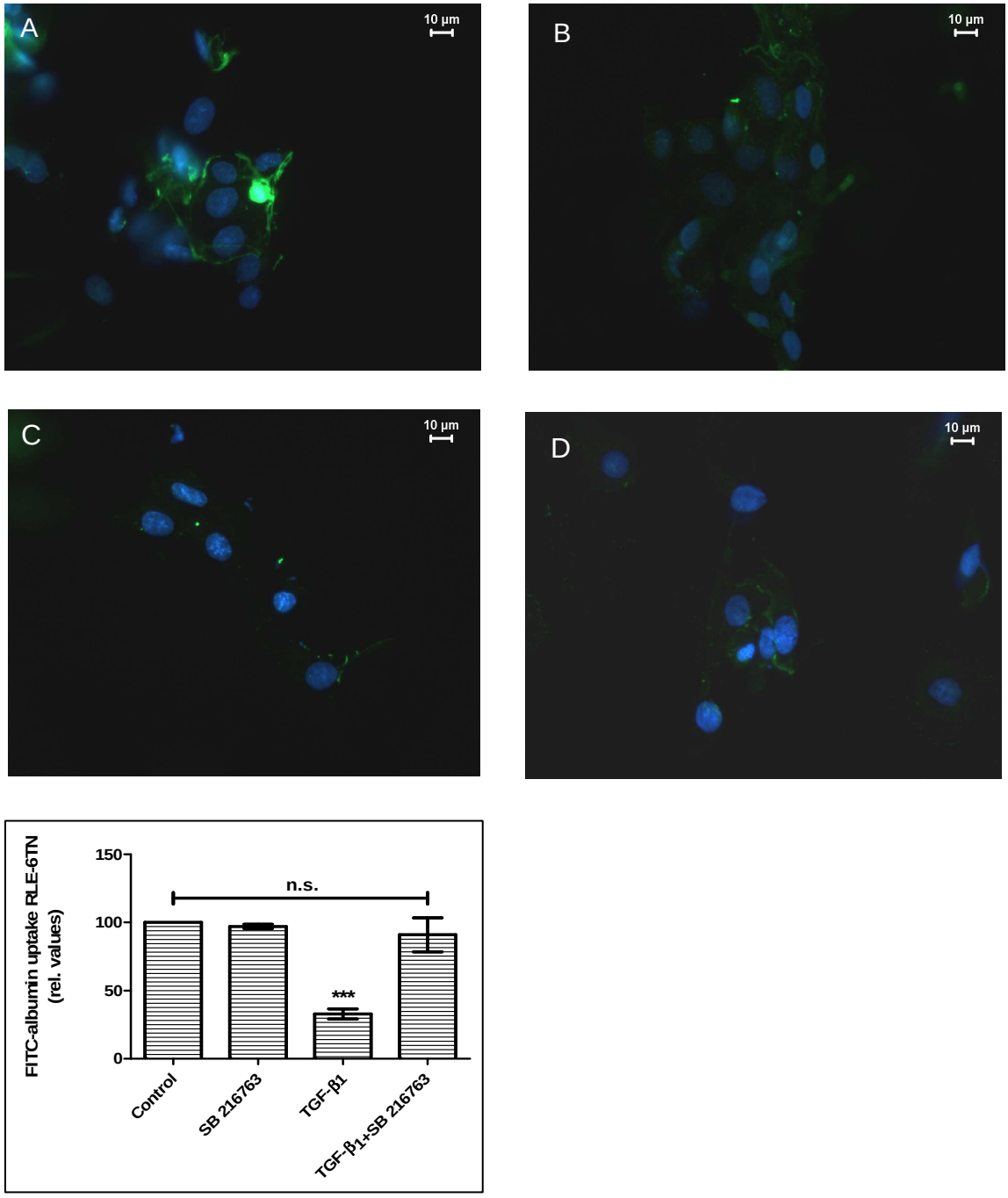

Figure 49: ***Treatment with SB 216763 reverses the effect of TGF-β1 on FITC-albumin uptake in RLE-6TN cells.***
RLE-6TN cells were first challenged with TGF-β1 and subsequently treated with SB 216763. FITC-albumin uptake was detected by fluorescence.****p<0,001; n=3.*

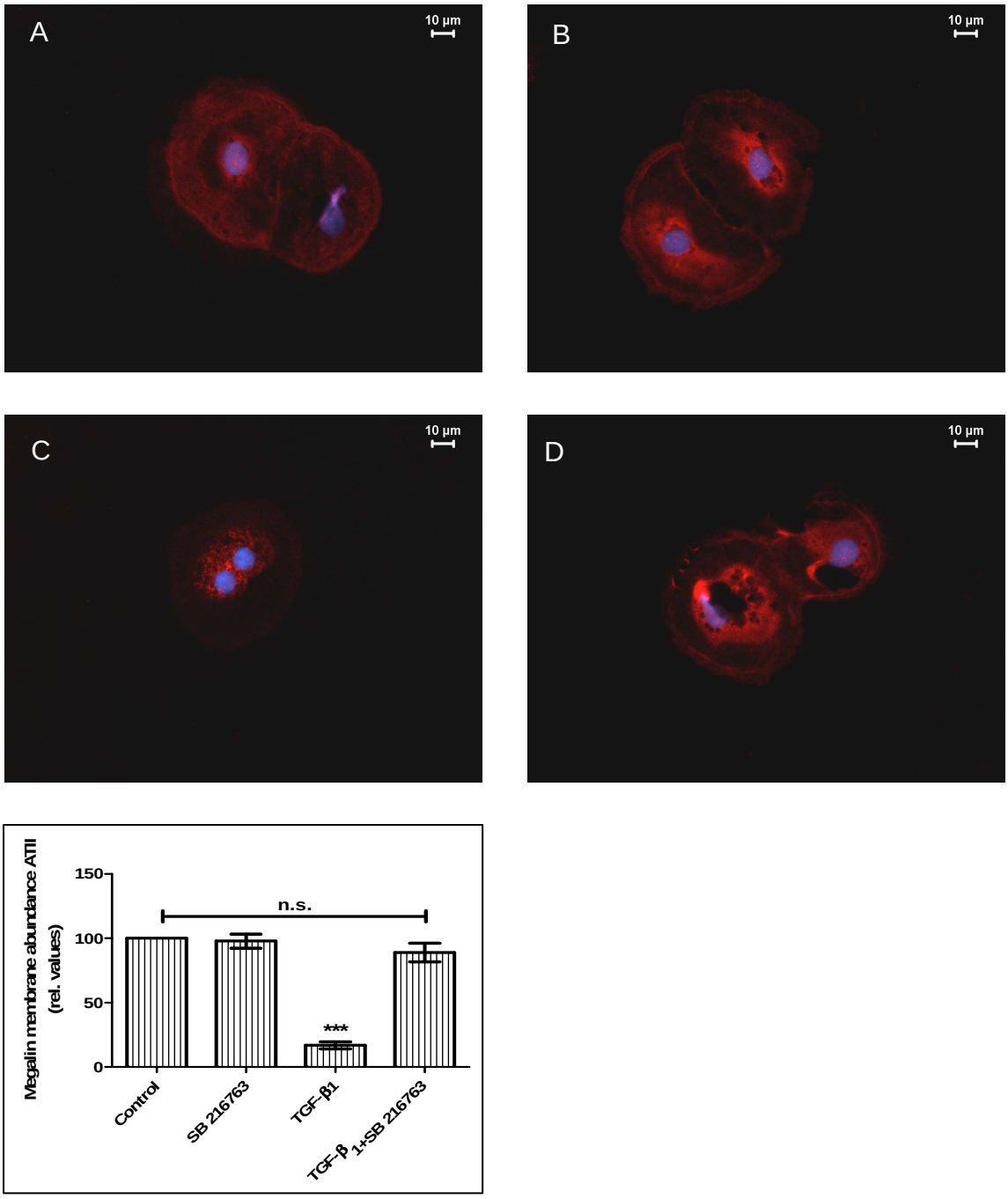

Figure 50: ***Treatment with SB 216763 reverses the effect of TGF-β1 on megalin surface distribution in primary ATII cells.***
ATII cells were challenged with TGF-β1 and treated with SB 216763, megalin membrane distribution was assessed by immunofluorescence.****p<0,001;n=3.*

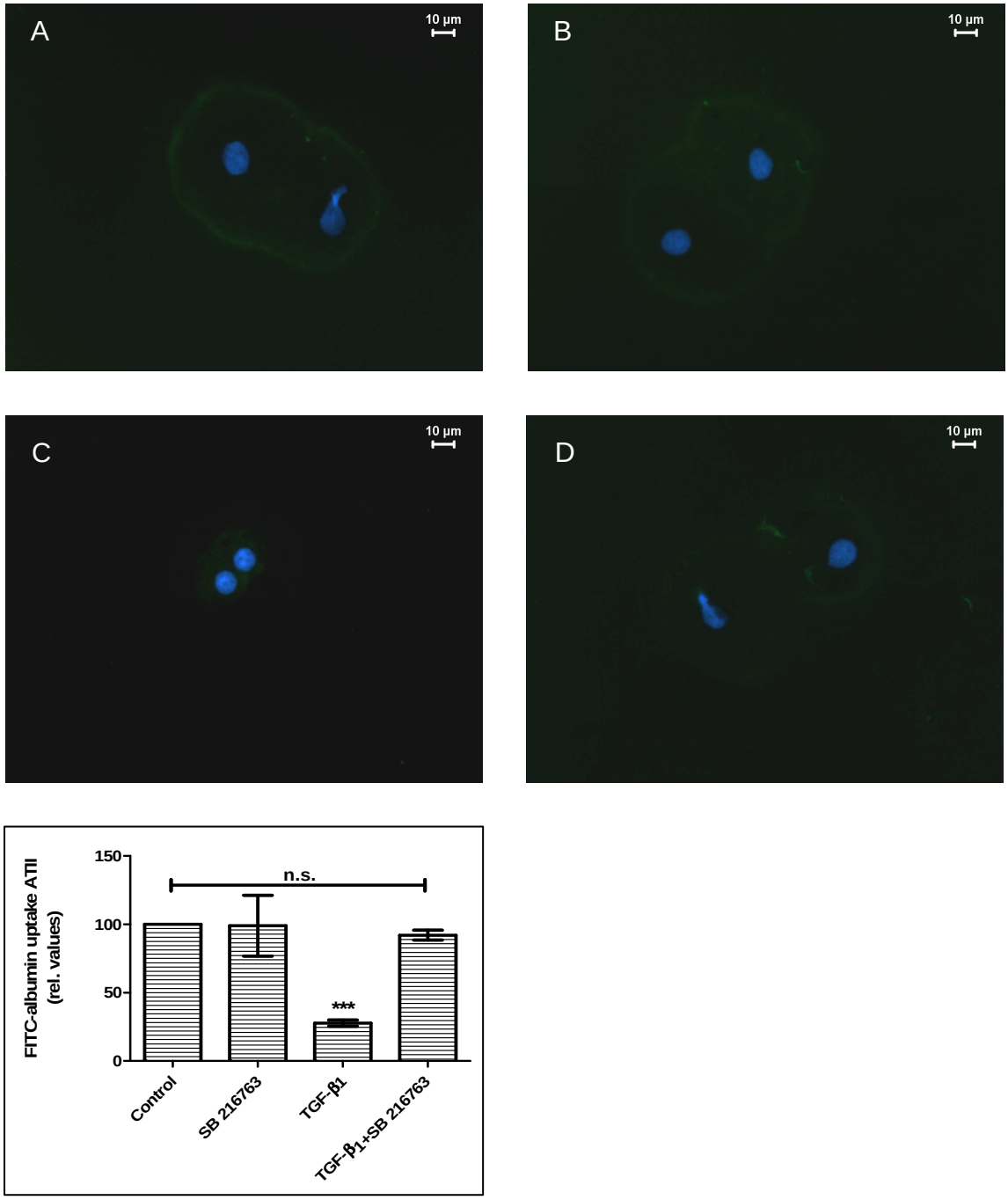

Figure 51: ***Treatment with SB 216763 restores physiological FITC-albumin uptake in primary ATII cells.***
ATII cells were treated with SB 216763 after TGF-β1 challenge and FITC-albumin uptake was detected by fluorescence microscopy. ****p<0,001; n=3.*

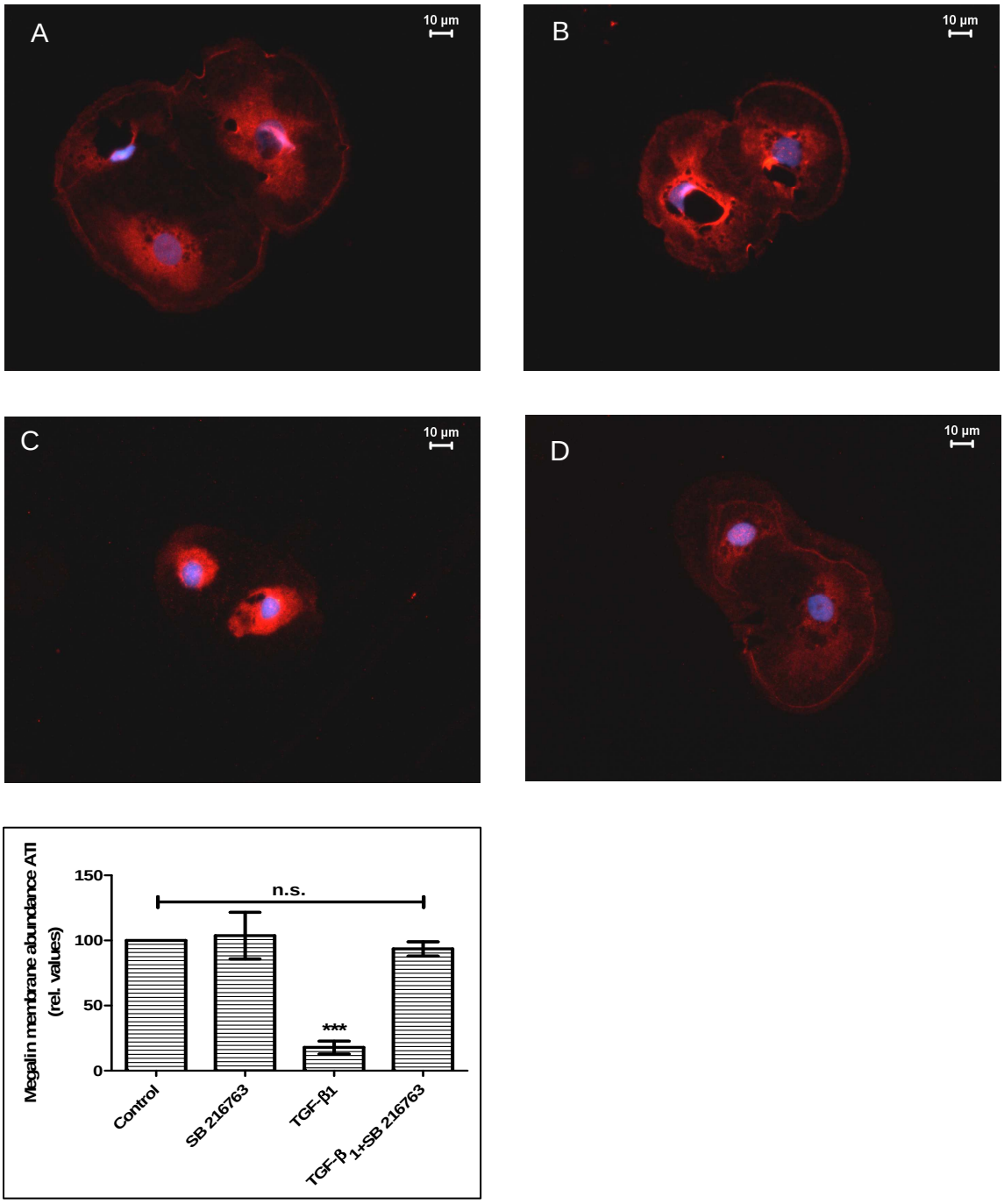

Figure 52: ***Treatment with SB 216763 restores megalin surface expression in primary ATI-like cells.***
ATI-like cells were challenged with TGF-β1 and subsequently treated with SB 216763, we assessed megalin membrane expression by immunofluorescence. ****p<0,001; n=3.*

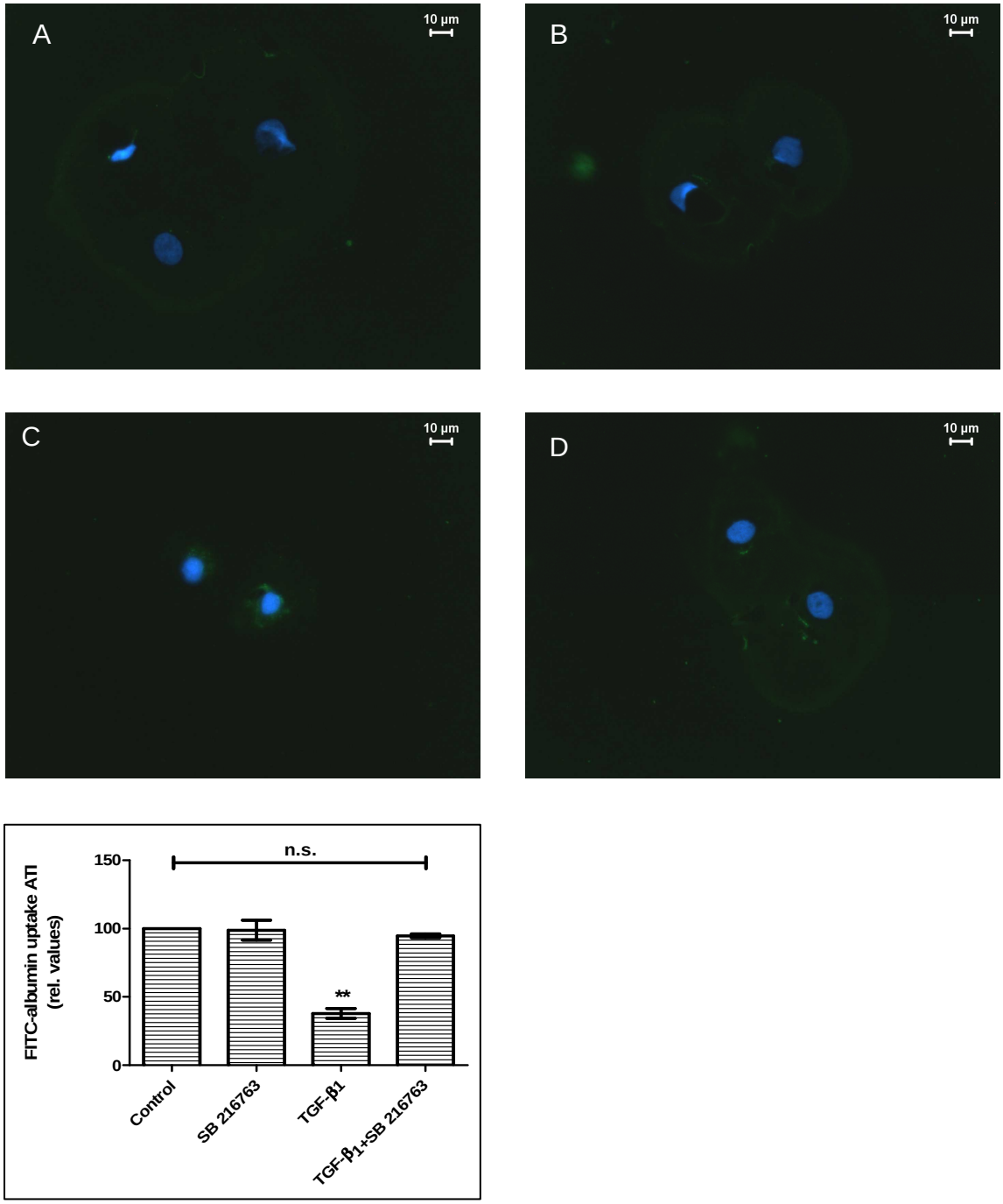

Figure 53: ***Treatment with SB 216763 restores FITC-albumin uptake in primary ATI-like cells.***
ATI-like cells were first challenged with TGF-β1 and treated with SB 216763. FITC-albumin uptake was detected by fluorescence microcopy. ***p<0,01;n=3.*

To confirm these findings we plated our alveolar epithelial cells on permeable supports and conducted cellular transport studies to assess binding, uptake and transepithelial transport of ^{125}I-albumin when cells were treated with SB 216763 after TGF-β1 challenge.

In RLE-6TN cells ^{125}I-albumin surface binding was increased to 93.7 ± 4.3 % after SB 216763 treatment. In ATII cells the inhibitor increased ^{125}I-albumin surface binding from 52.2 ± 7.1 % (with TGF-β1) to 92.6 ± 2.7 %. And in ATI-like cells the amount of surface bound ^{125}I-albumin went back to 93.9 ± 1.3 % after application of SB 216763 (**Figure 54**).

Uptake of ^{125}I-albumin by RLE-6TN cells increased to 99.1 ± 8.2 % after SB 216763 treatment. ATII cells presented with a decelerated ^{125}I-albumin uptake of 57.3 ± 6.6 % after TGF-β1 application and with an increased uptake rate of 89.5 ± 2.5 % after inhibitor treatment. In ATI-like cells, SB 216763 restored ^{125}I-albumin uptake to 92.3 ± 4.3 %, compared to controls (**Figure 55**).

Transepithelial transport ^{125}I-albumin across the cell monolayer displayed a delayed transport rate in RLE-6TN cells after TGF-β1 challenge and was increased to 99.5 ± 7.7 % after inhibitor treatment. In ATII cells, transport was elevated to 97.9 ± 8.7 % when cells were treated with SB 216763 after TGF-β1 application. In ATI-like cells, treatment with the inhibitor increased transepithelial transport to 89.9 ± 5.2 % (**Figure 56**).

The results of the cellular transport studies are in line with our microscopic findings and may suggest a potential role for the specific GSK3 inhibitor SB 2167663 as a novel therapeutic substance in the therapy of acute lung injury and ARDS.

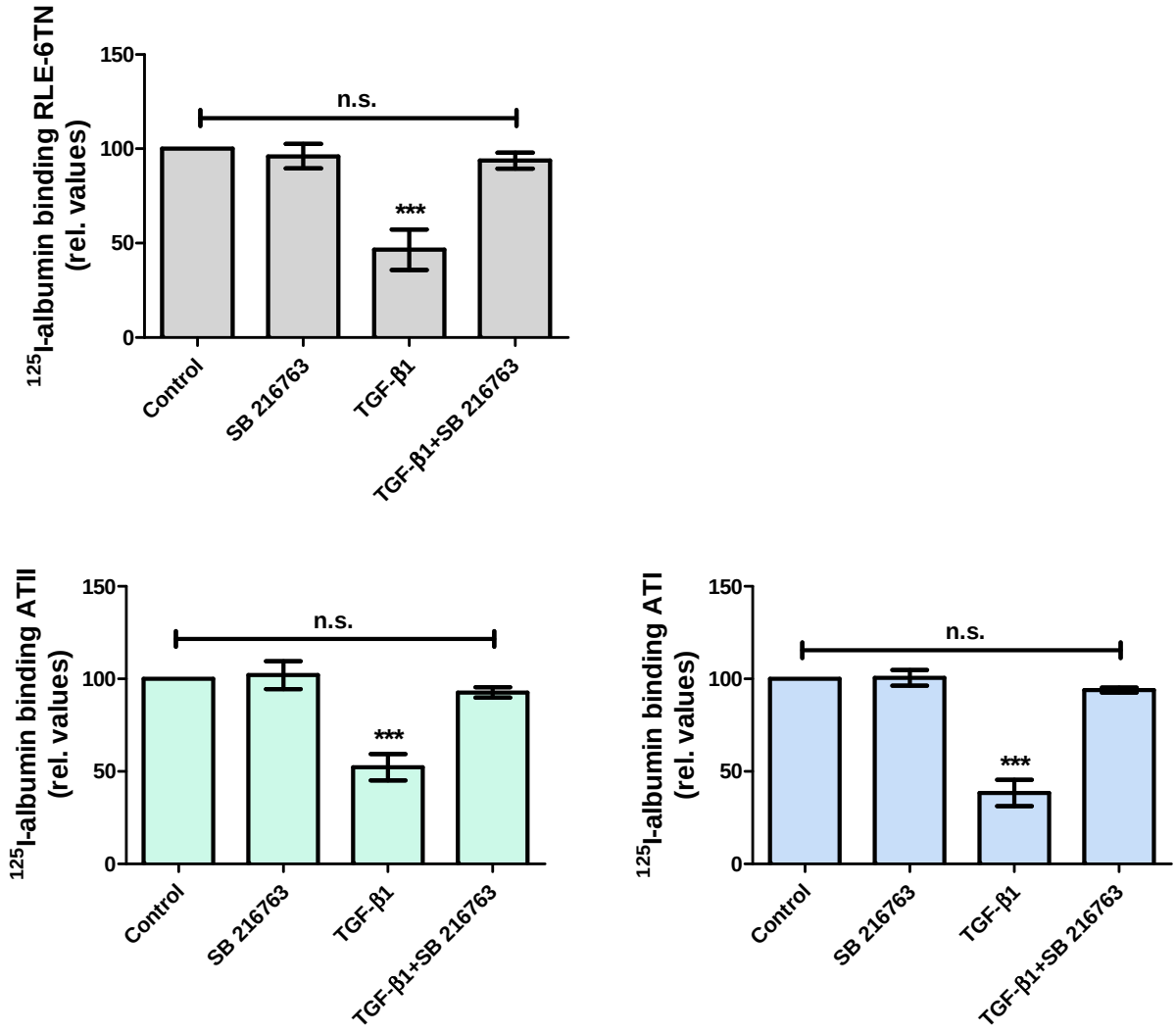

Figure 54: ***SB 216763 treatment after TGF-β1 challenge and its effect on ^{125}I-albumin binding to alveolar epithelial cells.***
RLE-6TN cells, ATII and ATI-like cells were treated with SB 216763 after challenge with TGF-β1. The amount of surface bound ^{125}I-albumin was assessed by γ-radiation. ****p<0,001; n=4.*

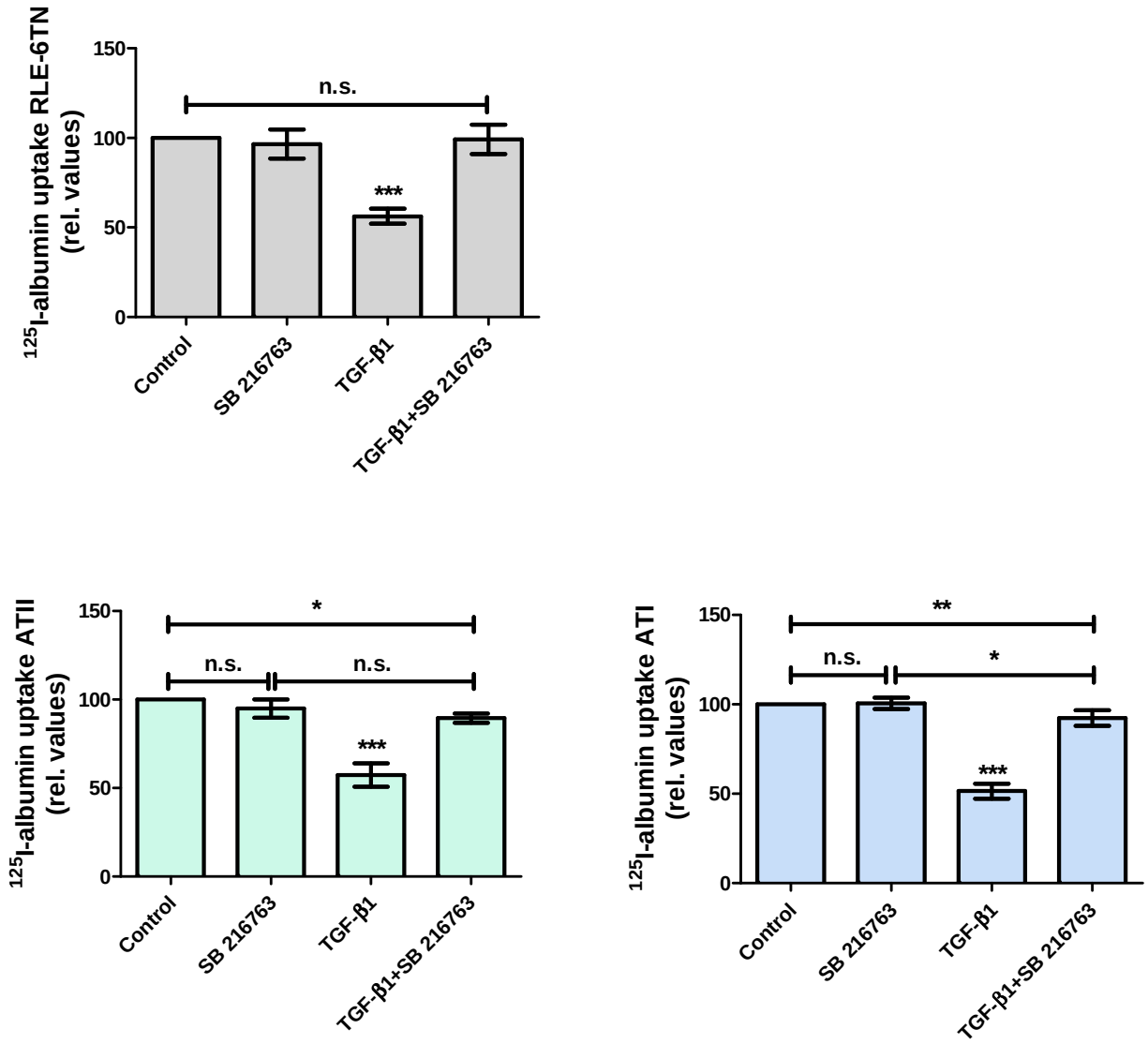

Figure 55: ***SB 216763 treatment after TGF-β1 challenge and its effect on ^{125}I-albumin uptake by alveolar epithelial cells.***
Epithelial cells were challenged with TGF-β1 and treated with SB 216763. Uptake of ^{125}I-albumin was assessed by γ-radiation.****p<0,001;**p<0,01;*p<0,05; n=4.*

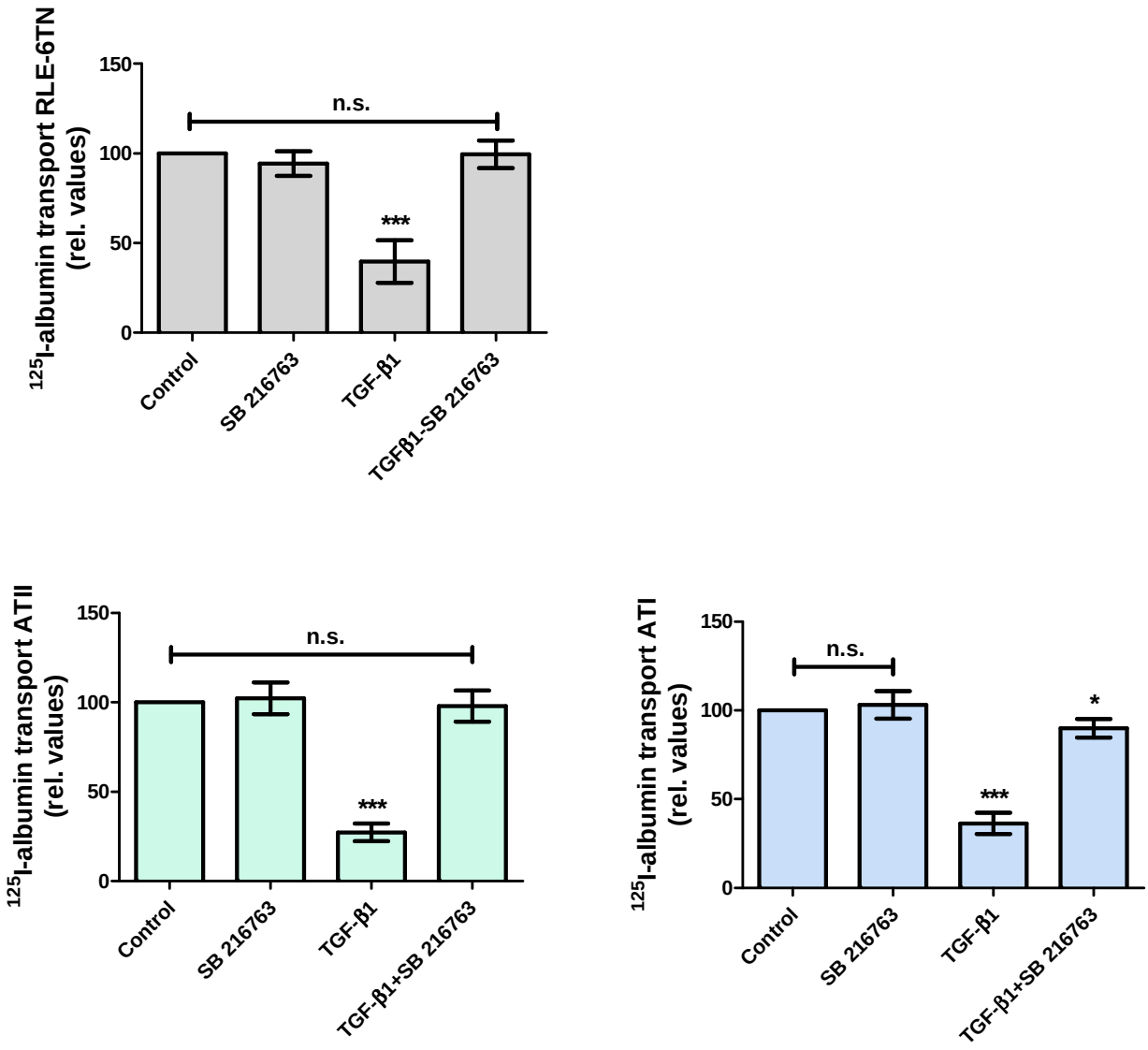

Figure 56: ***SB 216763 treatment after TGF-β1 challenge restores transepithelial transport rates of ^{125}I-albumin across monolayers of alveolar epithelial cells.***
RLE-6TN cells, ATII and ATI-like cells were first challenged with TGF-β1 and subsequently treated with SB 216763 before transepithelial transport of ^{125}I-albumin was assessed by γ-radiation. ****p<0,001;*p<0,05; n=4.*

4. Discussion

4.1 The importance of protein clearance in ARDS

The acute respiratory distress syndrome (ARDS) displays mortality rates of up to 40 % in approximately 200,000 critically ill patients in the United States annually. The clinical disorders that can cause the development of ARDS include sepsis, pneumonia and major trauma. ARDS is characterized by accumulation of protein-rich edema in the alveolar space, which causes severe hypoxemia and impaired carbon dioxide excretion. The lung injury is primarily caused by neutrophil-dependent and platelet-dependent damage to the endothelial and epithelial barriers of the lung. Resolution is delayed because of the epithelial injury, which prevents removal of alveolar edema fluid and therefore deprives the lung of adequate quantities of surfactant (Matthay and Zemans 2011). Of great importance is the clearance of plasma proteins from the alveolar space. Sodium and fluid is cleared from the lung quite rapidly via active transport processes, leading to increased protein concentration in the alveolar compartment. This increased concentration of protein creates an oncotic gradient which leads to a re-entry of fluid, thereby preventing edema resolution. Moreover, precipitates of excess protein can accumulate in the alveolar space and it has been demonstrated that non-survivors of ARDS exhibit threefold higher levels of precipitated protein in their edema fluid than survivors of the disease (Bachofen and Weibel 1977). In addition, excess protein in the alveolar compartment may contribute to hyaline membrane formation and promote lung fibrosis (Kobashi and Manabe 1993; Tomashefski 1990). Thus, resolution of alveolar edema is crucial for the patient's survival and better understanding of the mechanisms by which proteins are cleared from the distal air spaces may contribute to find new therapeutic approaches and to improve outcome.

4.2 Albumin transport in primary alveolar epithelial cells is an active process

Whether albumin transport across the alveolo-capillary barrier is an active process remains controversial. Fluid-filled lungs have been used for decades to investigate transport properties of the lung. Transport rates of albumin, which were assessed through this experimental model vary from 0.06 %/min in sheep (Peterson, Dickerson et al. 1989), 0.02 %/min in rabbits (Hastings, Grady et al. 1992) and 0.007 %/min in rats (Jayr, Garat et al. 1994). These data led to the conclusion that albumin transport is extremely slow. The intactness of the alveolo-capillary barrier has been accounted for the low transport rate of albumin (Hastings, Grady et al. 1992; Hastings, Wright et al. 1994; Wangensteen, Bartlett et al. 1996). In addition, the protein which was instilled into the lungs comprised a high quantity of plasma proteins, including native albumin (Hastings, Wright et al. 1994; Wangensteen, Bartlett et al. 1996). Thus, it is likely that these studies assessed passive transport of albumin whereas active transport was competitive inhibited by native albumin. Previous studies by our group established a ^{125}I-albumin transport rate of 0.25 %/min in the isolated, ventilated and perfused rabbit lung (Rummel 2007). Albumin clearance from the isolated lung was a temperature-sensitive process and was nearly completely shut down at 4 °C (Rummel 2007). At this temperature all active transport properties are completely inhibited (Rutschman, Olivera et al. 1993) and albumin transport can only occur *via* passive transepithelial movement. Another attribute of active transport, besides temperature-sensitivity, is that it can be saturated. Recent studies in our lab in cultured A549 cells demonstrated almost complete blockage of ^{125}I-albumin uptake in presence of a 1000fold molar excess of native albumin (Rummel 2007). Although A549 cells are a widely accepted *in vitro* model of type II pneumocytes (Foster, Oster et al. 1998), these cells are lacking important features of primary epithelial cells. A549 cells do not polarize and are unable to form completely developed intercellular junctions. Thus, these cells are not capable of forming electrophysiologically tight monolayers (Foster, Oster et al. 1998) and therefore can not be employed to investigate transepithelial transport. A549 cells only represent type II pneumocytes and type I cells are found in similar numbers in the alveolar epithelium (Mutlu and Sznajder 2005). Furthermore, type I cells represent more than 95 % of the alveolar surface area (Mutlu and Sznajder 2005) and are known to regulate fluid balance in the lung *via* epithelial sodium channels and aquaporin water channels (Johnson et al. 2002; Matthay et al. 2002). Moreover, exhibiting high abundance of microvessicles, ATI cells may also contribute to transport of macromolecules (Gumbleton et

al. 2003), such as proteins. Considering comparable transport rates in both cell types, the contribution of ATI cells to the transport of macromolecules would be highly relevant. Additionally, one may speculate that because of their flat shape, passage of macromolecules across type I cells might be more rapid. Thus, we employed both cell types of the alveolar epithelium as primary isolated rat ATII and ATI-like cells to investigate the mechanisms of protein transport in the lung. Since it is technically difficult to isolate and culture alveolar epithelial type I cells, many investigators have exploited the transformation of isolated AT II cells to AT I-like cells in vitro (Borok et al.1998; Campbell et al. 1999). We and others have previously demonstrated that ATII cells at day seven transform into ATI-like cells (Ridge et al. 1997). Therefore, we used primary cells for experiments at day three (ATII) and day seven (ATI-like).

We conducted cellular transport studies in which we detected the transport of radiolabeled albumin (^{125}I-albumin) across tight monolayers of primary alveolar epithelial cells. We set out to determine whether albumin transport across primary ATII and ATI-like cells is facilitated by an active process. One typical characteristic of an active transport process is that it can be competed out by an excess of the substrate. Thus, we applied a 1000fold molar excess of unlabeled native albumin to the cell monolayers before incubation of ^{125}I-albumin. We assessed binding of ^{125}I-albumin to the cell surface of ATII and ATI-like cells, as well as ^{125}I-albumin uptake by the cells. Since cells were plated on permeable supports measurement of transepithelial transport was also possible. Binding, uptake and transepithelial transport of ^{125}I-albumin were almost completely blocked by competition with unlabeled albumin, in both alveolar epithelial cell lines. In addition, we used fluorescence microscopy to detect uptake of FITC-albumin in presence of excess native albumin and obtained similar results. These data indicate that ^{125}I-albumin uptake by primary alveolar epithelial cells and its subsequent transcytosis are facilitated by an active transport process which can be competitively inhibited. Furthermore, these data implicate a receptor-mediated endocytic process since non-specific fluid-phase uptake (macropinocytosis) is a much slower process (John, Vogel et al. 2001; Kim and Malik 2003) and can not be competed out by the presence of other macromolecules (Conner and Schmid 2003).

4.3 Albumin uptake in the alveolar epithelium is mediated by megalin via clathrin-dependent endocytosis

A high efficiency of endocytosis is achieved by specific high-affinity receptors (receptor-mediated endocytosis) (Conner and Schmid 2003). The main receptor-mediated endocytic pathways include caveolae-mediated and clathrin-dependent endocytosis. Caveolin-coated vesicles (caveolae) and clathrin-coated pits are both present in alveolar type I and type II cells (Mostov and Cardone et al. 1995; Kasper, Reimann et al. 1998; Campbell, Hollins et al. 1999; John, Vogel et al. 2001). A ~ 60 kDa plasma membrane sialoglycoprotein (gp 60) was identified as an endothelial albumin receptor that facilitates protein uptake *via* caveolae-mediated endocytosis (Schnitzer and Ulmer et al. 1990). This receptor has also been proposed to play a role in epithelial albumin uptake (John, Vogel et al. 2001; Kim and Malik 2003). Previous studies by our group have demonstrated that inhibition of caveolae-mediated endocytosis resulted in a partial inhibition of ^{125}I-albumin clearance from the alveolar space in isolated rabbit lungs (Rummel 2007). Interestingly, two recent sudies have documented that the involvement of caveolae-mediated endocytosis of albumin *via* gp 60 in alveolar epithelial cells played only a minor role compared to clathrin-dependent processes (Yumoto et al. 2006; Ikehata and Yumoto et al. 2008). Since application of indomethacin (Visser, stevanovic et al. 2004), methyl-β-cyclodextrin and nystatin (Kim et al. 2007) , inhibitors of cavelolae-mediated endocytosis, in cultured RLE-6TN cells (Yumoto et al. 2006) and in rat primary type II and type I-like cells (Ikehata and Yumoto et al. 2008) resulted in a non-significant reduction of FITC-albumin uptake by these cells. Additionally, these studies reported a very low expression of *caveolin-1* mRNA and *caveolin-1* protein in type II cells. The role of clathrin-dependent endocytosis was also investigated by employing chlorpromazine (Wang, Rothberg et al. 1993) and phenylarsine oxide (Visser, Stevanovic et al. 2004), two known inhibitors of this endocytic pathway. Application of these inhibitors significantly decreased FITC-albumin uptake in type II and type I-like cells. Furthermore, these reports documented a high expression of clathrin heavy chain mRNA in both cell types, suggesting that clathrin-dependent endocytosis is the key mediator of albumin uptake in alveolar epithelial cells. These findings are in line with several studies that established clathrin-dependent endocytosis as the predominant pathway for macromolecule uptake along epithelia (Mukherjee et al. 1997; Schmid 1997; Christensen and Birn 2002).

Potential receptors for clathrin-dependent endocytosis of albumin in the alveolar epithelium are the tandem endocytic receptors megalin and cubilin. These receptors are

known to play an important role in clathrin-mediated endocytosis of proteins including albumin, in the kidney (Christensen and Birn, 2001). Renal proximal tubular epithelial cells reabsorb and subsequently metabolize proteins in glomerular filtrates. Disruption of clathrin-dependent and megalin-mediated endocytosis of albumin can induce cell damage, proteinuria and promote the development of chronic kidney disease (Saito et al. 2009). Moreover, megalin deficient mice present with severe forebrain abnormalities and lung defects (Willnow et al. 1996) and usually die perinatally. Survivors serve as an animal model for low molecular weight proteinuria (LeHeste et al. 1999).

Megalin, a member of the low-density lipoprotein receptor gene family, is a multiligand endocytic receptor and is abundantly expressed and located in clathrin-coated pits in the apical membrane of renal proximal tubular epithelial cells (Farquhar et al. 1995). Cubilin, another multi-ligand endocytic receptor, is co-expressed with megalin in renal proximal tubules. Since cubilin, in contrast to megalin, has no transmembrane domain, megalin is assumed to mediate endocytosis of cubilin and its ligands (Christensen and Birn 2001). The two receptors co-localize in several tissues that include absorptive epithelia, such as the alveolar epithelium. Moreover, expression of megalin and cubilin has been shown in alveolar type II and type I-like cells (Kolleck et al. 2002; Ikehata et al. 2008).

Although megalin and cubilin are expressed in alveolar epithelial cells, involvement of the receptors in albumin uptake by ATII and ATI-like cells has not yet been reported. To investigate whether megalin and cubilin mediate albumin uptake in a certain cell type, one can employ receptor associated protein (RAP) which binds to both receptors with high affinity and therefore partially blocks albumin-binding by competition (Verroust et al. 2002). Adminsitration of RAP in cultured opossum kidney proximal tubule cells resulted in almost complete inhibition of BSA-FITC uptake (Zhai et al. 2000). Thus, we treated rat primary ATII and ATI-like cells with RAP before we conducted cellular transport studies and assessed its impact on binding, uptake and transepithelial transport of ^{125}I-albumin. Binding of ^{125}I-albumin to the cell surface, uptake by epithelial cells and transepithelial transport were significantly decreased when cells were treated with RAP in both, type II and type I-like cells. These findings were confirmed by fluorescence microscopy, where we detected the effect of RAP on FITC-albumin uptake in both cell types.

However, pharmacological inhibitors may have non-specific effects on unrelated proteins, receptors and signaling pathways. RAP, for instance, is also known to modulate ligand interactions with LDL receptor-related protein (LRP), another multi-ligand receptor in the low-density lipoprotein receptor family (Herz at al. 1991). Thus, to further elucidate the

specific role of megalin and cubilin in albumin uptake by alveolar epithelial cells, a genetic approach to specifically knock down megalin was employed. Since only megalin exhibits a transmembrane domain and therefore is presumed to facilitate endocytosis of ligands and cubilin, we set out to silence megalin gene expression by RNA interference. It is commonly known that primary alveolar epithelial cells display very low transfection efficiency, therefore we used cultured rat lung epithelial cells (RLE-6TN). Since this immortalized cell line presents with several characteristics of primary ATII cells, such as alkaline phosphatase activity and expression of cytokeratin 19 mRNA (Yumoto et al. 2006), RLE-6TN cells have been established as an *in vitro* model system for ATII cells.

Importantly, we observed comparable albumin transport kinetics in RLE-6TN cells as in primary ATII and ATI-like cells. Therefore, assuming that the mechanisms of albumin transport are the same in RLE-6TN cells as in ATII and ATI-like cells, we knocked down megalin gene expression by short interference RNA and performed cellular transport studies. In megalin knocked down cells the uptake of ^{125}I-albumin and FITC-albumin was almost completely blocked, as well as the binding and transepithelial transport of ^{125}I-albumin. Collectively, these findings indicate that megalin facilitates albumin endocytosis in the alveolar epithelium of the lung.

4.4 TGF-β impairs uptake and transepithelial transport of albumin across the alveolar epithelium by downregulating megalin surface abundance

Numerous cytokines are participating in the development of ARDS (Baughman et al. 1996). Since transforming growth factor (TGF)-β contributes to cell proliferation and fibrosis, it is considered to play a significant role in the pathology of lung injury. The association between mortality and pulmonary fibrosis in ARDS has been well documented (Martin, Papazian et al. 1995). Tissue injury induces upregulation of the TGF-β1 gene, and TGF-β1 is directly involved in fibrosis and wound repair (Singer and Clark 1999). Since fibroproliferative ARDS is a pathologic type of tissue repair, TGF-β1 might be a key molecule in the pathophysiology of ARDS, and particularly of progressive lung fibrosis (Fahy et al. 2003). In addition, several animal models of acute lung injury implicate a role for TGF-β1 in ARDS. After inducing acute lung injury in mice by bleomycin or *Escherichia coli* endotoxin, development of pulmonary edema was prevented by pharmacological inhibition of TGF-β by a TGF-β soluble

receptor (Pittet et al. 2001). The same inhibitor reduced bleomycin induced fibrosis in hamsters (Wang et al. 1999). Recent studies have documented elevated levels of active TGF-β1 in BAL fluids of patients with ARDS within the first 24 hours of diagnosis (Fahy et al. 2003), suggesting a critical role for TGF-β1 in the acute phase of ARDS. In immortalized rat renal proximal tubule cells, TGF-β1 reduced albumin binding to confluent cell monolayers and therefore its subsequent uptake. This effect of TGF-β1 was imputed to a decreased megalin expression in the cells (Russo et al. 2007). In our study we sought to investigate the effect of TGF-β1 on albumin clearance from the alveolar space. We applied TGF-β1, at a concentration that is pathophysiologically relevant in patients with acute lung injury, to the isolated, ventilated and perfused rabbit lung and detected its effect on ^{125}I-albumin clearance. Movement of the radio-labeled tracer from the alveolar space to the vasculature was measured by γ-radiation in real-time and the rate of active albumin clearance from the alveolar space was decreased by ~ 48 % when TGF-β1 was applied. To further elucidate the effect of TGF-β1 on albumin transport we conducted cellular studies in primary ATII, ATI-like and RLE-6TN cells. The amount of surface bound ^{125}I-albumin was significantly decreased when cells were challenged with TGF-β1, and accordingly uptake and transepithelial transport of ^{125}I-albumin were markedly reduced. Presence of TGF-β1 has been shown to facilitate development of pulmonary edema (Pittet et al. 2001) and promote lung fibrosis (Wang et al. 1999). In the present study, TGF-β1 markedly impaired albumin transport across the alveolo-capillary barrier in an intact rabbit lung model. Thus, we identified a novel mechanism by which TGF-β1 may contribute to the pathogenesis of ARDS.

In the present study we have shown that protein transport in alveolar epithelial cells is mediated by megalin. Since TGF-β1 decreased albumin transport in our experiments, we were wondering if the growth factor might interfere with the receptor. In immortalized rat renal proximal tubule cells, stimulation with TGF-β1 for 24 hours reduced albumin binding to confluent cell monolayers and its subsequent uptake. This effect of TGF-β1 was attributed to a decreased megalin expression in the cells (Russo et al. 2007). In another study, treatment of proximal-tubule-derived opossum kidney cells with TGF-β1 for 48 hours resulted in downregulation of megalin-cubilin-mediated endocytosis of albumin. This effect was ascribed to a reduced cubilin and megalin expression in the membrane fraction of the cells (Gekle et al. 2003). Since in our study, impairment of protein transport was a rapid effect, downregulation of megalin expression by TGF-β1 seems rather unlikely. Therefore, we assumed that the effect of TGF-β1 on megalin-mediated albumin uptake was facilitated by posttranslational modification of the receptor. Phosphorylation has been reported to play a key role in cell

surface stability of megalin (Yuseff et al. 2007). To investigate whether TGF-β1 affects surface expression of megalin, we applied the growth factor to primary ATII and ATI-like cells, as well as cultured RLE-6TN cells and analyzed megalin membrane distribution by immunofluorescence. We detected markedly decreased megalin membrane abundance in response to TGF-β1 in all three cell types. As assessed by fluorescence microscopy, reduced megalin surface distribution under TGF-β1 stimulation directly correlated with decreased uptake of FITC-albumin in alveolar epithelial cells. These findings support the presumption that TGF-β1 mediates endocytosis of megalin from the plasma membrane and thereby impairs albumin transport in the lung.

As mentioned before, endocytosis of megalin is facilitated by phosphorylation of the receptor. The cytoplasmic domain of megalin contains phosphorylation sites for several kinases, including PKC, CK-II and PKA, all of which were able to phosphorylate the receptor *in vitro* but failed to phosphorylate megalin under *in vivo* conditions. Yuseff et al. (2007) identified a PPPSP motif in the cytoplasmic domain which represented a phosphorylation site for GSK3. Moreover, it has been demonstrated that active GSK3 was able to phosphorylate megalin *in vivo* which resulted in decreased megalin membrane expression by promoting endocytosis of the receptor.

Unlike most kinases, GSK3 is constitutively phosphorylated in the cell, which represents the inactive form of the kinase. In order for GSK3 to be activated it must be dephosphorylated at Ser-21(GSK3 α) or at Ser-9 (GSK3 β) (Cross et al. 1995). Activity of the kinase increases proportional to the grade of dephosphorylation at the serine residues. Several studies have indicated an association of GSK3 activation with various pathological conditions, including diabetes mellitus, obesity, inflammation, neurological disorders and tumor development (Wada 2009; Rayasam 2009; Woodgett 2003). Since TGF-β1 has been reported to alter GSK3 activity in human pulmonary artery smooth muscle cells (Clifford et al. 2008), we were wondering if TGF-β1 might affect GSK3 activity in alveolar epithelial cells as well, thereby leading to downregulation of megalin. Stimulation of primary alveolar type II cells with a pathologically relevant concentration of TGF-β1 resulted in significant dephosphorylation and therefore activation of both GSK3 subunits. Interestingly, we observed maximal dephosphorylation of GSK3 within minutes, which is in line with our data that show rapid impairment of albumin uptake in presence of TGF-β1.

To further investigate the correlation between TGF-β1-mediated GSK3 activation, reduced megalin surface expression and impaired albumin uptake, we set out to inhibit GSK3 activity in primary alveolar epithelial and RLE-6TN cells prior to administration of TGF-β1.

The best studied inhibitor of GSK3 is lithium (Stambolic et al. 1996) which has been used for treatment of mental diseases since the middle of the 20th century and inhibits the kinase by Mg^{2+}-competition (Ryves and Harwood 2001). However, it has been established that lithium exhibits low specificity for GSK3 and affects other enzymes as well. In addition, high doses of lithium are required to inhibit GSK3 in cell culture (Stambolic et al. 1996). Still, lithium has shown beneficial effects in the treatment of bipolar disorder, indicating that GSK3 activity plays a role in causing the disease (Detera-Wadleigh 2001; Manji et al. 1999). Later on valproate was identified to show a similar mood stabilizing effect by GSK3 inhibition (Chen et al. 1999). Beside of GSK3 inhibition, lithium and valproate also interfere with neuronal inositol metabolism which, meanwhile, has been proposed to be the underlying mechanism of their mood-stabilizing efficiency (Williams 2002). To investigate the role of GSK3 in the pathology of different diseases, a number of new inhibitors have been recently developed. Most of them facilitate inhibition by ATP-competition and are highly specific for the kinase (Martinez et al. 2002a; Martinez et al. 2002b). SB 216763 is such an inhibitor, a maleimide that inhibits activity of both subunits of GSK3 by ATP competition (Cross et al. 2001; Smith et al. 2001). The selectivity of SB 216763 has been established by testing the inhibitor against 26 kinases, none of which were affected at concentrations were GSK3 was already significantly inhibited (Smith et al. 2001). This inhibitor has been used in a variety of studies to investigate involvement of GSK3 in the pathology of diseases. In one study investigating ischemic preconditioning, perfused rat hearts have been pretreated with SB 216763 before ischemia was induced (Tong et al. 2002). This study established that inhibition of GSK3 mimics the effect of ischemic preconditioning, since inactivation of the kinase appeared cardioprotective by improving postischemic function and reducing infarct size. When we employed the specific GSK3 inhibitor SB 216763 in the current study and conducted cellular transport studies, the effects of TGF-β1 on albumin uptake were prevented. Binding of ^{125}I-albumin to the cell surface as well as uptake by the cells and transepithelial transport across monolayers of alveolar epithelial cells were restored. Furthermore, SB 216763 restored megalins' membrane distribution and FITC-albumin uptake in ATII, ATI-like and RLE-6TN cells. These findings further suggest that TGF-β1 induced activation of GSK3α/β mediates increased phosphorylation and decreased cell surface expression of megalin and thereby, impairs albumin endocytosis in alveolar epithelial cells.

4.5 Inhibition of GSK3 as a therapeutic approach

Although ALI/ARDS has been described over four decades ago (Ashbaugh et al. 1967), no suitable pharmacological therapy has been established. In a multi-center clinical trial, patients were mechanically ventilated with either 12 ml/kg or 6 ml/kg with plateaus pressure restriction of < 30 cm H_2O (ARDSNet 2000). Application of a lung protective lower tidal volume resulted in a reduction of mortality rate by 22 % and is, up until now, the only strategy to decrease mortality in ARDS. Tremendous efforts have been undertaken to identify substances to treat the disease, however, none of them translated to a clinical benefit. Surfactant replacement therapy, for instance, has been shown to be beneficial in pediatric acute lung injury, which is associated with impaired surfactant production (Liechty et al. 1991). In adult ARDS surfactant therapy failed to improve mortality rate (Anzueto et al. 1996). In another trial, application of inhaled vasodilators that directly target pulmonary vasculature, such as nitric oxide (NO) (Pepke-Zaba et al. 1991) and prostacyclins (Walmrath et al. 1993) resulted in temporarily improved oxygenation but failed to decrease mortality (Troncy et al. 1998; Van Heerden et al. 1996). Moreover, glucocorticoids exhibit both, anti-inflammatory and anti-fibrotic properties (Newton 2000) and therefore were proposed to be beneficial in ARDS. Mechanical ventilated patients were prophylactically treated with high-dose methylprednisolone (Weigelt et al. 1985) but the development of ARDS could not be prevented. The same strategy failed to improve mortality rate in established ARDS (Bernard et al. 1982). Glucocorticoid treatment in the late proliferative phase of lung injury did also fail to have a therapeutic effect (Meduri et al. 1998), even though bleomycin-induced fibrosis in rats was inhibited by application of dexamethasone (Dik 2003).

Inhibition of GSK3 as a therapeutic strategy has been presumed to be beneficial for various diseases. The best studied application of GSK3-inhibitors as a therapeutic agent is the treatment of mental diseases. One example is the treatment of fragile X syndrome (FXS), a hereditary disease, which besides mental retardation, exhibits symptoms like attention deficits, anxiety, hypersensitivity to stimuli and childhood-seizures (Baumgardner et al. 1995; Fisch et al. 1999). Studies in a transgenic mouse model for FXS (Bakker and Consortium 1994) established that the symptoms are triggered by activation of GSK3 and thus, the impact of SB216763 on seizure sensitivity and open field hyperactivity was investigated. SB 216763 significantly decreased sensitivity to seizures and normalized hyperactivity (Min et al. 2009). Leroy et al. (2007) detected increased GSK3 activity in the frontal cortex of patients with Alzheimer's disease (AD). Furthermore, it has been established that GSK3 enhances insoluble

β-amyloid (Aβ) production and thereby promotes hyperphosphorylation of tau which results in neurodegeneration by neurofibrillary tangles formation (Hooper at al. 2008). Inhibition of GSK3 activity by lithium treatment prevented tau phosphorylation in transgenic mice which phenotypically over-express GSK3β and tau (Engel et al. 2006) and inhibited Aβ induced neurodegeneration in cultured neurons (Alvarez et al. 1999). GSK3 activity is increased in type II diabetes (Eldar-Finkelman et al. 1999) resulting in inactivation of glycogen synthase (Cohen et al. 1998). A new potent GSK3 inhibitor (CHIR 99021) has been tested in three different rodent models of type II diabetes. CHIR 99021 successfully suppressed glucose production in the liver and increased glycogen synthesis by activation of glycogen synthase and therefore, normalized blood glucose levels (Cline et al. 2003).

In the present study we demonstrated a direct correlation between TGF-β1-mediated activation of GSK3 and decreased albumin clearance and thus, set out to investigate the role of GSK3 inhibition as a therapeutic strategy. In cellular transport studies we treated primary alveolar epithelial cells and RLE-6TN cells with the specific inhibitor SB 216763 after cells were challenged with TGF-β1 and incubated them with ^{125}I-albumin or FITC-albumin. Treatment of the cells with SB 216763 after TGF-β1 challenge restored normal megalin surface distribution and albumin transport. These findings may suggest a potential role for the specific GSK3 inhibitor SB 216763 as a novel therapeutic agent in ALI/ARDS.

4.6 Summary

We used alveolar epithelial cells and an intact organ model to investigate the mechanisms of protein clearance from the alveolar space. In tight monolayers of ATII and ATI-like cells, transport of ^{125}I- or FITC-albumin was almost completely blocked by competition with unlabeled albumin, indicating that albumin transport is facilitated by an active and receptor-mediated transport process. Since several studies have established that clathrin-dependent endocytosis is the major pathway for macromolecule uptake along epithelia (Mukherjee et al. 1997; Schmid 1997; Christensen and Birn 2002), we set out to investigate the role of the multi-ligand receptors megalin and cubilin which are known to facilitate clathrin-dependent endocytosis of proteins in the kidney (Christensen and Birn, 2001). Parmacological inhibition and gene silencing of megalin resulted in significantly decreased protein transport. Collectively, our findings suggested that under physiological conditions, albumin endocytosis in the alveolar epithelium was mediated by megalin. Importantly, we detected comparable albumin transport rates in type I and type II cells, which is of high relevance, since type I cells represent more than 95% of the alveolar surface area (Mutlu and Sznajder 2005).

To determine the mechanisms of albumin transport in the pathophysiology of acute lung injury we applied TGF-β1, a key mediator of ALI/ARDS, to alveolar epithelial cells and to the isolated, ventilated and perfused rabbit lung and detected significantly impaired albumin transport rates. Furthermore, we observed markedly decreased megalin membrane abundance in response to a pathologically relevant concentration of TGF-β1. We found evidence that TGF-β1 rapidly activates both subunits of GSK3, a kinase that phosphorylates megalin and thereby induces endocytosis of the receptor. Furthermore, pharmacological inhibition of GSK3 activity prior to TGF-β1 challenge and after TGF-β1 challenge completely prevented the TGF-β1 induced downregulation of megalin and thus, protein transport. These findings may suggest a potential role for GSK3 inhibition as a novel therapeutic approach in ALI/ARDS.

5. Zusammenfassung

Das Acute Respiratory Distress Syndrome (ARDS) führt jährlich bei ungefähr 200,000 kritisch erkrankten Patienten zu einer Mortalitätsrate von bis zu 40 %, allein in den USA. Leitsymptom ist die Anreicherung einer proteinreichen Ödemflüssigkeit in den Lungenalveolen. Die Lungeninsuffizienz wird durch eine Schädigung der endothelialen und epithelialen Schranke des Lungenparenchyms verursacht. Aus klinischer Sicht ist vor allem der Abtransport von Plasmaproteinen aus dem Alveolarraum von großer Bedeutung. Da Ionen und Flüssigkeit relativ schnell über aktive Prozesse abtransportiert werden können, erhöht sich die Proteinkonzentration in der Alveole zunehmend. Es entsteht ein onkotischer Druck, der das Lungenödem verschlimmert und eine Heilung verhindert. Der Abtransport von Proteinen und die Auflösung des Ödems sind entscheidend für das Überleben des Patienten, allerdings sind die Mechanismen des Albumintransports noch weitgehend unbekannt.

In der vorliegenden Studie wurden primäre Pneumozyten und ein intaktes Organmodel verwendet, um die Mechanismen des Proteintransports im Alveolarraum zu untersuchen. In dichten Monolayern aus Typ II und Typ I Pneumozyten wurde der Transport von ^{125}I-Albumin fast vollständig durch Kompetition mit unmarkiertem Albumin blockiert, ähnliche Ergebnisse lieferten mikroskopische Untersuchungen mit FITC-Albumin. Diese Daten implizieren, dass Albumin über einen aktiven Rezeptor-vermittelten Prozess transportiert wird. In mehreren Studien wurde festgestellt, dass in Epithelien hauptsächlich die Clathrin-abhängige Endozytose die Aufnahme von Makromolekülen, wie Proteinen, bewerkstelligt. In diesem Zusammenhang wurde auch von den Multiliganden Rezeptoren Megalin und Cubilin berichtet, die die Clathrin-abhängige Endozytose von Albumin in der Niere vermitteln. Um die Bedeutung der Megalin-vermittelten und Clathrin-abhängigen Endozytose beim Proteintransport in der Lunge zu untersuchen, behandelten wir Pneumozyten mit Receptor Associated Protein (RAP), einem Inhibitor der Megalin-vermittelten Endozytose, was deutlich die Aufnahme und den Transport von Albumin verminderte. Da Pharmakologische Hemmstoffe mit unspezifischen Nebenwirkungen einhergehen können, setzten wir einen genetischen Ansatz ein um die Bedeutung von Megalin als Albuminrezeptor zu ermitteln. Dazu wurde das Megalin-Gen mittels RNA Interferenz spezifisch ausgeschalten. Wegen ihrer hohen Transfektioneffizienz verwendeten wir kultivierte RLE-6TN Zellen, ein etabliertes *in vitro* Model für Typ II Pneumozyten. Das Gen-Silencing führte in diesen Zellen zu einer fast vollständigen Blockierung der Albuminaufnahme. Insgesamt deuten diese Ergebnisse darauf hin, dass Megalin, unter physiologischen Bedingungen, die Aufnahme von Albumin durch

das alveolare Epithel vermittelt. Interessanterweise konnten wir vergleichbare Transportraten in Typ I und Typ II Zellen feststellen, was von besonderer Bedeutung ist, da Typ I Zellen mehr als 95% der alveolaren Oberfläche darstellen.

Um den Albumintransport in der Pathophysiologie von ARDS zu untersuchen, applizierten wir Transforming Growth Factor (TGF)-β1, ein Schlüsselmolekül in der Entstehung von ARDS, in Pneumozyten und in der isolierten, ventilierten und perfundierten Kaninchenlunge. Eine pathologisch relevante Konzentration an TGF-β1 führte innerhalb kurzer Zeit zu deutlich vermindertem Albumintransport in beiden Modellen. Des Weiteren stellten wir eine verminderte Expression von Megalin in der Plasmamembran fest. Wir fanden Hinweise auf eine Aktivierung beider Untereinheiten der Glykogen Synthase Kinase 3 (GSK3) durch TGF-β1. Die GSK3 kann Megalin phosphorylieren und dadurch die Endozytose des Rezeptors verursachen. Maximale Aktivierung der GSK3 zeigte sich innerhalb weniger Minuten, was mit unseren vorangegangenen Ergebnissen übereinstimmt, die eine zeitlich gesehen schnelle Störung des Albumintransportes durch TGF-β1 dokumentieren. Als wir den spezifischen GSK3 Inhibitor SB 216763 applizierten, wurde die TGF-β1-vermittelte Herabsetzung der Megalinexpression in der Zellmembran verhindert und der Albumintransport blieb unverändert. Diese Daten deuten darauf hin, dass eine TGF-β1-vermittelte Aktivierung der GSK3 zur Endozytose von Megalin führt, wodurch der alveolare Albumintransport gestört wird.

Da die GSK3 Hemmung in verschiedenen Erkrankungen als therapeutische Maßnahme erfolgreich eingesetzt wurde, untersuchten wir eine mögliche Bedeutung in der Therapie von ARDS. Pneumozyten wurden zuerst mit TGF-β1 stimuliert und anschließend mit SB 216763 behandelt. Diese Behandlung stellte die ursprüngliche Verteilung von Megalin in der Zellmembran und den physiologischen Albumintransport wieder her. Diese Daten könnten auf eine mögliche Bedeutung der GSK Hemmung als neuartige Strategie in der Therapie von ARDS hinweisen.

6. Abstract

The acute respiratory distress syndrome (ARDS) displays mortality rates of up to 40 % in approximately 200,000 critically ill patients in the United States annually. The disease is characterized by accumulation of protein-rich edema in the alveolar space due to impaired endothelial and epithelial barrier function in the lung. Of great importance is the clearance of plasma proteins from the alveolar space. Sodium and fluid is cleared from the lung quite rapidly via active transport processes, leading to increased protein concentration in the alveolar compartment. This increased concentration of protein creates an oncotic gradient which further promotes alveolar edema formation, thereby preventing recovery. Albumin clearance and edema resolution are crucial for the patient's survival. However, the mechanisms by which albumin transport is facilitated have not been fully elucidated.

In the present study we used primary alveolar epithelial cells and an intact organ model to investigate the mechanisms of protein clearance from the alveolar space. In tight monolayers of alveolar epithelial type II cells and type I-like cells, transport of ^{125}I-albumin was almost completely blocked by competition with unlabeled albumin. Similar results were obtained by assessing the uptake of FITC-albumin by fluorescence microscopy, indicating that albumin transport is facilitated by an active and receptor-mediated transport process. A number of previous studies have reported that clathrin-dependent endocytosis is the main pathway for protein uptake along epithelia, and the multi-ligand receptors megalin and cubilin have been established to facilitate clathrin-dependent endocytosis of proteins in the kidney. To investigate the role of clathrin-dependent endocytosis and megalin in the physiological significance of albumin transport in the lung, we applied receptor associated protein (RAP), an inhibitor of megalin-mediated endocytosis, to our cell monolayers and detected significantly decreased albumin transport rates. Since pharmacological inhibitors may have non-specific effects on unrelated proteins, we employed a genetic approach to further elucidate the role of megalin in albumin uptake by alveolar epithelial cells. We sought to specifically silence the megalin gene by RNA interference. Since primary ATII cells display very low transfection efficiency, we employed cultured RLE-6TN cells, an established *in vitro* model system for ATII cells. In these cells, gene silencing of megalin resulted in an almost complete block of albumin uptake. Collectively, our findings suggested that under physiological conditions, albumin endocytosis in the alveolar epithelium was mediated by megalin. Importantly, we observed similar protein transport rates in both alveolar epithelial

cell types. These findings are of high significance, since type I pneumocytes represent more than 95% of the alveolar surface area.

To determine the mechanisms of albumin transport in the pathophysiology of acute lung injury we applied TGF-β1, a key mediator of ALI/ARDS, to alveolar epithelial cells and to the isolated, ventilated and perfused rabbit lung and detected significantly impaired albumin transport rates (within 30 minutes in cell monolayers and within 120 minutes in the isolated rabbit lung). Furthermore, we observed markedly decreased megalin membrane abundance in response to a pathologically relevant concentration of TGF-β1 *via* immunofluorescence. We found evidence that TGF-β1 activates both subunits of glycogen synthase kinase 3 (GSK3), a kinase that phosphorylates megalin and thereby induces endocytosis of the receptor. Importantly, maximal activation of GSK3 under TGF-β1 stimulation was observed within minutes, which was in line with the rapid impairment of albumin transport we detected under TGF-β1 challenge in primary alveolar epithelial cells and in the isolated rabbit lung. When GSK3 activity was inhibited by administration of the specific inhibitor SB 216763, TGF-β1-mediated downregulation of megalin membrane expression was prevented and albumin transport remained unaffected. These data implied that TGF-β1-mediated activation of GSK3 induced phosphorylation and subsequent endocytosis of megalin, thereby disrupting albumin transport in the alveolar epithelium.

Since inhibition of GSK3 as a therapeutic strategy has been presumed to be beneficial for several diseases, we set out to investigate a potential role for SB 216763 in the therapy of acute lung injury. Treatment of alveolar epithelial cells with the specific GSK3 inhibitor after TGF-β1 challenge restored normal megalin surface distribution and albumin transport. These findings may suggest a potential role for GSK3 inhibition as a novel therapeutic approach in ALI/ARDS.

7. References

Adamson, I. Y., D. H. Bowden (1975). "Derivation of type 1 epithelium from type 2 cells in the developing rat lung. " Lab Invest **32**:736-745.

Alvarez, G., J. R. Munoz-Montana, J. Satrustegui, J. Avila, E. Bogonez and J. az-Nido (1999). "Lithium protects cultured neurons against beta-amyloid-induced neurodegeneration. " FEBS Lett. **453**:260-264.

Anzueto, A., R. P. Baughman, K. K. Guntupalli et al. (1996)."Aerosolized surfactant in adults with sepsis-induced acute respiratory distress syndromke. Exosurf Acute Respiratory Distress Syndrome Sepsis Study Group. " N Engl J Med **334**:1417-1421.

Ashbaugh, D.G., D.B. Bigelow, T.L. Petty, B.E. Levine (1967). "Acute respiratory distress in adults. "Lancet **2**:319-23.

ARDSNet (2000). "Ventilation with lower tidal volumes as compared with traditional tidal volumes for acute lung injury and the acute respiratory distress syndrome." N Engl J Med **342**: 1301-8.

Bachofen, M. and E. R. Weibel (1977). "Alterations of the gas exchange apparatus in adult respiratory insufficiency associated with septicemia." Am Rev Respir Dis **116**: 589-615.

Bakker, C. E., Consortium D-BFX (1994). "Fmr1 knockout mice: a model to study fragile X mental retardation. " Cell **78**:23-33.

Bartram, U., Speer, C. P. (2004). "The role of transforming growth factor β in lung development and disease. " CHEST **125**: 754-765.

Baughman, R. P., K. L. Gunther, M. C. Rashkin, D. A. Keeton, and E. N. Pattishall (1996). "Changes in inflammatory response of the lung during acute respiratory distress syndrome: prognostic indicators. "Am. J. Respir. Crit. Care Med. **154**:76-81

Baumgardner, T. L., A. L. Reiss, L. S. Freund, M. T. Abrams (1995). "Specification of the neurobehavioral phenotype in males with fragile X syndrome. " Pediatrics **95**:744-752.

Bernard, G. R., A. Artigas, K. L. Brigham, J. Carlet, K. Falke, et al. (1994). "The American-European Consensus Conference on ARDS. Definitions, mechanisms, relevant outcomes, and clinical trial coordination. " Am. J. Respir. Crit. Care Med. **149**(3 Pt 1):818-24

Bernard, G. R., J. M. Luce, C. L. Sprung et al. (1987). "High-dose corticosteroids in patients with the adult respiratory distress syndrome. " N Engl J Med **317**:1565-1570.

Berthiaume, Y., K. H. Albertine, M. Grady, G. Fick and M. A. Matthay (1989). "Protein clearance from the air spaces and lungs of unanesthetized sheep over 144 h." J Appl Physiol **67**: 1887-97.

Berthiaume, Y., V. C. Broaddus, M. A. Gropper, T. Tanita and M. A. Matthay (1988). "Alveolar liquid and protein clearance from normal dog lungs." J Appl Physiol **65**: 585-93.

Birn, H. and E. I. Christensen (2006). "Renal albumin absorption in physiology and pathology." Kidney Int **69**: 440-9.

Birn, H., J. C. Fyfe, C. Jacobsen, F. Mounier, P. J. Verroust, H. Orskov, T. E. Willnow, S. K. Moestrup and E. I. Christensen (2000). "Cubilin is an albumin binding protein important for renal tubular albumin reabsorption." J Clin Invest **105**: 1353-61.

Borok, Z., S. I. Danto, L. L. Dimen, X. L. Zhang, and R. L. Lubman (1998). "Na(+)-K(+)-ATPase expression in alveolar epithelial cells: upregulation of active ion transport by KGF. " Am J Physiol. **274**: 149-158

Breuss, J. M., J. Gallo, H. M. DeLisser, I. V. Klimanskaya, H. G. Folkesson, J. F. Pittet, S. L. Nishimura, K. Aldape, D. V. Landers, and W. Carpenter (1995). "Expression of the beta 6 integrin subunit in development, neoplasia and tissue repair suggests a role in epithelial remodeling. " J. Cell Sci. **108**:2241-2251.

Campbell, L., A. J. Hollins, A. Al-Eid, G. R. Newman, C. von Ruhland and M. Gumbleton (1999). "Caveolin-1 expression and caveolae biogenesis during cell transdifferentiation in lung alveolar epithelial primary cultures." Biochem Biophys Res Commun **262**: 744-51.

Caruso-Neves, C., S. H. Kwon and W. B. Guggino (2005). "Albumin endocytosis in proximal tubule cells is modulated by angiotensin II through an AT2 receptor-mediated protein kinase B activation." Proc Natl Acad Sci U S A **102**: 17513-8.

Chen, G., L. D. Huang, Y. M. Jiang and H. K. Manji (1999). "The moodstabilizing a agent valproate inhibits the activity of glycogen synthase kinase-3. " J. Neurochem. **72**:1327-1230.

Chiancone, E., E. Thulin et al. (1986). "Evidence for the interaction between the calcium indicator 1,2-bis(o-aminophenoxy)ethane-N,N,N',N'- tetraacetic acid and calcium-binding proteins. " J Biol Chem **261**:16306-16308.

Christensen, E.I. and Birn, H.(2001). "Megalin and cubilin: synergistic endocytic receptors in renal proximal tubule. " Am J Physiol Renal Physiol **280**: F562– F573

Clark, J. G., J. A. Milberg, K. P. Steinberg, and L. D. Hudson (1994). "Elevated lavage levels of N-terminal peptide of type III procollagen are associated with increased fatality inadult respiratory syndrome. "Chest **105**:126-127.

Clifford, R. L., K. Deacon, A. J. Knox (2008). "Novel regulation of vascular endothelial growth factor-A (VEGF-A) by transforming growth factor (beta)1: requirement for Smads, (beta)-CATENIN, and GSK3(beta). " J Biol Chem. **283**:35337-35353-

Cline, G. W. et al. (2003). "Effects of a novel glycogen synthase kinase-3 inhibitor on insulin-stimulated glucose metabolism in Zucker Diabetic Fatty (fa/fa) rats." Diabetes **51**:2903-2910.

Cohen, P. (1998). "Identification of a protein kinase cascade of major importance in insulin signal transduction." Phil. Trans. R. Soc. Lond. B **354**:485-495.

Conner, S. D. and S. L. Schmid (2003). "Regulated portals of entry into the cell." Nature **422**: 37-44.

Cross, D. A., D. R. Alessi, P. Cohen, M. Andjelkovich and B. A. Hemmings (1995). "Inhibition of glycogen synthase kinase-3 by insulin mediated by protein kinase B." Nature **378**:785789.

Cross, D. A. et al. (2001). "Selective small-molecule inhibitors of glycogen synthase kinase-3 activity protect primary neurones from death. "J. Neurochem. **77**:94-102

Das, K., R. Y. Lewis, P. E. Scherer and M. P. Lisanti (1999). "The membrane-spanning domains of caveolins-1 and -2 mediate the formation of caveolin hetero-oligomers. Implications for the assembly of caveolae membranes in vivo." J Biol Chem **274**: 18721-8.

Detera-Wadleigh, S. D. (2001). "Lithium-related genetics of bipolar disorder." Ann. Med. **33**:272-285.

Dik, W. A., R. J. McAnulty, M. A. Versnel et al. (2003). "Short course dexamethasone treatment following injury inhibits bleomycin induced fibrosis in rats." Thorax **58**:765-771.

Doble, B.W. and Woodgett, J.R. (2003). "GSK3: tricks of the trade for a multi-tasking kinase. "J. Cell. Sci. **116**:1175-1186.

Drab, M., P. Verkade, M. Elger, M. Kasper, M. Lohn, B. Lauterbach, J. Menne, C. Lindschau, F. Mende, et al. (2001). "Loss of caveolae, vascular dysfunction, and pulmonary defects in caveolin-1 gene-disrupted mice." Science **293**: 2449-52.

Driscoll, K. E., J. M. Carter, P. T. Iype, H. L. Kumari, L. L. Crosby, M. J. Aardema, R. J. Isfort, D. Cody, M. H. Chestnut, et al. (1995). "Establishment of immortalized alveolar type II epithelial cell lines from adult rats." In Vitro Cell Dev Biol Anim **31**: 516-27.

Eisner, M. D., T. Thompson, L. D. Hudson, J. M. Luce, D. Hayden, et al. (2001). "Efficacy of low tidal volume ventilation in patients with different clinical risk factors for acute lung injury and the acute respiratory distress syndrome. " Am. J. Respir. Crit. Care Med. **164**:231-36.

Eldar-Finkelman, H., S. A. Schreyer, M. M. Shinohara, R. C. LeBoeuf and E. G. Krebs (1999). "Increased glycogen synthase kinase-3 activity in diabetes and obesity-prone C57BL/6J mice." Diabetes **48**:1-5.

Embi, N. et al. (1980). "Glycogen synthase kinase-3 from rabbit skeletal muscle. Separation from cyclic-AMP-dependent protein kinase and phosphorylase kinase. "Eur. J. Biochem. **107**:519-527

Engel, T., P. Goni-Oliver, J. J. Lucas, J. Avila and F. Hernandez (2006). "Chronic lithium administration to FTDP-17 tau and GSK-3beta overexpressing mice prevents tau hyperphosphorylation and neurofibrillary tangle formation, but pre-formed neurofibrillary tangles do not revert. " J. Neurochem. **99**:1445-1455.

Evans MJ, Cabral LJ, Stephens RJ, Freeman G (1975). "Transformation of alveolar type 2 cells to type 1 cells following exposure to NO2. "Exp Mol Pathol. **22**:142-50.

Fahy, R. J., F. Lichtenberger, C. B. McKeegan, G. J. Nuovo, C. B. Marsh, and M. D. Wewers (2003). "The acute respiratory distress syndrome: A role for transforming growth factor-β1. "Am. J. Respir. Cell Mol. Biol. **28**: 499-503

Farquhar, M. G., A. Saito, D. Kerjaschki and R: A. Orlando (1995). "The Heymann nephritis antigenic complex: megalin (gp330) and RAP. " J. Am. Soc. Nephrol. **6**:35-47

Fehrenbach, H., M. Kasper, T. Tschernig, M. S. Shearman, D. Schuh, M. Muller (1998). "Receptor for advanced glycation endproducts (RAGE) exhibits highly differential cellular and subcellular localisation in rat and human lung. "Cell Mol Biol (Noisy-legrand) **44**:1147-1157.

Fisch, G. S., N. J. Carpenter, J. J. Holden, R. Simensen, P. N. Howard-Peebles, A. Maddalena,A. Pandya, W. Nance (1999). "Longitudinal assessment of adaptive and maladaptive behaviours in fragile X males : growth, development, and profiles. " American Journal of Medical Genetics **83**:257-263.

Flick, M. R., A. Perel, N. C. Staub (1981). "Leucocytes are required for increased lung microvascular permeability after microembolization in sheep. " Circ. Res. **48**:344-51

Flori, H. R., D. V. Glidden, G. W. Rutherford, M. A. Matthay (2005). "Pediatric acute lung injury: prospective evaluation of risk factors associated with mortality. " Am. J. Respir. Crit. Care Med. **171**:995-1001.

Folkesson, H. G., M. A. Matthay, C. A. Hebert, V. C. Broaddus (1995). "Acid aspiration-induced lung injury in rabbits mediated by interleukin-8-dependent mechanisms. " J. Clin. Investig. **96**:107-16

Folkesson, H. G., M. A. Matthay, B. R. Westrom, K. J. Kim, B. W. Karlsson and R. H. Hastings (1996). "Alveolar epithelial clearance of protein." J Appl Physiol **80**: 1431-45.

Folkesson, H. G., B. R. Westrom, M. Dahlback, S. Lundin and B. W. Karlsson (1992). "Passage of aerosolized BSA and the nona-peptide dDAVP via the respiratory tract in young and adult rats." Exp Lung Res **18**: 595-614.

Folkesson, H. G., B. R. Westrom and B. W. Karlsson (1990). "Permeability of the respiratory tract to different-sized macromolecules after intratracheal instillation in young and adult rats." Acta Physiol Scand **139**: 347-54.

Folkesson, H. G., B. R. Westrom, S. G. Pierzynowski, J. Svendsen and B. W. Karlsson (1993). "Lung to blood passage of albumin and a nonapeptide after intratracheal instillation in the young developing pig." Acta Physiol Scand **147**: 173-8.

Foster, K. A., C. G. Oster, M. M. Mayer, M. L. Avery and K. L. Audus (1998). "Characterization of the A549 cell line as a type II pulmonary epithelial cell model for drug metabolism." Exp Cell Res **243**: 359-66.

Fukuda, Y., M. Ishizaki, Y. Masuda, G. Kimura, O. Kawanami and Y. Masugi (1987). "The role of intraalveolar fibrosis in the process of pulmonary structural remodeling in patients with diffuse alveolar damage. " Am. J. Pathol. **126**:171-182.

Gekle, M., P. Knaus, R. Nielsen, S. Mildenberger, R. Freudinger, V. Wohlfarth, C. Sauvant, E. I. Christensen (2003). "Transforming growth factor-beta1 reduces megalin- and cubilin-mediated endocytosis of albumin in proximal-tubule-derived opossum kidney cells. "J Physiol **552**:471-481.

Gerst, J. E. (2003). "SNARE regulators: matchmakers and matchbreakers." Biochim Biophys Acta **1641**: 99-110.

Ghosh, A. K., W. Yuan, Y. Mori, and J. Varga (2001), "Antagonistic regulation of type I collagen gene expression by interferon-gamma and transforming growth factor-beta: integration at the level of p300/CBP transcriptional coactivators. " J. Biol. Chem. **276**:11041-11048.

Gorin, A. B. and P. A. Stewart (1979). "Differential permeability of endothelial and epithelial barriers to albumin flux." J Appl Physiol **47**: 1315-24.

Grande, J. P. (1997). "Role of transforming growth factor- β in tissue injury and repair." Proc Soc Exp Biol Med **214**:27-40

Greenlee, K. J., Z. Werb and F. Kheradmand (2007). "Matrix metalloproteinases in lung: multiple, multifarious, and multifaceted." Physiol Rev **87**: 69-98.

Gross, N. J. (1995). "Extracellular metabolism of pulmonary surfactant: the role of a new serine protease." Annu Rev Physiol **57**: 135-50.

Gumbiner, B. (1987). "Structure, biochemistry, and assembly of epithelial tight junctions." Am J Physiol **253**(6 Pt 1): C749-58.

Gumbleton, M., A. J. Hollins, Y. Omidi, L. Campbell, G. Taylor (2003). "Targeting caveolae for vesicular drug transport. "J Control Release **87**:139-151.

Hammad, S. M., J. L. Barth, C. Knaak, W. S. Argraves (2000). "Megalin acts in concert with cubilin to mediate endocytosis of high density lipoproteins. " J Biol Chem **275**: 12003-12008.

Hastings, R. H., H. G. Folkesson and M. A. Matthay (2004). "Mechanisms of alveolar protein clearance in the intact lung." Am J Physiol Lung Cell Mol Physiol **286**: L679-89.

Hastings, R. H., H. G. Folkesson, V. Petersen, R. Ciriales and M. A. Matthay (1995). "Cellular uptake of albumin from lungs of anesthetized rabbits." Am J Physiol **269**(4 Pt 1): L453-62.

Hastings, R. H., M. Grady, T. Sakuma and M. A. Matthay (1992). "Clearance of different-sized proteins from the alveolar space in humans and rabbits." J Appl Physiol **73**: 1310-6.

Hastings, R. H., J. R. Wright, K. H. Albertine, R. Ciriales and M. A. Matthay (1994). "Effect of endocytosis inhibitors on alveolar clearance of albumin, immunoglobulin G, and SP-A in rabbits." Am J Physiol **266**(5 Pt 1): L544-52.

Herz, J., J. L. Goldstein, D. K. Strickland, Y. K. Ho and M. S. Brown (1991). "39-kDa protein modulates binding of ligands to low density lipoprotein receptor-related protein/alpha 2-macroglobulin receptor. " J. Biol. Chem. **226**:21232-21238.

Hooper, C., R. Killick, S. Lovestone (2008). "The GSK3 hypothesis of Alzheimer's disease." J Neurochem. **104**:1433-1439.

Hostetter, M. W., C. A. Dawson and V. L. Moore (1981). "Influence of temperature on the absorption of inhaled bovine serum albumin through isolated rabbit lungs." Proc Soc Exp Biol Med **167**: 412-8.

Ikehata, M., R. Yumoto, K. Nakamura, J. Nagai and M. Takano (2008). "Comparison of albumin uptake in rat alveolar type II and type I-like epithelial cells in primary culture. " Pharm Research **25**: 913-922.

Jayr, C., C. Garat, M. Meignan, J. F. Pittet, M. Zelter and M. A. Matthay (1994). "Alveolar liquid and protein clearance in anesthetized ventilated rats." J Appl Physiol **76**: 2636-42.

Johansson, B. R. (1979). "Size and distribution of endothelial plasmalemmal vesicles in consecutive segments of the microvasculature in cat skeletal muscle." Microvasc Res **17**: 107-17.

John, T. A., S. M. Vogel, R. D. Minshall, K. Ridge, C. Tiruppathi and A. B. Malik (2001). "Evidence for the role of alveolar epithelial gp60 in active transalveolar albumin transport in the rat lung." J Physiol **533**(Pt 2): 547-59.

John, T. A., S. M. Vogel, C. Tiruppathi, A. B. Malik and R. D. Minshall (2003). "Quantitative analysis of albumin uptake and transport in the rat microvessel endothelial monolayer." Am J Physiol Lung Cell Mol Physiol **284**: L187-96.

Johnson, M.D., J.H. Widdicombe, L. Allen, P. Barbry, L.G. Dobbs (2002). "Alveolar epithelial type I cells contain transport proteins and transport sodium, supporting an active role for type I cells in regulation of lung liquid homeostasis. "Proc Natl Acad Sci U S A **99**:1966-1971

Kaidanovic, O., and Eldar-Finkelman, H. (2002). "The role of glycogen synthase kinase-3 in insulin resistance and Type 2 diabetes. " diabetes. Expert Opin. Ther. Targets **6**:555-561.

Kaminski, N., J. D. Allard, J. F. Pittet, F. Zuo, M. J. Griffiths, D. Morris, X. Huang, D. Sheppard, andR. A. Heller (2000). "Global analysis of gene expression in pulmonary fibrosis reveals distinct programs regulating lung inflammation and fibrosis. " Proc. Natl. Acad. Sci. USA **97**:1778-1783.

Kasper, M., T. Reimann, U. Hempel, K. W. Wenzel, A. Bierhaus, D. Schuh, V. Dimmer, G. Haroske and M. Muller (1998). "Loss of caveolin expression in type I pneumocytes as an indicator of subcellular alterations during lung fibrogenesis." Histochem Cell Biol **109**: 41-8.

Kim, K. J. and A. B. Malik (2003). "Protein transport across the lung epithelial barrier." Am J Physiol Lung Cell Mol Physiol **284**: L247-59.

Kim, K. J., Y. Matsukawa, H. Yamahara, V. K. Kalra, V. H. Lee and E. D. Crandall (2003). "Absorption of intact albumin across rat alveolar epithelial cell monolayers." Am J Physiol Lung Cell Mol Physiol **284**: L458-65.

Kim, H. R., S. Gil, K. Andrieux, V. Nicolas, M. Appel, H. Chacun, D. Desmaele, F. Taran, D. Georgin, and P. Couvreur (2007). "Low-density lipoprotein receptor-mediated endocytosis of PEGylated nanoparticles in rat brain endothelial cells. " Cell. Mol. Life Sci. **64**:356-364

Kobashi, Y. and T. Manabe (1993). "The fibrosing process in so-called organized diffuse alveolar damage. An immunohistochemical study of the change from hyaline membrane to membranous fibrosis." Virchows Arch A Pathol Anat Histopathol **422**: 47-52.

Kolleck, I., H. Wissel, F. Guthmann, M. Schlame, P. Sinha and B. Rustow (2002). "HDL-holoparticle uptake by alveolar type II cells: effect of vitamin E status." Am J Respir Cell Mol Biol **27**: 57-63.

Laukoetter, M. G., M. Bruewer and A. Nusrat (2006). "Regulation of the intestinal epithelial barrier by the apical junctional complex." Curr Opin Gastroenterol **22**: 85-9.

LeHeste, J. R., B. Rolinski, H. Vorum et al. (1999). "Megalin knock out mice as an animal model of low molecular weight proteinuria. " Am J Pathol **155**:1361-1370.

Leroy, K., Z. Yilmaz and J. P. Brion (2007). "Increased level of active GSK-3beta in Alzheimer's disease and accumulation in argyrophilic grains and in neurones at different stages of neurofibrillary degeneration. " Neuropathol. Appl. Neurobiol. **33**:43-45.

Liechty, E. A., E. Donovan, D. Purohit et al. (1991). "Reduction of neonatal mortality after multiple doses of bovine surfactant in low birth weight neonates with respiratory distress syndrome. " Pediatrics **88**:19-28.

Lin, C. T., J. Garbern and J. Y. Wu (1982). "Light and electron microscopic immunocytochemical localization of clathrin in rat cerebellum and kidney." J Histochem Cytochem **30**: 853-63.

Looney, M. R., X. Su, J. A. Van Ziffle, C. A. Lowell, M. A. Matthay (2006). "Neutrophils and their Fcγ receptors are essential in amouse model of transfusion-related acute lung injury. " J. Clin. Investig. **116**:1615-23

Lunn, G., E. Sansone (1994). "Degradation and disposal of some enzyme inhibitors. Scientific note. " Appl Biochem Biotechnol. **48**:57-59.

Manji, H. K., G. J. Moore and G. Chen (1999). "Lithium at 50: have the neuroprotective effects of this unique cation been overlooked?" Biol. Psychiatry **46**:929-940.

Marsh, M. and H. T. McMahon (1999). "The structural era of endocytosis." Science **285**: 215-20.

Marshall, R. P., G. Bellingan, S. Webb, A. Puddicombe, N. Goldsack, R. J. McAnulty and G. J. Laurent (2000). "Fibroproliferation occurs early in the acute respiratory distress syndrome and impacts on outcome. " Am. J. Respir. Crit. Care Med. **162**:1783-1788.

Martin, C., L. Papazian, M. J. Payan, P. Saux, and F. Gouin (1995). "Pulmonary fibrosis correlates with outcome in adult respiratory distress syndrome: a study in mechanical ventilated patients. Chest **107**:196-200.

Martinez, A., M. Alonso, A. Castro, C. Perez and F. J. Moreno (2002a). "First non-ATP competitive glycogen synthase kinase 3 beta (GSK-3beta) inhibitors: thiadiazolidinones (TDZD) as potential drugs for treatment of Alzheimer's disease. " J. Med. Chem. **45**:1292-1299.

Martinez, A., A. Castro, I. Dorronsoro and M. Alonso (2002b). "Glycogen synthase kinase 3 (GSK-3) inhibitors as new promising drugs for diabetes, neurodegeneration, cancer, and inflammation. " Med. Res. Rev. **22**:73-384.

Mason, R. J., M. C. Williams, J. H. Widdicombe, M. J. Sanders, D. S. Misfeldt, L. C. Berry (1982)."Transepithelial transport by pulmonary alveolar type II cells in primary culture. " Proc Natl Acad Sci U S A **79**:6033-6037.

Matthay, M. A. (2002). "Alveolar fluid clearance in patients with ARDS: does it make a difference?" Chest **122**(6 Suppl): 340S-343S.

Matthay, M. A., Y. Berthiaume and N. C. Staub (1985). "Long-term clearance of liquid and protein from the lungs of unanesthetized sheep." J Appl Physiol **59**: 928-34.

Matthay, M. A., H. G. Folkesson and C. Clerici (2002). "Lung epithelial fluid transport and the resolution of pulmonary edema." Physiol Rev **82**: 569-600.

Matthay, M. A. and J. P. Wiener-Kronish (1990). "Intact epithelial barrier function is critical for the resolution of alveolar edema in humans." Am Rev Respir Dis **142**(6 Pt 1): 1250-7.

Matthay, M. A., Zemans, R. L. (2011): "The acute respiratory distress syndrome: pathogenesis and treatment. " Annu. Rev. Pathol. **6**:147-63

Matthay, M. A., G. A. Zimmerman (2005). "Acute lung injury and the acute respiratory distress syndrome: four decades of inquiry into pathogenesis and rational management. " Am. J. Respir. Cell Mol. Biol. **33**:319-27

Meduri, G. U., A. S. Headly, E. Golden et al. (1998). "Effect of prolonged methylprednisolone therapy in unresolving acute respiratory distress syndrome: a randomized controlled trial. " JAMA **280**:159-165.

Mehta, D. and A. B. Malik (2006). "Signaling mechanisms regulating endothelial permeability." Physiol Rev **86**: 279-367.

Meyer, E. C., R. Ottaviano and J. J. Higgins (1977). "Albumin clearance from alveoli: tissue permeation vs. airway displacement." J Appl Physiol **43**: 487-97.

Meyer, E. C., R. Ottaviano and J. J. Higgins (1978). "Fibrinogen clearance from alveoli." J Appl Physiol **45**: 516-20.

Min, W. W., C. J. Yuskaitis, Q. Yan, C. Sikorski, S. Chen, R. S. Jope, R. P. Bauchwitz (2009). "Elevated glycogen synthase kinase-3 activity in Fragile X mice: key metabolic regulator with evidence for treatment potential. " Neuropharmacology **56**:463-472.

Minshall, R. D. and A. B. Malik (2006). "Transport across the endothelium: regulation of endothelial permeability." Handb Exp Pharmacol(176 Pt 1): 107-44.

Moestrup, S. K. and R. Kozyraki (2000). "Cubilin, a high-density lipoprotein receptor." Curr Opin Lipidol **11**: 133-40.

Moestrup, S. K., R. Kozyraki, M. Kristiansen, J. H. Kaysen, H. H. Rasmussen, D. Brault, F. Pontillon, F. O. Goda, E. I. Christensen, et al. (1998). "The intrinsic factor-vitamin B12 receptor and target of teratogenic antibodies is a megalin-binding peripheral membrane protein with homology to developmental proteins." J Biol Chem **273**: 5235-42.

Monks, J. and M. C. Neville (2004). "Albumin transcytosis across the epithelium of the lactating mouse mammary gland." J Physiol **560**(Pt 1): 267-80.

Mostov, K. E. and M. H. Cardone (1995). "Regulation of protein traffic in polarized epithelial cells." Bioessays **17**: 129-38.

Mostov, K. E. and D. L. Deitcher (1986). "Polymeric immunoglobulin receptor expressed in MDCK cells transcytoses IgA." Cell **46**: 613-21.

Mu, D., S. Cambier, L. Fjellbirkeland, J. L. Baron, J. S. Munger, H. Kawakatsu, D. Sheppard, V. C. Broaddus, and S. L. Nishimura (2002). "The integrin alpha(v)beta8 mediates epithelial homeostasis through MT1-MMP-dependent activation of TGF-beta1. " J. Cell Biol. **157**:493-507.

Mukherjee, S., R. N. Ghosh and F. R. Maxfield (1997). "Endocytosis. " Physiol Rev **77**:759-803

Murphy-Ullrich, J. E., and M. Poczatek (2000). "Activation of latent TGF-beta by thrombospondin-1: mechanisms and physiology. " Cytokine Growth Factor Rev. **11**:59-69.

Mutlu, G. M. and J. I. Sznajder (2005). "Mechanisms of pulmonary edema clearance." Am J Physiol Lung Cell Mol Physiol **289**: L685-95.

Newton, R. (2000). "Molecular mechanisms of glucocorticoid action: what is important? " Thorax **55**:603-613.

Pearse, B. M. (1976). "Clathrin: a unique protein associated with intracellular transfer of membrane by coated vesicles." Proc Natl Acad Sci U S A **73**: 1255-9.

Pelkmans, L. and M. Zerial (2005). "Kinase-regulated quantal assemblies and kiss-and-run recycling of caveolae." Nature **436**: 128-33.

Pepke-Zaba, J., T. W. Higenbottam, A. T. Dinh-Xuan et al. (1991). "Inhaled nitric oxide as a cause of selective pulmonary vasodilation in pulmonary hypertension. " Lancet **338**:1173-1174.

Peterson, B. T., K. D. Dickerson, H. L. James, E. J. Miller, J. W. McLarty and D. B. Holiday (1989). "Comparison of three tracers for detecting lung epithelial injury in anesthetized sheep." J Appl Physiol **66**: 2374-83.

Pittet, J. F., M. J. Griffiths, T. Geiser, N. Kaminski, S. L. Dalton, X. Huang, L.A. Brown, P. J. Gotwals, V. E. Koteliansky, M. A. Matthay and D. Sheppard (2001). "TGF-beta is a critical mediator of acute lung injury. " J. Clin. Invest. **107**:1537-1544.

Pugin, J., G. Verghese, M.C. Widmer and M. A. Matthay (1999). "The alveolar space is the site of intense inflammatory and profibrotic reactions in the early phase of acute respiratory distress syndrome. " Crit. Care. Med. **27**:304-312.

Randolf, A. G. (2009). "Management of acute lung injury and acute respiratory distress syndrome in children. " Crit. Care. Med. 37:2448-54

Rayasam, G.V. et al. (2009). " Glycogen synthase kinase 3: more than a namesake. " Br J Pharmacol. **156**:885–898.

Razani, B., X. B. Wang, J. A. Engelman, M. Battista, G. Lagaud, X. L. Zhang, B. Kneitz, H. Hou, Jr., G. J. Christ, et al. (2002). "Caveolin-2-deficient mice show evidence of severe pulmonary dysfunction without disruption of caveolae." Mol Cell Biol **22**: 2329-44.

Ridge, K. M., D. H. Rutschman, P. Factor, A. I. Katz, A. M. Bertorello and J. L. Sznajder (1997). "Differential expression of Na-K-ATPase isoforms in rat alveolar epithelial cells. " Am J Physiol. **273**(1 Pt 1):L246-255.

Rivett, A. J. (1990). "Eukaryotic protein degradation." Curr Opin Cell Biol **2**: 1143-9.

Rodewald, R. and J. P. Kraehenbuhl (1984). "Receptor-mediated transport of IgG." J Cell Biol **99**(1 Pt 2): 159s-164s.

Rubenfeld, G. D., E. Caldwell, E. Peabody, J. Weaver, D. P. Martin, et al. (2005). "Incidence and outcomes of acute lung injury. " N. Engl. J. Med. **353**:1685-93.

Rummel, S. (2007). "Mechanisms of alveolar protein clearance in isolated rabbit lungs: role of clathrin- and caveolae-mediated endocytosis of albumin by the alveolar epithelium. "Laufersweiler Verlag.

Rutschman, D. H., W. Olivera and J. I. Sznajder (1993). "Active transport and passive liquid movement in isolated perfused rat lungs." J Appl Physiol **75**: 1574-80.

Russo, L. M., E. del Re, D. Brown, H. Y. Lin (2007). "Evidence for a role of transforming growth factor (TGF)-beta1 in the induction of postglomerular albuminuria in diabetic nephropathy: amelioration by soluble TGF-beta type II receptor. "Diabetes **56**:380-388.

Ryves, W. J. and Harwood, A. J. (2001). "Lithium inhibites glycogen synthase kinase-3 by competition for magnesium. " Biochem. Biophys. Res. Commun. **280**:720-725.

Saito A, Pietromonaco S, Loo AK, Farquhar MG. (1994). "Complete cloning and sequencing of rat gp330/megalin, a distinctive member of the low density lipoprotein receptor gene family. "Proc Natl Acad Sci U S A. **91**:9725-9.

Saito, A., H. Sato, N. Iino and T. Takeda (2010). "Molecular mechanisms of receptor-mediated endocytosis in the renal proximal tubular epithelium. " J Biomed Biotechnol. **2010**: 403272

Sakagami, M., P. R. Byron and F. Rypacek (2002). "Biochemical evidence for transcytotic absorption of polyaspartamide from the rat lung: effects of temperature and metabolic inhibitors." J Pharm Sci **91**: 1958-68.

Schmid, S. L. (1997). "Clathrin-coated vesicle formation and protein sorting: An integrated process. " Annu Rev Biochem **66**:511-548.

Schnitzer, J. E. (1992). "gp60 is an albumin-binding glycoprotein expressed by continuous endothelium involved in albumin transcytosis." Am J Physiol **262**(1 Pt 2): H246-54.

Schnitzer, J. E., J. Allard and P. Oh (1995). "NEM inhibits transcytosis, endocytosis, and capillary permeability: implication of caveolae fusion in endothelia." Am J Physiol **268**(1 Pt 2): H48-55.

Schnitzer, J. E., P. Oh, E. Pinney and J. Allard (1994). "Filipin-sensitive caveolae-mediated transport in endothelium: reduced transcytosis, scavenger endocytosis, and capillary permeability of select macromolecules." J Cell Biol **127**: 1217-32.

Schnitzer, J. E., J. B. Ulmer and G. E. Palade (1990). "A major endothelial plasmalemmal sialoglycoprotein, gp60, is immunologically related to glycophorin." Proc Natl Acad Sci U S A **87**: 6843-7.

Seeger, W., D. Walmrath, F. Grimminger, S. Rosseau, H. Schutte, H. J. Kramer, L. Ermert and L. Kiss (1994). "Adult respiratory distress syndrome: model systems using isolated perfused rabbit lungs." Methods Enzymol **233**: 549-84.

Serikov, V. B., M. Grady and M. A. Matthay (1993). "Effect of temperature on alveolar liquid and protein clearance in an in situ perfused goat lung." J Appl Physiol **75**: 940-7.

Sharma, D. K., J. C. Brown, A. Choudhury, T. E. Peterson, E. Holicky, D. L. Marks, R. Simari, R. G. Parton and R. E. Pagano (2004). "Selective stimulation of caveolar endocytosis by glycosphingolipids and cholesterol." Mol Biol Cell **15**: 3114-22.

Singer, A. J., and R. A. Clark (1999). "Cutaneous wound healing. " N. Engl. J. Med. **341**:738-746.

Smith, D. G. et al. (2001). "3-Anilino-4-arylmaleimides: potent and selective inhibitors of glycogen synthase kinase-3 (GSK-3). "Bioorg. Med. Chem. Lett. **11**:635-639.

Stambolic, V., L. Ruel, and J.R. Woodgett (1996). "Lithium inhibits glycogen synthase kinase-3 activity and mimics wingless signalling in intact cells. "Curr. Biol. **6**:1664-1668.

Staub, N. C. (1974). "Pulmonary edema. " Physiol. Rev. **54**:678-811.

Staub, N. C. (1981). "Pulmonary edema due to increased microvascular permeability. " Annu. Rev. Med. **32**:291-312.

Steinman, R. M., S. E. Brodie and Z. A. Cohn (1976). "Membrane flow during pinocytosis. A stereologic analysis." J Cell Biol **68**: 665-87.

Stenbeck, G. and M. A. Horton (2004). "Endocytic trafficking in actively resorbing osteoclasts." J Cell Sci **117**(Pt 6): 827-36.

Tagawa, M., R. Yumoto, K. Oda, J. Nagai and M. Takano (2008). "Low-affinity transport of FITC-albumin in alveolar type II epithelial cell line RLE-6TN. " Drug Metab. Pharmacokinet. **23**: 318-327

Tamai, K., Zeng, X., Liu, C., Zhang, X., Harada, Y., Chang, Z., He, X., (2004). "A mechanism for Wnt coreceptor activation. "Mol Cell **13**:149-156.

Taylor, A. E. and K. A. Gaar, Jr. (1970). "Estimation of equivalent pore radii of pulmonary capillary and alveolar membranes." Am J Physiol **218**: 1133-40.

Tiruppathi, C., A. Finnegan and A. B. Malik (1996). "Isolation and characterization of a cell surface albumin-binding protein from vascular endothelial cells." Proc Natl Acad Sci U S A **93**: 250-4.

Tiruppathi, C., W. Song, M. Bergenfeldt, P. Sass and A. B. Malik (1997). "Gp60 activation mediates albumin transcytosis in endothelial cells by tyrosine kinase-dependent pathway." J Biol Chem **272**: 25968-75.

Tomashefski, J. F., Jr. (1990). "Pulmonary pathology of the adult respiratory distress syndrome." Clin Chest Med **11**: 593-619.

Tomashefski, J. F., Jr. (2000). "Pulmonary pathology of the acute respiratory distress syndrome." Clin Chest Med **21**: 435-466.

Tong, H., K. Imahashi, C. Steenbergen, E. Murphy (2002). "Phosphorylation of glycogen synthase kinase-3beta during preconditioning through a phosphatidylinositol-3-kinase-dependent pathway is cardioprotective." Circ Res. **90**:377-379.

Troncy, E., J. P. Collet, S. Shapiro et al. (1998). "Inhaled nitric oxide in acute respiratory distress syndrome: a pilot randomized controlled study. " Am J Respir Crit Care Med **157**:1483-1488.

Tuma, P. L. and A. L. Hubbard (2003). "Transcytosis: crossing cellular barriers." Physiol Rev **83**: 871-932.

Ueda, T., M. Ikegami and A. H. Jobe (1995). "Clearance of surfactant protein A from rabbit lungs." Am J Respir Cell Mol Biol **12**: 89-94.

Vadasz, I., R. E. Morty, M. G. Kohstall, A. Olschewski, F. Grimminger, W. Seeger and H. A. Ghofrani (2005a). "Oleic acid inhibits alveolar fluid reabsorption: a role in acute respiratory distress syndrome?" Am J Respir Crit Care Med **171**: 469-79.

Vadasz, I., R. E. Morty, A. Olschewski, M. Konigshoff, M. G. Kohstall, H. A. Ghofrani, F. Grimminger and W. Seeger (2005b). "Thrombin impairs alveolar fluid clearance by promoting endocytosis of Na+,K+-ATPase." Am J Respir Cell Mol Biol **33**: 343-54.

Vadasz, I. and J. I. Sznajder (2006). "Hypoxia-induced alveolar epithelial dysfunction." Journal of Organ Dysfunction **2**: 244-249.

Van Heerden, P. V., D. Blythe, S. A. Webb (1996). "Inhaled aerosolized prostacyclin and nitric oxide as selective pulmonary vasodilators in ARDS-a pilot study. " Anaesth Intensive Care **24**:564-568.

Verroust, P. J., H. Birn, R. Nielsen, R. Kozyraki, E. I. Christensen (2002). "The tandem endocytic receptors megalin and cubilin are important proteins in renal pathology. " Kidney International **62**:745-756.

Visser, C. C., S. Stevanovic, L. Heleen Voorwinden, P. J. Gaillard, D. J. Crommelin, M. Danhof and A. G. De Boer (2004). "Validation of the transferrin receptor for drug targeting to brain capillary endothelial cells in vitro." J Drug Target **12**: 145-50.

Wada A. (2009)."GSK-3 inhibitors and insulin receptor signaling in health, disease, and therapeutics. " Front Biosci. **14**:1558–1570.

Wakeham, D. E., J. A. Ybe, F. M. Brodsky and P. K. Hwang (2000). "Molecular structures of proteins involved in vesicle coat formation." Traffic **1**: 393-8.

Walmrath, D., T. Schneider, J. Pilch et al. (1993). "Aerosolised prostacyclin in adult respiratory distress syndrome. " Lancet **342**:961-962.

Wang, E., P. S. Brown, B. Aroeti, S. J. Chapin, K. E. Mostov and K. W. Dunn (2000). "Apical and basolateral endocytic pathways of MDCK cells meet in acidic common endosomes distinct from a nearly-neutral apical recycling endosome." Traffic **1**: 480-93.

Wang, L. H., K. G. Rothberg and R. G. Anderson (1993). "Mis-assembly of clathrin lattices on endosomes reveals a regulatory switch for coated pit formation." J Cell Biol **123**: 1107-17.

Wang, Q., Y. Wang, D. M. Hyde, P. J. Gotwals, V. E. Koteliansky, S.T. Ryan, and S. N. Giri (1999). "Reduction of bleomycin induced lung fibrosis by transforming growth factor beta soluble receptor in hamsters. "Thorax **54**:805-812

Wangensteen, O. D., M. M. Bartlett, J. K. James, Z. F. Yang and P. S. Low (1996). "Riboflavin-enhanced transport of serum albumin across the distal pulmonary epithelium." Pharm Res **13**: 1861-4.

Ware, L. B. and M. A. Matthay (2000). "The acute respiratory distress syndrome. "N. Engl. J. Med. **342**:1334-49

Ware, L. B. and M. A. Matthay (2001). "Alveolar fluid clearance is impaired in the majority of patients with acute lung injury and the acute respiratory distress syndrome." Am J Respir Crit Care Med **163**: 1376-83.

Weigelt, J. A., J. F. Norcross, K. R. Borman et al. (1985). "Early steroid therapy for respiratory failure. " Arch Surg **120**:536-540.

Wiedemann, H. P., A. P. Wheeler, G. R. Bernard, B. T. Thompson, D. Hayden, et al. (2006). "Comparison of two fluid-management strategies in acute lung injury. " N. Engl. J. Med. **354**:2564-75.

Wiener-Kronish, J. P., K. H. Albertine, M. A. Matthay (1991): "Differential responses of the endothelial and epithelial barriers of the lung in sheep to *Escherichia coli* endotoxin. " J. Clin. Investig. **88**:864-75

Williams, R. S., L. Cheng, A. W. Mudge and A. J. Harwood (2002). "A common mechanism of action for three mood-stabilizing drugs. " Nature **417**:292-295.

Willnow, T. E., J. Hilpert, S. A. Armstrong et al. (1996). "Defective forebrain development in mice lacking gp330/megalin. " Proc Natl Acad Sci USA **93**:8460-8464.

Woodgett, J. R. (1990). "Molecular cloning and expression of glycogen synthase kinase-3/factor A. " EMBO J **9**:2431-2438.

Woodgett, J. R. (2003). "Physiological roles of glycogen synthase kinase-3: potential as a therapeutic target for diabetes and other disorders. " Curr Drug Targets Immune Endocr Metabol Disord. **3**:281–290.

Wu, D. and Pan, W. (2010). "GSK3: a multifaceted kinase in Wnt signaling. "Trends Biochem Sci. **35**: 161–168.

Yumoto, R., H. Nishikawa, M. Okamoto, H. Katayama, J. Nagai and M. Takano (2006). "Clathrin-mediated endocytosis of FITC-albumin in alveolar type II epithelial cell line RLE-6TN." Am J Physiol Lung Cell Mol Physiol **290**: L946-55.

Yussef, M. S., P. Farfan, G. Bu, M. P. Marzolo (2007). " A cytoplasmic PPPSP motif determines megalin's phosphorylation and regulates receptor's recycling and surface expression. " Traffic **8**:1215-1230.

Zemans, R. L., S. P. Colgan, G. P. Downey (2009). "Transepithelial migration of neutrophils: mechanisms and implications for acute lung injury. " Am. J. Respir. Cell Mol. Biol. **40**:519-35.

Zhai, X. Y., R. Nielsen, H. Birn, K. Drumm, S. Mildenberger, R. Freudinger, S. K. Moestrup, P. J. Verroust, E. I. Christensen and M. Gekle (2000). "Cubilin- and megalin-mediated uptake of albumin in cultured proximal tubule cells of opossum kidney. "Kidney Int. **58**:1523-1533.

Zheng, G., D. R. Bachinsky, I. Stamenkovic, et al. (1994). "Organ distribution in rats of two members of the low-density lipoprotein receptor gene family, gp330 and LRP/alpa 2MR, and the receptor-associated protein (RAP). "J Histochem Cytochem **42**:531-542.

8. Danksagung

Mein erster Dank gilt Herrn Prof. Dr. Werner Seeger, Direktor der medizinischen Klinik und Poliklinik II des Universitätsklinikums Giessen und Marburg, für die Bereitstellung des Themas und für die Unterstützung bei der Durchführung meiner Arbeit.

Ein besonderer Dank gilt Herrn Dr. Istvan Vadasz für die ständige Unterstützung bei der Anfertigung meiner Arbeit und für die wissenschaftliche Ausbildung.

Ich danke Miriam Wessendorf für ihre tatkräftige Unterstützung bei den Zellversuchen.

Gerd Weigand möchte ich danken für seine Unterstützung bei der Auswertung der Isotopenversuche.

Ich danke meinen Teamkollegen für ihre ständige Hilfsbereitschaft und für das wunderbare Arbeitsklima.

Mein Dank gilt weiterhin meiner Familie und meinen Freunden, besonders Marten Schlüter, für den starken Rückhalt.

Der größte Dank gilt meiner Mutter, die mir diesen Werdegang ermöglicht hat und meinem Großvater, der immer an mich geglaubt hat.

Der Lebenslauf wurde aus der elektronischen Version der Arbeit entfernt.

The curriculum vitae was removed from the electronic version of the paper.

List of publication

Original articles:

Yasmin Buchäckert, Sebastian Rummel, Christine U. Vohwinkel, Nieves M. Gabrielli, Benno A. Grzesik, Konstantin Mayer, Susanne Herold, Rory E. Morty, Werner Seeger and István Vadász
Megalin mediates transepithelial albumin clearance from the alveolar space of intact rabbit lungs
J Physiol. 2012 Oct 15;590(Pt 20):5167-81.

Mike Althaus, Martin Fronius, **Yasmin Buchäckert**, István Vadász, Wolfgang G. Clauss, Werner Seeger, Roberto Motterlini, and Rory E. Morty
Carbon Monoxide Rapidly Impairs Alveolar Fluid Clearance by Inhibiting Epithelial Sodium Channels
Am. J. Respir. Cell Mol. Biol. 41: 639-650.

Oral and poster presentations:

I. Vadasz, **Y. Buchaeckert**, R. Ruehl, W. Seeger, R. E. Morty
Extracellular signal-regulated kinase mediates Na,K-atpase endocytosis and prevents alveolar fluid reabsorption after a single recruitment maneuver.
Eur. Resp. J. 2009, 34(53):148

M. Althaus, M. Fronius, **Y. Buchäckert**, I. Vadász, W. Clauss, W. Seeger, R. Motterlini, R. Morty
Carbon monoxide modulates the activity of sodium channels in the alveolar epithelium: a role for ENaC?
Eur. Resp. J. 2009, 34(53):876

I Vadasz, **Y Buchaeckert**, R Ruehl, W Seeger, and RE Morty
Recruitment Maneuvers Impair Alveolar Epithelial Function by Inhibiting Na,K-ATPase Function in Rabbit Lungs.
Am. J. Respir. Crit. Care Med., Apr 2009; 179: A4945.

M Althaus, M Fronius, **Y Buchaekert**, I Vadasz, WG Clauss, W Seeger, R Motterlini, and RE Morty
Carbon Monoxide Modulates the Activity of Sodium Channels in the Alveolar Epithelium: A Role for δENaC?.
Am. J. Respir. Crit. Care Med., Apr 2009; 179: A4950.

Yasmin Buchäckert, Sebastian Rummel, Miriam Schmidt, Rory E. Morty, Werner Seeger and István Vadász
Clathrin-dependent endocytosis mediates active transport of albumin across the alveolo-capillary barrier.
8th Annual Retreat of the International Graduate Programs
Molecular Biology and Medicine of the Lung and the Max Planck Research School for Heart and Lung Research

Rauischholzhausen, August 09-11, 2010
Yasmin Buchäckert, Sebastian Rummel, Miriam Schmidt, Rory E. Morty, Werner Seeger and István Vadász
Effects of alveolar recruitment maneuvers on epithelial barrier integrity in rabbit lungs (molecular biology).
7th Annual Retreat of the International Graduate Programs
Molecular Biology and Medicine of the Lung and the Max Planck Research School for Heart and Lung Research
Rauischholzhausen, July 27-29, 2009

Yasmin Buchäckert, Sebastian Rummel, Miriam Schmidt, Rory E. Morty, Werner Seeger and István Vadász
Effects of alveolar recruitment maneuvers on epithelial barrier integrity in rabbit lungs (physiology).
6th Annual Retreat of the International Graduate Programs
Molecular Biology and Medicine of the Lung
Rauischholzhausen, July 28-30, 2008

Invited talk:

Yasmin Buchäckert and Ramona Rühl
Real-time visualisation of transepithelial sodium transport in isolated lungs.
The first scientific symposium of the University of Giessen and Marburg Lung Center School
Burg Staufenberg, Hessen, Germany
28th – 29th September, 2010

10. Erklärung

Ich erkläre: Ich habe die vorgelegte Dissertation selbständig, ohne unerlaubte fremde Hilfe und nur mit den Hilfen angefertigt, die ich in der Dissertation angegeben habe. Alle Textstellen, die wörtlich oder sinngemäß aus veröffentlichten oder nicht veröffentlichten Schriften entnommen sind, und alle Angaben, die auf mündlichen Auskünften beruhen, sind als solche kenntlich gemacht. Bei den von mir durchgeführten und in der Dissertation erwähnten Untersuchungen habe ich die Grundsätze guter wissenschaftlicher Praxis, wie sie in der "Satzung der Justus-Liebig-Universität Gießen zur Sicherung guter wissenschaftlicher Praxis" niedergelegt sind, eingehalten.

édition scientifique
VVB LAUFERSWEILER VERLAG

VVB LAUFERSWEILER VERLAG
STAUFENBERGRING 15
D-35396 GIESSEN

Tel: 0641-5599888 Fax: -5599890
redaktion@doktorverlag.de
www.doktorverlag.de

ISBN: 978-3-8359-5961-3

Cover Photo: © Mopic - Fotolia.com